INTRAMYOCELLULAR TOPOGRAPHY OF LIPID DROPLETS AND OXPAT IN OBESITY AND TYPE II DIABETES

Vasco Rui Carvalho Pereira Fernandes Fachada

Master's Thesis
Exercise Physiology
Department of Biology of
Physical Activity
University of Jyväskylä
Supervisors: Heikki Kainulainen,
Paavo Rahkila, Urho Kujala

ABSTRACT

Fachada, Vasco 2010. Intramyocellular Topography of Lipid Droplets and OXPAT in Obesity and Type II Diabetes. Department of Biology of Physical Activity and Department of Health Sciences, University of Jyväskylä. Master Thesis. 99 pp.

Nowadays in the westernized world, high caloric diet and sedentarism are driving populations to accumulate ectopic fat, especially in skeletal muscle. Such is associated with the development of insulin resistance (IR) related metabolic diseases, as type II diabetes (T2D) and obesity (OB). Like IR individuals, athletes also show high intramyocellular lipids (IMCL) contents, denoting qualitative rather than quantitative differences between insulin sensitive (IS) and IR individuals IMCL. PAT proteins and OXPAT specifically, are among the main regulators of lipid droplets (LDs) in skeletal muscle. We hypothesized that different IS profiles are distinguishable through LD and OXPAT localization and colocalization (COLOC) in different skeletal muscle fiber types.

Biopsies from *vastus lateralis* were collected from 3 groups: lean controls (LC) (n=7), obese non diabetic (OB) (n=8) and type 2 diabetic (T2D) (n=10). Immunocytochemistry protocols and fluorescence microscopy were used, followed by bioinformatic methods. We assessed LD and OXPAT geography in relation to sarcolemma in different fiber types. Moreover, assessed data was also correlated with anthropometrical and blood variables. For group comparisons a Mann Whitney U test ($P<0.001$) was used and for variable correlations a Spearman test ($P<0.05$ and $P<0.01$) was used.

LDs, OXPAT and COLOC showed more peripheral in T2D followed by OB when comparing to LC. OXPAT showed more peripheral than LDs in all fiber types of all groups, especially in type II fibers where OXPAT showed always more peripheral. LDs followed the same pattern with the exception of OB, where LDs showed more peripheral in type I than type II fibers. Moreover, such particle closeness to membrane correlated positively with tissue and plasma lipids, especially in T2D.

When comparing to LC, the more peripheral values of LD and OXPAT in T2D and OB may be explained by tissue and plasma lipid availability. In type II fibers, more peripheral values may be explained by lesser capacity of these fibers in internalizing and metabolizing lipids. In OB type I fibers, more peripheral LDs may foresee an IR developing symptom. OXPAT more peripheral than LDs may be explained by OXPAT's proposed role in packaging freshly internalizing lipids into new LDs for immediate oxidation.

Our study brings novel insights concerning OXPAT localization in skeletal muscle. Additionally, we developed a powerful tool to study histological particle topography.

Keywords: Lipid metabolism; lipid droplets; PAT proteins; OXPAT; mitochondria; skeletal muscle; distribution; insulin resistance; diabetes; obesity; fiber type

ACKNOWLEDGEMENTS

I wish to express deep gratitude towards the people without whom, this present work could not be possible. My parents Nuno Fachada and Maria da Luz Pereira, for always believing and fully supporting their sons' endeavors. A word of humble gratefulness goes to Paavo Rahkila, for being a true master and pedagogue in the arts of biochemical laboratory techniques. I foremost sincerely acknowledge the possibility and trust I was given to study and work on this wider project by Heikki Kainulainen.

Important participation in this thesis should be also recognized for Tuomas Turpeinen for development of key software applications and my brother Nuno Fachada for Matlab methodological instructions. Equally important, was the possibility to have additional control group biopsy samples provided by Urho Kujala. An additional word should go towards Heikki Kyröläinen for early guidance in this Master's thesis and towards both the Department of Biology of Physical Activity and the Department of Health Sciences for infrastructural and logistic support provided by all responsible and lab personnel.

Less directly but still important, I would like to thank all people that in one way or another are present in this work. My Family and Friends: Avó Julinha, Avô Zé Maria, Avó Mariazinha, André, Tomás, Magda, Luisa, Tio Quico, Tio Quim Zé, Tia Nucha, Catarina, Patrícia, Rita, José Luís, Tânia, Sara, Ana, Miguel, Manel Zé, Joca, Maria Adelaide. My Colleagues and Friends: Luís Branco, Georgios, Miguel Torres, Ma, Gurutze, Rachel, Natalia, Sira, Mika, Juha, Susanne, Sini, Lisa, Jussi, Liisa, Elinä, Siiri, Ritva, and Armaghan.

One final note of appreciation to my former professors in Évora who initiated me in Human Physical Activity Sciences and impelled me in pursuing my goals in Jyväskylä: Orlando Fernandes, Peter Vogelaere, Armando Raimundo and José Marmeleira.

LIST OF TERMS AND ABBREVIATIONS

A-Band	Also known as Anisotropic Band, is the wide darker band of a sarcomere, where actin filaments superimpose with myosin filaments. See page 29.
ACBP	Acyl-CoA binding protein is an intracellular FA transporter.
AD board	Analogical to digital converter.
Adipocyte	Adipose tissue cell.
ADP	Adenosine Di Phosphate.
ADRP	Adipophilin, a protein belonging to the PAT family. See page 33.
AMP	Adenosine Mono Phosphate.
Amphipathic	With hydrophobic and hydrophilic properties.
Antibody	Protein produced by an immune system to destroy a specific antigen.
Antigen	Substance recognized by an immune system as foreign to the organism.
Antigenicity	Capacity of a molecule or an antigen to induce an immune response.
Apoptosis	Cell death.
Artifacts	Relative to microscopy. An image effect produced by any material not concerning the structures meant to be observed.
ATGL	Adipose Triglyceride Lipase. See page 18.
ATP	Adenosine Tri Phosphate. Main energy substrate of eukaryote organisms.
BAT	Brown Adipose Tissue.
Bile	Liver secreted fluid for lipid digestion aiding in small intestine.
Bleaching	Also referred as *photobleaching*. When fluorchromes wear off by over excitation.
BMI	Body Mass Index.
BSA	Bovine Serum Albumin.
Caveolae	Plasmalemma invaginations involved in the Endocytosis process.
Caveolins	Group of proteins involved in Endocytosis process, leading to formation of caveolae from the plasma membrane.
CD36	Cell membrane protein involved in assisting FA endocytosis; also known as FAT. See page 15.
CDS	Chanarin-Dorfman Syndrome is a disease where neutral lipids are excessively stored in various tissues' Lipid Droplets, including skeletal muscle.
CGI-58	Co-activator protein of intracellular lipases. See page 19.

CHO	Carbohydrates.
Chylomicrons	Large lipoprotein consisting in about 90% of TAG.
CM	Confocal Microscope. Allows isolate observation of very thin layers of a larger sample.
Colipase	Intestinal lipase secreted by pancreas in order to prevent the hydrolysis inhibitory effects of bile salts.
COLOC	Measured variable, colocalization of LDs and OXPAT accordingly to Costes et al. 2004
Colocalization	Degree of pixel overlap between two different fluorescent labels.
Concave	Curving inwards, like the inner surface of a sphere.
Conjugate	Fluorphores bond to an antibody.
Convex	Curving outwards, as the exterior of a sphere.
Copixelization	Term created for pointing out the fragility of "colocalization"'s biological meaning.
COX	Cytochrome c oxidase or complex IV, mitochondrial transmenbrane protein, antigen marker for mitochondria.
CPAT	Constitutive PAT proteins.
Cytoplasm	Intracellular content disregarding the nucleus.
Cytosol	Intracellular liquid surrounding organelles.
DAG	Diacylglycerol.
Dynein	Complex microtubular motor protein; transports intracellular contents along microtubules.
Endocytosis	Content Internalization in cell.
Endosome	Organelle involved in endomembrane sorting and transport systems, interacting between plasmalemma, lysosomes, Golgi complex etc.
Enterocytes	Intestinal absorptive cells.
EPAT	Exchangeable PAT proteins.
ER	Endoplasmatic reticulum.
Esterification	Formation of an ester as the reaction product (Adding of FA to Glycerol, MAG, or DAG compound).
EX and EM	Excitation and emission.
Exocytosis	Content Externalization from cell.
FA	Fatty Acid.
FABP	Fatty Acid Binding Protein. See page 15.
FABP3	Muscle Fatty Acid Binding Protein. Main cytosolic FA transporter in muscle. Also known as H-FABP. See page 16.
FABPpm	Plasma Membrane Fatty Acid Binding Protein. See page 15.
FastMyo	Fast Myosin Heavy-Chain.
FAT%	Body fat percentage.

FATPs	Group of plasma membrane proteins responsible for FFA endocytosis. See page 15.
FFA	Free Fatty Acid.
FFM	Fat free mass.
Fluorchromes	Also referred as *fluorphores*, they are fluorescent compounds, emitting fluorescence.
FM	Fluorescence Microscope; also Fat Mass.
Galvanometer mirrors	Mechanism inside the CM scan head which dynamically redirects the laser beam in the X and Y axis, scanning thus the entire specimen.
Gluconeogenesis	Recycling of non-carbohydrate byproducts to regenerate glucose (liver; kidneys; heart).
Glycemia	Blood glucose.
H-Band	Also known as H-Zone, is the sarcomere central and clearer region where myosin filaments stand alone. See page 29.
HDL	High Density Lipoprotein. Here also so used as the measured variable, plasma HDL.
Hepatocytes	Liver basic cell.
Heterotypic interaction	Interaction between LDs and other organelles, like endosomes, peroxisomes, mitochondria etc.
Homotypic interaction	Interaction between Lipid Droplets, like fusion, fission etc.
HSL	Hormone Sensitive Lipase. See page 18.
Hydrolysis	Fission of FAs and glycerol in neutral lipids; chemical separation of water molecules into hydrogen cations and hydroxide anions.
Hydrophilic	Not binding to or repelling water molecules.
Hydrophobic	Having the capacity for binding to water molecules.
I-Band	Also known as Isotropic Band, is the adjacent area to Z-lines where actin filaments stand alone with no superimposition with myosin filaments. See page 29.
ICA	Intensity Correlation Analysis.
IMCL	Intramyocellular lipids (lipids inside muscle fibre). Sometimes used as IMTG synonym.
IMF	Intermyofibrillar. Intramyocellular region in between myofibrils.
Immunocytochemistry	Biochemical procedure for marking specific cellular sites with antibodies.
Immunolabelling	Visualization of antibody markers.
IMTG	Intramyocellular triglycerides (TAG inside muscle fiber).
Intramyocellular	Inside muscle cell.
IR	Insulin resistance or Insulin resistant. In Figure 13 it represents insulin receptor.
IS	Insulin sensitivity or Insulin sensitive.
Kinesin	Microtubular motor protein; transports intracellular contents along microtubules.
KO	Knock-Out; silencing genes for observing organism response in the absence of these.
LC	Lean Controls.
LCFA	Long-Chained Fatty Acids.

LD	Lipid Droplets.
LDL	Low Density Lipoprotein. Here also so used as the measured variable, plasma LDL.
Lipase	Enzyme responsible for catalyzing lipid hydrolysis.
Lipolysis	Breakdown of TAG into FAs.
Lipotoxicity	Intracellular toxic effect caused by lipidic agents, like FFA, DAG, ceramides etc.
LPL	Lipoprotein lipase.
LSD-1 LSD-2	Lipid storage droplet-1,2; PAT proteins in *Drosophila melanogaster.*
M-Line	Sarcomere middle line. See page 29.
MAG	Monoacylglycerol.
MAM	Mitochondria-associated membrane; continuum ER membrane structure involving mitochondria; lipid synthesis probable site.
MGL	Monoglycerol Lipase. See page 18.
Microvilli	Microscopic membrane protrusions which increase cells' surface area.
Mitochondrion	Organelle responsible for many cell functions, important in ATP production.
Myocyte	Myocardium or skeletal muscle cell.
Myofibril	Bundle of myofilaments repeatedly organized more or less cylindrically and longitudinally through muscle fibers.
Myofilaments	F-Actin or Myosin filaments in parallel organization into myofibrils.
Neutral Lipid	TAG; some DAG and MAG; sterol esters.
Normoglycemic	Situation where normal range glucose levels are present in blood.
OB	Obesity/Obese.
Optical sections	Thin virtual layers observed with no light interference from the adjacent planes.
OXPAT	Protein belonging to the PAT family. Highly present in oxidative tissues. See page 36.
PAT proteins	Group of specific proteins coating LD, standing for "Perilipin; Adipophilin and TIP47". See page 31.
PBS	Phosphate buffered saline.
Perilipin	Perilipin, a protein belonging to the PAT family. See page 32.
Peroxisome	Organelle crucial for metabolic processing of FA and converting hydrogen peroxide into water, all by oxidation.
Pexopodia	I this case they are peroxisomal protrusions which penetrate into other organelles.
Photobleaching	See Bleaching.
PKA	Protein Kinase A; family of enzymes whose activity is dependent on the level of cyclic AMP or adrenalin stimulus for instance.
Plasmalemma	Cellular membrane.
PMT	Photomultiplier tube (converts fluorescence into voltage).
PPAR	Peroxisome proliferator-activated receptors; nuclear receptors involved in fuel

	selection and lipid metabolism.
Quantum efficiency	Ratio between energy emitted and energy absorbed.
RT	Room temperature.
S3-12	Protein belonging to the PAT family. See page 35.
Sarcolemma	Cellular membrane of muscle fibers.
Sarcomere	Skeletal muscle basic unit; repeated myofibril zone from one Z-line to another.
SCFA	Short Chained Fatty Acid.
sec61α	Protein present and typically used as an ER marker.
SER	Smooth Endoplasmic Reticulum.
SERCA	Sarco/Endoplasmic reticulum Ca^{2+} -ATPase. Protein present and typically used as an SR marker.
Slide	Thin transparent material putted under the objective for specimen observation.
SNARE	Family of large proteins involved in vesicle fusion among other functions.
SR	Sarcoplasmic Reticulum.
SS	Subsarcolemmal. Thin intramyocellular region between sarcolemma and IMF region.
Steroidogenic	Agent that produces steroids in living organisms.
T2D	Type 2 Diabetes/Type 2 Diabetic.
TAG	Triacylglycerol.
TAGemia	Triglyceridemia, same as triacylglycerol in blood.
TCHOL	Total cholesterol in blood.
TIP47	Tail Interacting Protein of 47 kD, a protein belonging to the PAT family. See page 34.
Topography	In this document sense it refers to the position and characteristics of particles within muscle cells.
VLCFA	Very Long Chained Fatty Acid.
VLDL	Very Low Density Lipoprotein.
VO_2max	Maximal Oxygen consumption or aerobic capacity.
WAT	White Adipose Tissue.
Wavelength	Here the term refers to Light spectrum in microscopy, wherein human capacity can detect roughly between 380–750 nanometers.
Wildefield	Referring to Microscopy which allows visualization of total volume of sample only.
β-oxidation	FA breakdown into Acetyl-CoA in mitochondria for ATP production or in Peroxisomes for different cellular purposes. See page 16.
Z-Line	Delimiting structures of a sarcomere. See page 29.

CONTENTS

1 INTRODUCTION

A dysfunctional lipid metabolism has been long shown to associate with several common and expensive diseases across the world, among these are atherosclerosis, cardiomyopathy, Chanarin-Dorfman Syndrome (CDS), metabolic syndrome, obesity (OB) and type 2 diabetes (T2D) (Bickel et al. 2009). Especially these last two, have been a growing concern due to its epidemic characteristics. It is also known that OB and T2D are broadly related to sedentary lifestyles and physical inactivity which reduces energy demands, resulting in increased fat storage in skeletal muscle, the great “fat burner” in our organism. This increased intramuscular lipid reserves has long characterized insulin resistant (IR) populations like OB and T2D. However, more recent studies gave visibility to a metabolic paradox, as extremely insulin sensitive (IS) individuals, such as endurance athletes have been repeatedly shown to have equal or even increased intramuscular lipid reserves (van Loon & Goodpaster 2006). Therefore, it is important to better understand and closely examine different populations’ skeletal muscle and their own triacylglycerol (TAG) depots, the intramuscular triglycerides or IMTG.

As equally and dependently interesting, the study of skeletal muscle micro morphology, is an active research area which urgently needs to be integrated along with lipid metabolism research. Specific physical and functional characteristics of the striated muscle fiber prohibit safe direct assumptions or analogies from among other more commonly studied cell types, as adipocytes or hepatocytes. Hence, it is also for the utmost importance, to help clarify or at least further question the intramyocellular arrangement of lipid metabolism participating agents.

2 LIPID METABOLISM OVERVIEW

2.1 Lipids in Humans

As naturally occurring molecules, lipids are easily found in virtually all living beings. Through nourishing, the average person in the western world ingests 100 to 150 grams of triacylglycerol (TAG) per day, which is the main source of lipids in the human organism attending for more than 95% of total body fat (Maughan et al. 1997). Besides TAG, other forms of lipids such as cholesterol, phospholipids or long-chained fatty acids (LCFA) are also ingested in the western daily diet (Silverthorn 2007).

In its various shapes, lipids are present throughout the human body, from plasma and lymph as free fatty acids (FFA) or lipoproteins, to cell and organelle membranes as cholesterol or phospholipids (Silverthorn 2007). Still, the adipocyte is the grand winner as a deposit for lipid stores, mainly as TAG reservoirs. Nonetheless, there are other important organs with significant TAG store capacity besides the adipose tissue, namely the liver and the skeletal muscle (Maughan et al. 1997).

Lipids have a wide variety of functions in the human metabolism, where they provide an endless fuel source. They grant the largest and more efficient nutrient store of chemical energy for biological work, including muscle contraction (Maughan et al. 1997), moreover, it is calculated that around 90% of the calories used by humans come from intracellular TAG pools (Silverthorn 2007), whereby, for the same weight unit, lipids can origin more than double of the energy provided by carbohydrates (CHO) (Maughan et al. 1997). Besides fueling purposes, lipids have very important metabolic roles as they are active accomplices in hormonal regulation, intracellular signaling among other important functions (Mooren & Völker 2005).

2.2 Systemic review

2.2.1 Digestion and absorption

When ingested, lipids start to be digested already in the mouth by small amounts of lipases present in saliva. However, it is in the small intestine where major lipid digestion and absorption occurs. Free cholesterol does not require special mechanisms of digestion and therefore, can be absorbed by active transport into intestine epithelial cells called enterocytes (Silverthorn 2007).

Contrary to cholesterol, the TAG molecule is too big and complex to be absorbed by enterocytes, it first needs to be broken down into three molecules of FA and one of glycerol, passing through the forms of diacylglycerol (DAG) and monoacylglycerol (MAG) during the process. Since fat is characterized by its water insolubility, in order to pancreatic lipase being able to perform its function, secreted bile and colipase act together to respectively emulsify and disaggregate fewer and bigger fat droplets into more and smaller ones, therefore facilitating TAG hydrolysis into FA and glycerol by lipases (Silverthorn 2007).

Once broken down to FA and MAG, fats can be diffused into enterocytes in the microvilli. After endocytosis, some short-chained fatty acids (SCFA) are externalized and absorbed into blood capillaries, however, most FA are reassembled into TAG along with MAG in the smooth endoplasmic reticulum (SER) in a process called esterification. Still inside enterocytes, TAG combine with cholesterol and proteins to give birth to chylomicrons. These are then packed in Golgi complex before being exocytosed. Given its too large dimensions for blood capillary absorption, chylomicrons are absorbed into lacteals, where they enter the lymphatic system before being transferred into blood stream in the subclavian vein (Silverthorn 2007).

2.2.2 Circulation

Lipoproteins are the main transport form of lipids in blood stream. Chylomicrons, which are around 85% composed of TAG, usually do not last more than an hour in plasma. This happens due to their interaction with high-density lipoproteins (HDL) where both classes of lipoproteins exchange material. In addition, like in other lipoproteins, TAG in chylomicrons are mainly hydrolyzed by an insulin-stimulated enzyme named lipoprotein lipase (LPL), present in capillary endothelium, thus freeing FA and glycerol into plasma (Figure 1) (Maughan et al. 1997).

Not only directly digested TAG is present in blood. Both HDL and very low-density lipoproteins (VLDL) carry TAG in plasma after being produced in hepatocytes. While HDL carry cholesterol from the blood towards the liver for producing bile, low density-lipoproteins (LDL) hydrolyzed from VLDL by LPL, carry lipids in the opposite direction, i.e., from hepatocytes towards circulation (Maughan et al. 1997). Moreover, adipose tissue is an important plasma free fatty acids (FFA) provider when adipocytes undergo lipolysis (Maughan et al. 1997).

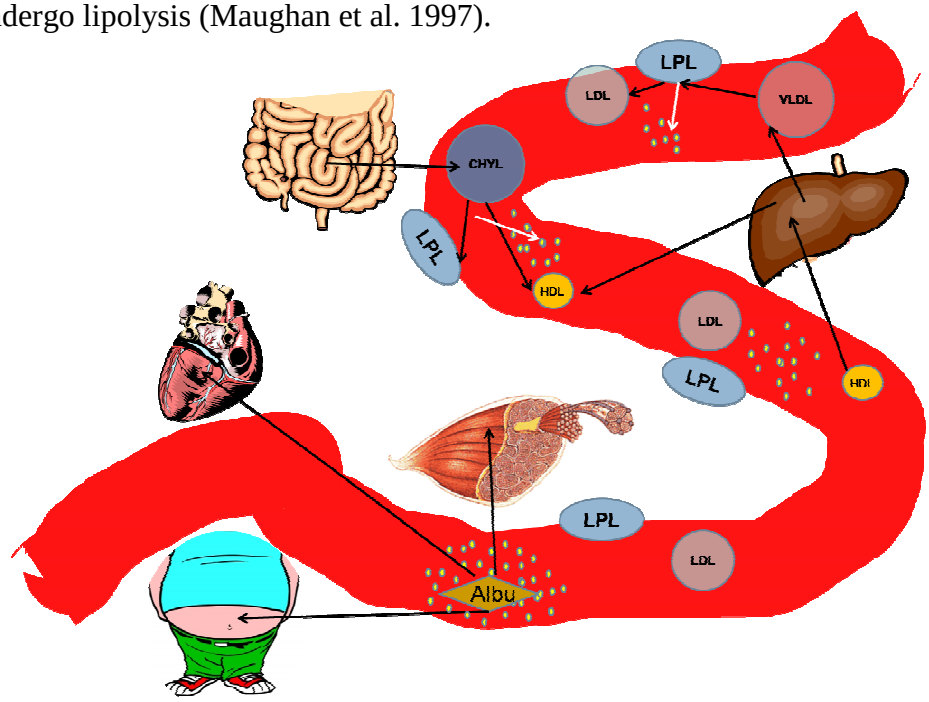

FIGURE 1. Illustration of plasma lipids processing.

Once in plasma and due to skeletal muscle limited capacity for processing it, glycerol is mostly taken by the liver and kidneys where it partakes in gluconeogenesis. On the other hand, FFA are bound to albumin and then can be transported towards cells, namely myocytes, adipocytes and others (Figure 1) (Maughan et al. 1997).

2.3 Intramyocellular trafficking

Now that we have roughly seen how different lipids are digested, absorbed and transported systemically, it is time for understanding the intracellular complexity of lipid metabolism, especially in the muscle cell wherein this thesis focuses more on.

2.3.1 Fatty acids endocytosis

Independent of the cascades regulating FA endocytosis, the rate of internalization seems to be associated with FFA gradients between extracellular space and cytosol (Mooren & Völker 2005). In fact, the FFA cellular uptake topic is presently an active field of research where models are constantly putted in proof in different cell types. It has been believed that FA could enter the cell both by passive diffusion and by protein mediated mechanisms (Mooren & Völker 2005), but recent research strengthens the paradigm that FA internalizes cells by protein facilitation (Su & Abumrad 2009).

Several transmembranal proteins were shown to take part in FA myocyte intake, among these are FATP1-6, FABPpm and CD36. The latter two are the most studied for this matter and have been positively correlated with FA internalization rates and subsequently higher levels of IMTG. Furthermore, both protein and mRNA of FABPpm and CD36 have been shown to increase chronically with muscle contraction, while acute insulin-stimulated and contraction-stimulated FA uptake seems also to involve CD36 (Mooren & Völker 2005). In addition, colocalization between CD36 and caveolin-3 (a muscle specific caveolin) observed under confocal microscope, suggests that caveolae might have an important role in FA uptake in human skeletal muscle, especially in type I

fibres where it is more expressed (Vistisen et al. 2004). The role of caveolae in FA uptake would be in accordance with its shown ability to internalize albumin (Nabi & Le 2003). After being coupled to the sarcolemma, FAs have to be transported efficiently to the cell's interior. For this, attractive models based on cytosolic fatty acid-binding proteins have been proposed. Such strong evidenced models suggest that muscle fatty acid-binding protein (FABP3 or H-FABP), which is estimated to be present at the micrometer range throughout cytosol, is proposed to be an intramuscular version of serum albumin, binding and internalizing membrane coupled FA (Figure 2). Moreover, FABP3 role in oxidative pathways is strengthened by its increased concentrations in more oxidative muscle fibres. What is more, FABP3 has been shown to chaperone both saturated and unsaturated FA in addition to interact with CD36 itself (Glatz et al. 2003).

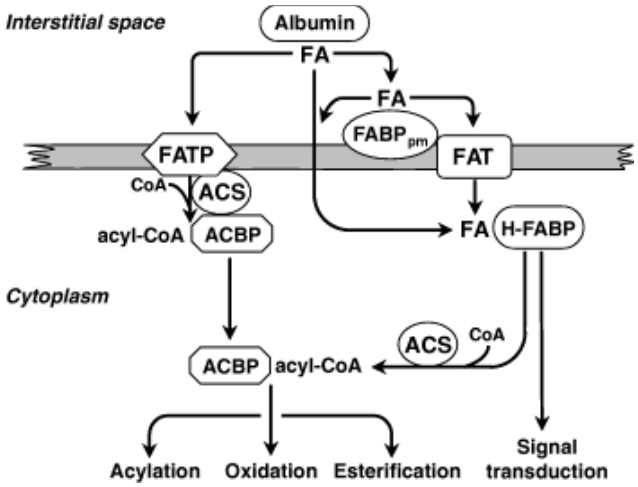

FIGURE 2. Free Fatty Acid endocytosis and intracellular transport (Glatz et al. 2003).

2.3.2 Lipid Synthesis, Lipolysis and β-Oxidation

At the time FA are finally internalized they bind to Coenzyme A (CoA) to form the ester acyl-CoA, whereby FABP3 loses its affinity to acylated FA and gives place to acyl-CoA binding protein (ACBP) for farther FA transport towards several possible anabolic or, less likely, catabolic destinations (Glatz et al. 2003; Kanaley et al. 2009). For immediate catabolic utilization after being internalized, FA in the form of acyl-CoA, may be transported via carnitine mediation – which seems to be a rate limiting factor – into mitochondria or into peroxisomes. When inside these organelles, acyl-CoA is broken

down into acetyl-CoA in a process called β-oxidation. Despite having more metabolic roles, the main destination of acetyl-CoA is ATP production within the mitochondrial matrix (Maughan et al. 1997).

Besides the not so solid possibility of being directly transported for oxidation, endocytosed FA seem more likely to be anabolized by esterification into TAG by enzymatic action of glycerol-3-phosphates (GPATs), lipin and diacylglycerol acyltransferases (mainly DGAT2) so to be used when the body requires so (Moro et al. 2008; Kanaley et al. 2009; Watt 2009). In fact, when concerning performance, IMTG are thought to be more decisive in energy production than plasma TAG, which could be accounted by the fact that plasma FA uptake rates are not able to keep up with intracellular FA oxidation rates during higher aerobic demands (Maughan et al. 1997). Nevertheless, according to Bonen and colleagues, in resting muscle, plasma FFA accounts for 90% of the lipid metabolism, while only 10% is provided from IMTG. Such values seem to change during muscle contraction, being then, the oxidized FA coming increasingly from IMTG (Bonen et al. 1998). In some reviews it is possible to understand that IMTG utilization in different metabolic states is still a very debatable issue, with its values changing along with different methods and subjects characteristics (Kiens 2006). However, a recent multi-methodological study in over than 60 human subjects, greatly strengthened the relatively old model first proposed by Dagenais in which plasma FA were said to be first esterified into intracellular TAG pools rather than directly oxidated (Dagenais et al. 1976; Kanaley et al. 2009).

It is now known however, along with other lipids and specific proteins, that IMTG are dynamically stored inside key organelles which go by the name of lipid droplets (LD) (Walther & Farese 2008). Furthermore, cytosolic FFA may have more than one purpose in being converted into TAG along with glycerol, for it has been shown that cytosolic FFA are responsible for lipotoxicity and eventual apoptotic signalling, a phenomenon also related to Alzheimer's disease (Listenberger et al. 2003; Fujimoto et al. 2008). Consequently, it is for the utmost importance that FA are at the right times and rates, efficiently stored and hydrolyzed in TAG inside the LD, wherein PAT proteins have an important but somewhat undisclosed role.

Despite antonyms, lipid synthesis and lipolysis are not complete antagonists and cannot be separated from one another. All happens around LDs and their incorporated IMTG. In normal individuals, even during lipolytic/oxidative conditions, like muscle contraction, TAG is synthesised by FFA esterification, yet the catabolism/hydrolysis rate of the same TAG is superior to its anabolism/esterification (Mooren & Völker 2005). More recent research in muscle lipid metabolism, have been increasingly using the concept of IMTG turnover, which can be described as a "*composite measure of the dynamic balance between lipolysis and lipid synthesis*", wherein some factors are intimately regulating, such as muscle oxidative capacity, IMTG hydrolysis, FFA availability and re-esterification of sub-products like DAG for instance (Moro et al. 2008).

Hydrolysis of intramuscular neutral lipids into FFA is carried out at the LDs by important intracellular lipases and their co-activators after phosphorylation by protein kinase A (PKA) (Krahmer et al. 2009; Wang et al. 2009). For a long time the hormone sensitive lipase (HSL) was seen as the main intervenient lipase in intracellular TAG lipolysis. However, recent lines of research are pointing out to adipocyte triacylglycerol lipase (ATGL) as an important and critical lipase in this process, especially for TAG reduction into DAG, while HSL has been suggested to be more decisive in DAG hydrolysis into MAG. MAG is also believed to be reduced into the final FA plus the glycerol backbone mainly by monoacylglycerol lipase (MGL) (Figure 3). Nevertheless, such lipases role in LDs is yet to be fully resolved (Zimmermann et al. 2008), some authors even relay MGL to a non-significance in skeletal muscle lipolysis, given that ATGL and HSL together are responsible for about 95% of IMTG hydrolysis (Meex et al. 2009).

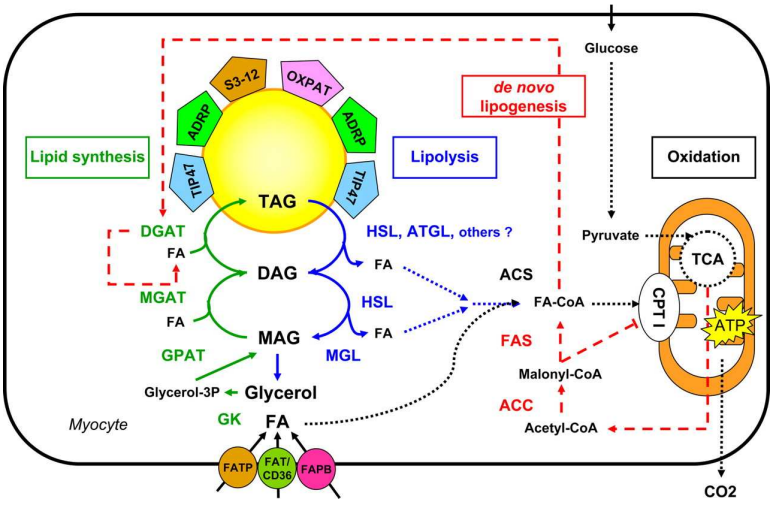

FIGURE 3. Biochemical pathways of human myocyte lipid metabolism (Moro et al. 2008).

Moreover, intracellular lipases activity itself is regulated by many different factors. For instance, ATGL has been shown to depend on activator and co-activator proteins such as CGI-58 or some PAT proteins (Lass et al. 2006; Granneman et al. 2009). Furthermore, other variables like the cell energy charge and calcium concentration correlate positively with HSL activation. Besides intracellular components, extracellular signalling factors, such as hormones, also seem play an important role in intracellular lipase regulation and consequent IMTG managing. Interestingly, in spite of stimulating LPL activity and consequently increasing lipoproteins lipolysis, insulin seems to inhibit HSL activity inside cells, resulting in sustained intracellular lipolysis. In an opposite manner, epinephrine stimulates HSL action and consequent intracellular lipolysis. Furthermore, leptin secretion was shown to increase TAG hydrolysis and FA oxidation along with reduced TAG esterification, while adiponectin is also related to increased FA oxidation (Mooren & Völker 2005).

Nevertheless, as an important ground for this dissertation, it should be noted that IMTG storage seems to be more decisive for insulin sensitivity than the rate of FA oxidation capacity (Moro et al. 2008).

3 INTRAMYOCELLULAR LIPID DROPLETS

The existence of lipid storage in skeletal muscle was first reported by Denton and Randle in 1967 (Denton & Randle 1967). Initially thought as simple random, unregulated liposomes or just fat depots, these structures, like many of their related proteins, are preserved from insects to humans and are now regarded as true organelles with dynamic life and functions, particularly in lipid metabolism (Martin & Parton 2006; Lay & Dugail 2009).

Despite being an organelle present in virtually every living cell, the LD exists differently in distinct cell types, wherein it varies considerably in size, distribution, function and probably protein regulation (Ducharme & Bickel 2008; Fujimoto et al. 2008). For instance, the classical adipocyte is mainly composed of an enormous LD which nearly fills all the cell volume, while hepatocytes and macrophages depend greatly in environmental factors in terms of LD profile and steroidogenic cells have LDs rich in steroid hormones precursors such as cholesterol (Murphy 2001).

This chapter focuses on the current knowledge concerning this organelle which just recently has been studied in its main dimensions besides its mere existence, like biogenesis, morphology and roles.

3.1 Morphology and composition

While in adipocytes LDs can reach gigantic dimensions within the 200 micrometers (Murphy 2001), the majority of LDs in skeletal muscle are within the range of nanometers, only occasionally surpassing 1 micrometer of diameter.

Much like lipoproteins in circulation, intracellular lipid droplets are delimited by a phospholipid monolayer giving this organelle a distinct amphipathic character (Tauchi-Sato et al. 2002). Phospholipids composing the LD membrane are very similar to ER membrane (Leber et al. 1994; Fujimoto et al. 2008) but the fatty acids composing the same phospholipids are rather distinct between LDs and ER membranes. Moreover, LDs seem to have considerably more free cholesterol than ER (Tauchi-Sato et al. 2002), some even suggesting this presence of cholesterol in LD membrane (Prattes et al. 2000).

While the hydrophilic heads shape the outer cytosol interacting surface, the hydrophobic tails of the phospholipid monolayer directly face and bind the inner constituents of the LD (Figure 4B). The LD core is composed of neutral lipids like DAG and sterol esters as cholesterol for instance, but the most abundant neutral lipid present in these organelles is by far TAG (Murphy 2001; Bartz et al. 2007; Walther & Farese 2008).

Interestingly, LD research using freeze fracture electron microscopy has revealed the inner structure of LDs as “onion like”, i.e., different layers throughout the core were observed (Figure 4A), suggesting that it could be an evidence of different TAG deposition processes in LDs, like esterification speed, FA composition or packing proteins, as DGATs or perhaps the PAT proteins (Tauchi-Sato et al. 2002; Robenek et al. 2008). However, whether these “onion-like” structures are indeed real or mere method-related artifacts, is still unclear and under debate (Fujimoto et al. 2008).

Additionally, many different types of protein physically relate to the LD. To begin with, as expected, esterifying enzymes like DGAT2 and hydrolyzing enzymes like ATGL and

HSL, are found in TAG pools, thus in LD, in order to perform their biological function (Kuerschner et al. 2008; Guo et al. 2009; Wang et al. 2009). Besides, various membrane-trafficking proteins were also traced in LDs, as Rab15, Rab18, ARF1 and even caveolins for instance (Fujimoto et al. 2001; Robenek et al. 2008; Walther & Farese 2008; Guo et al. 2009).

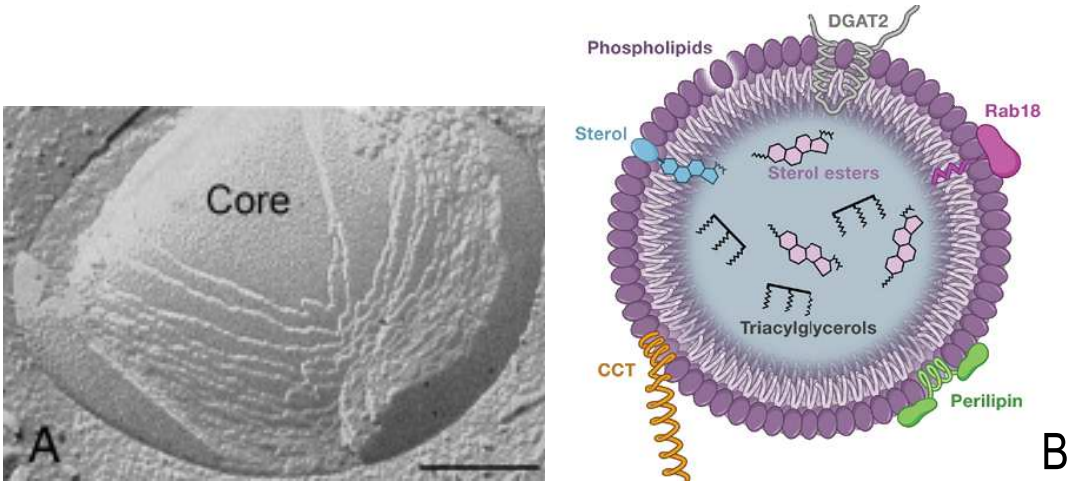

FIGURE 4. The Lipid Droplet in adipocyte. (A) Freeze fracture technique revealed LDs composed by several layers, suggesting distinct mechanisms by which TAG may be esterified (Adapted from Robenek et al. 2005). (B) Illustration of a LD with its main components, note that perilipin just localizes in LDs in adipocytes (Adapted from Krahmer et al. 2009).

Finally, important subjects of this dissertation, the PAT protein family is classically known for its relation with the LD, not only by coating LDs but also by being present in the core of this organelle (Robenek et al. 2008). In fact, Londos and colleagues stated that this group of proteins covers up to 20% of the LD monolayer in adipocytes (Londos et al. 1999). Ten years later, Wang and his colleagues further demonstrated the dynamic, non static position of PATs in the monolayer (Wang et al. 2009). It should be further noted that at least in adipocytes, different sized LD exhibit different PAT proteins (Walther & Farese 2008).

3.2 Biogenesis and development

The origin of LDs in mammalian cells is still largely speculative and especially mysterious in the poorly studied and architectonically complex skeletal muscle cell. If in prokaryote cells LDs seem to be originated from the plasmalemma, in the eukaryote cell this hypothesis is strongly challenged by LDs being originated in the ER (Walther & Farese 2008). Nevertheless, most literature facts and theories here reported are based in adipocyte research and it should be kept in mind that cell biology of skeletal muscle may not be completely analogous.

The fact that different caveolins were found in intracellular LDs actually strengthens the possibility of LDs being originated in the plasma membrane (Brasaemle et al. 2004; Liu et al. 2004; Rajendran et al. 2007), especially when increased plasma FFA led the same caveolins to be decreased in the plasma membrane and Golgi and increased in LDs (Pol et al. 2005). However, even though it was never clearly demonstrated, the most alluded belief is that ER is the source of LDs (Walther & Farese 2008; Krahmer et al. 2009).

The main restraint in explaining the source of LDs lies on their membrane composed of a phospholipid monolayer instead of a bilayer like other organelles, thus, the most accepted models rely on TAG synthesis and accumulation within the intra leaflet space of ER bilayer membrane, between the hydrophobic sides of the cytosolic and lumen leaflets of the ER membrane (Figure 5). Many model variations further speculate on the precise mechanism of LD biogenesis, from the possibility of LDs budding off like vesicles to the possibility of never completely leaving the ER (Martin & Parton 2006; Ducharme & Bickel 2008; Fujimoto et al. 2008; Olofsson et al. 2008; Walther & Farese 2008; Guo et al. 2009; Murphy et al. 2009). Nevertheless, both the presence of LDs next to lipid synthesis sites like mitochondria-associated membranes (MAM), plus the “eggcup” phenomenon (Appendix I) where the ER is shown to envelop LDs without any membrane fusion, together suggest that LDs may be born in the ER but may very well

become independent and mature elsewhere in association with different organelles (Vance & Moldave 2003; Robenek et al. 2008; Walther & Farese 2008).

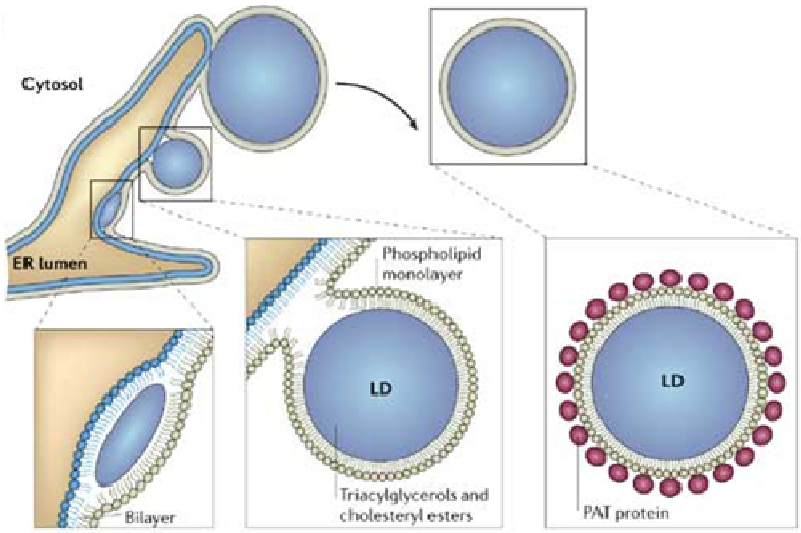

FIGURE 5. Principal model for Lipid Droplet Biogenesis. TAG accumulates in intra-leaflet space of ER, eventually generating phospholipid monolayered LDs. After birth, this organelle is ready for cellular life under regulation of PAT proteins (Adapted from Martin & Parton 2005).

Lipid droplets are dynamic organelles outlined by different sizes depending on the metabolic circumstances. Thus, LD development is a pertinent issue in literature with important implications in cell biology. Due to the presence of DGATs in the LD surface, TAG esterification has been questioned to occur in LDs themselves besides in the ER alone, which could mean LD growth independent from the ER (Wolins et al. 2006; Walther & Farese 2008). Moreover, the presence of phospholipid synthesising enzyme CCT seems to support droplet growth without a connection to ER (Guo et al. 2009).

Precise mechanisms by which this organelle grows or gets smaller during its maturation and development are still under debate. For better understanding of the main models, reading the work of Fujimoto and his colleagues is recommended (Fujimoto et al. 2008). The main points are here resumed in Figure 6.

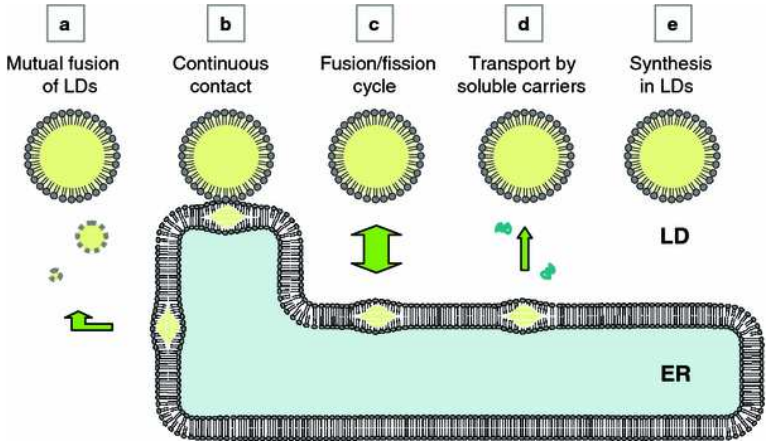

FIGURE 6. Possible mechanisms for Lipid Droplet growth. (a) By continuous fusion with other LDs. (b) ER permanent ester feeding. (c) Dynamic ER association, undergoing fission and fusion according to needs. (d) Soluble agents bringing lipid esters to LDs. (e) Esterification occurring within LDs (Adapted from Fujimoto et al. 2008).

In addition, research has been pointing to the possibility of LDs travelling along and coexisting with both ER and microtubules together (Figure 8), allowing different droplets to fuse with aid of SNARE proteins (Figure 7) (Bostrom et al. 2005; Goodman 2008; Olofsson et al. 2008; Walther & Farese 2008; Murphy et al. 2009). Moreover, LDs were shown to be transported towards both the minus-end and plus-end of microtubules by dynein and kinesin motor proteins (Welte et al. 2005; Walther & Farese 2008).

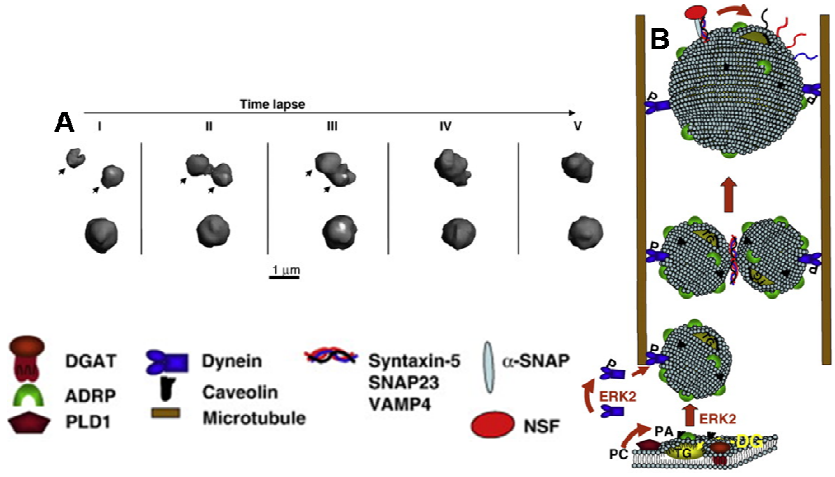

FIGURE 7. Lipid Droplet undergoing fusion. (A) LD fusion monitored with confocal microscopy. (B) ERK2 is required to phosphorylate motor protein dynein, allowing LDs to transfer on microtubules. This allows long-distance transport and fusion of LDs in the cell. Fusion is catalyzed by SNAREs (SNAP23, syntaxin-5 and VAMP4) (Adapted from Olofsson et al. 2008).

3.3 Distribution and functions

Now that we know how lipid droplets exist, it is time to better understand this organelle's main roles within the cell. Once again, most reported research is conducted in adipocytes and different cells other than skeletal muscle fibers. The adipose tissue cell is repeatedly demonstrated to have one or few major droplets in the centre while small LDs tend to locate more peripherally (Murphy 2001; Wolins et al. 2006).

One immediate thought concerning possible functions of LDs, is the obvious supply of FA for energetic purposes. Indeed, hydrolyzed FAs from LDs serve for mitochondrial β-oxidation (See 2.3.2). In fact, the LD-mitochondrion association was shown to be as proximal as 6-10 nm, suggesting functional coupling between both organelles (Sturmey et al. 2006). Expectedly, such an association is significantly increased after exercise in dog, goat and also human skeletal muscle (Vock et al. 1996; Tarnopolsky et al. 2007). These significant organelle relocations are more easily understood if one remembers the demonstrated interaction between LDs and microtubular motor proteins (Figure 7). The later not only allow LDs to travel at different and relatively high speeds throughout the cell, but also seem to be needed for LDs to undergo lipolysis (Murphy 2001; Bostrom et al. 2005; Welte et al. 2005; Murphy et al. 2009).

Consecutively, if LDs undergo lipolysis for energy production, they are also involved in FFA storing mechanisms. However, the function of storing lipids is not only for energy production or protection against lipotoxicity (See 2.3.2 and 3.2), but also for membrane biogenesis as a result of TAG hydrolysis into DAG, a component of phospholipids (Fujimoto et al. 2008). Also, due to the presence of cholesterol in LDs, it is believed that this organelle might have a role in managing cholesterol (Prattes et al. 2000).

Besides lipid storage and management, LDs also house many other biomolecules for different metabolic functions, such as protein storage and degradation, protein lipidation and also synthesis of signalling molecules (Fujimoto et al. 2008). In particular, LDs may

serve as protective storehouses to hold possibly harmful interactions between unfolded proteins and other organelles (Ohsaki et al. 2006; Welte 2007).

In addition to homotypic interactions and close association with mitochondria, LDs seem to physically interact with many other structures in which Murphy named as *heterotypic interactions* as illustrated in Figure 8 (Murphy et al. 2009). For instance, peroxisomes not only can interact but also invade LDs, and interestingly, some of LDs core contents are actually synthesized in peroxisomes (Binns et al. 2006; Bartz et al. 2007). Lipid droplets were also shown to interact with early endosomes under Rab regulation (Liu et al. 2007) and there is growing evidence of Rab18 being recruited to LDs surface during lipolytic stimulation in adipocytes (Murphy et al. 2009). Despite having semi-permanent contacts with other organelles, LDs appear to have quick "kiss and run" encounters with phagosomes in leukocytes (van Manen et al. 2005).

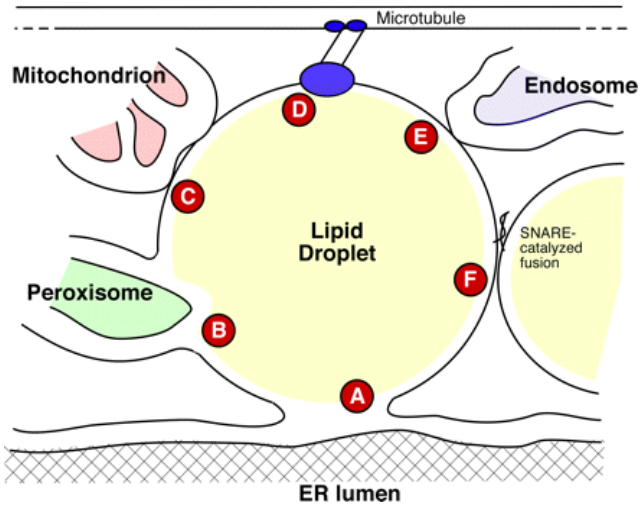

FIGURE 8. Lipid Droplet associations. (A) LD-ER physical association is still debatable if continuous, permanent or punctual. (B) Peroxisomes frequently associate with LDs and can insert pexopodia into the LD's core. (C) Mitochondrial interactions are one of the most obvious and cited in LDs. (D) LDs can travel through microtubules by motor protein transport. (E) There is increasing evidence of contact and material exchange between LDs and endosomes. (F) Homotypic interactions, LDs can fuse, probably with aid of SNAREs (Goodman 2008).

Though, still many LD functions are yet to be understood, as several proteins are associated with these new but ancient organelles, and not all these proteins are even

related to the lipid metabolism (Lay & Dugail 2009). Novel research has also started on LD interactions with bacterial and viral pathogens and promises to unveil further interesting results and applications (Guo et al. 2009).

A recently active research field, wherein this thesis wishes to contribute, concerns different possible roles of LDs depending on the PAT proteins family, i.e., it is believed that LD functions may vary accordingly to its protein composition (Walther & Farese 2008). More detailed information on these protein functions is presented in chapter 4, the PAT Proteins.

3.4 Myocyte features

Importantly, the structural design of skeletal muscle fibers is substantially different than adipocytes and most other cells. Single fibers are tightly arranged with sarcoplasmic reticulum (SR) enveloped myofibrils, which in turn, are densely composed of thick myosin and thin actin myofilaments (Ganong 1987) as seen in Figure 9. In skeletal muscle cells, LDs are frequently located in the vicinity of Z-lines (Figure 10) adjacent to intermyofibrillar (IMF) mitochondria (Morgan et al. 1969; Hoppeler et al. 1973; Tarnopolsky et al. 2007; Shaw et al. 2008). Even more intensely, these two oxidative organelles are extensively and closely present at the subsarcolemmal (SS) region, all together suggesting strategic interaction between both organelles (Hoppeler et al. 1973; Shaw et al. 2008).

Such a compact intracellular arrangement leaves little room for other organelles, especially when taking into account contractile properties of muscle, wherein the sarcomere length can change from roughly from 4.3 to 1.1 micrometers when contracted (Lieber et al. 1994). Thus, intramyocellular functionality has to be assured by a finely organized micro architecture wherein organelles, including LDs, must be physically and chemically stable enough to resist such violent mechanics.

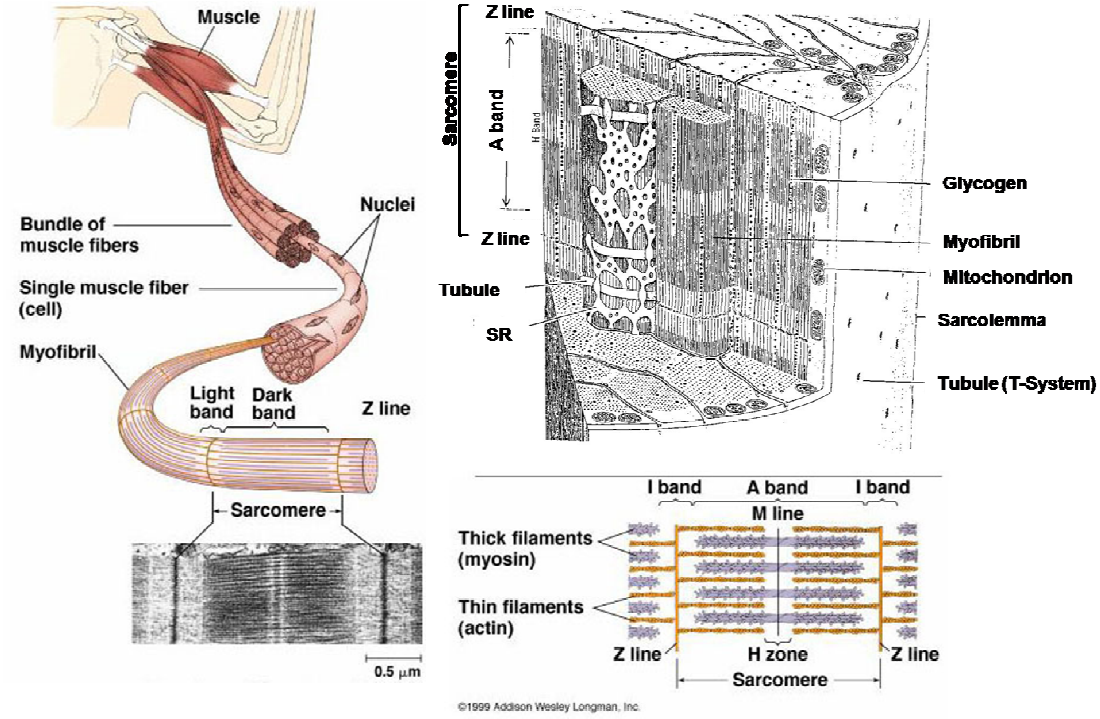

FIGURE 9. Compact architecture of the skeletal muscle cell (Adapted from Ganong 1987)

Up till now, the amazing majority of studies focusing LDs have been performed in the adipocytes, hepatocytes and others. That is, considerably few studies have focused on LDs in myocytes (Shaw et al. 2009). With high lipolytic turnover rates, muscle cells are normally characterized by having several minute sized LDs, which can be processed 250 times faster than in adipocytes (Murphy 2001). Moreover, it is known that type I fibers tend to possess more fat than type II muscle cells (Malenfant et al. 2001).

Likewise, the main proteins involved in LD regulation seem to differ according to the tissue. For example, the PAT family protein, OXPAT, is highly present in more oxidative myocytes and almost absent in white adipocytes. In opposition, S3-12, another PAT protein, seems to behave reversely (Wolins et al. 2006).

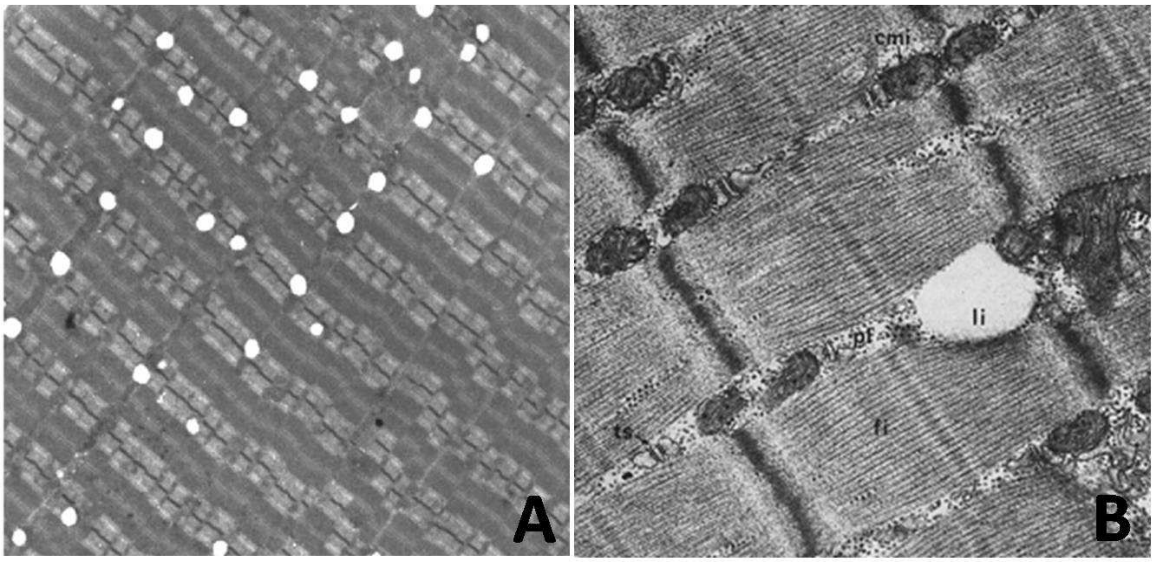

FIGURE 10. Lipid droplets in skeletal muscle. (A) Electron micrograph showing LDs in white, mostly localized adjacently to Z-lines (Meex et al. 2009). (B) Electron micrograph showing a LD (li) and intermyofibrillar mitochondria (cmi) close to Z-lines (Hoppeler et al. 1973).

Interestingly, a study performed in rat soleus muscle revealed that after muscle contraction and adrenalin stimulation, both SS and IMF IMTG content was reduced, explained by both the number and size of individual LDs (Prats et al. 2006).

Therefore, given the high rates of IMTG turnover and FA oxidation, the peculiar intracellular arrangement and biomechanics, plus the relatively few cellular studies performed so far, the skeletal muscle is an attractive tissue for carrying out research on lipid metabolism, particularly in lipid droplets, between populations with distinct lipid profiles.

4 PAT PROTEINS

Through this next chapter, the reader will further comprehend the complexity of the intracellular lipogenic/lipolytic regulation of TAG pools, known as IMTG turnover or LD dynamics. It is in the core of the lipid metabolism itself, where important lack of knowledge sustains and where a new research area arises, the PAT proteins.

In mammals, the PAT proteins family is a group of five resembling proteins which show high affinity for the LDs and other related proteins (Bickel et al. 2009). The first member, perilipin, was reported in 1990 by Londos' group, while the family was first characterized more recently by Miura and colleagues (Egan et al. 1990; Miura et al. 2002). Named after ***P****erilipin*, ***A****dipophilin* and ***T****IP47*, the PAT family shares similarity in their amino acid sequence (Figure 11), particularly in the N-terminus, also referred as PAT domain (Robenek et al. 2005). Not only sequence resemblance brings these proteins closer, also gene structure similarities suggest that they might share a common ancestral gene (Londos et al. 2005).

Each PAT protein has its distinctive role in regulating TAG in LD, they are differently distributed in diverse tissues and they have specific lipid binding properties and dissimilar subcellular localization (Wolins et al. 2006). In addition, due to their amphiphatic properties, most PATs can interact with both cytosol and LD membrane (Wolins et al. 2006). Such variability among so similar proteins suggests "sub roles" specificity in a general biological role. The later observation is reinforced when paralleling mammals' five PATs with insects' two PATs (LSD-1 and LSD-2) and fungi's MPL1, implying that greater tissue specialization in managing LDs requires more variable coating of these organelles (Miura et al. 2002; Dalen et al. 2007).

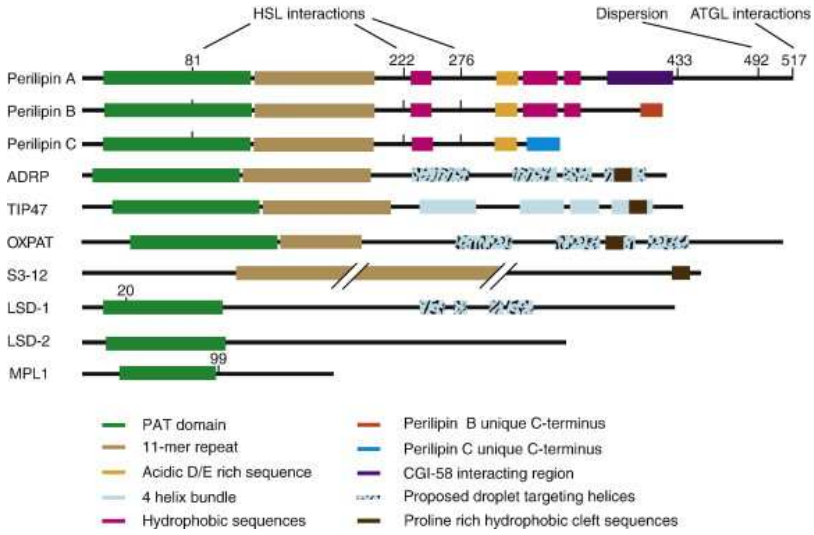

FIGURE 11. Currently studied structure and functions of PAT proteins. Many domains have been and are being identified to interact with LDs, lipases and their co-activators. Note the PAT domain, common between all proteins with exception of S3-12. (Bickel et al. 2009)

In this work only the PAT proteins present in humans are referred, with special attention to those more related with skeletal muscle. Despite the brief review on all human PATs, understandably more focus is given to OXPAT, as it is one of the main subjects of this study along with its regulated organelle, the lipid droplet.

4.1 Perilipin

Found during the late 1980's and later described by Londos and colleagues, the perilipins are LD proteins specific of adipocytes and steroidogenic cells. Moreover, perilipin exists mostly in the gigantic LDs in adipocytes and is believed to have a protective effect against TAG hydrolysis, while its total absence seems to lead to augmented leptin secretion in adipocytes and insulin resistance despite reduced body fat in mice (Londos et al. 2005; Wolins et al. 2006). To be noted, like other PATs, perilipin electrostatically associates with lipases and co-activators like HSL and CGI-58 (Wolins et al. 2006).

Nevertheless, since it is not a protein reported in skeletal muscle, little focus is given to perilipin in this work.

4.2 Adipophilin

First described by Jiang and Serrero (Jiang & Serrero 1992), *adipophilin* or *adipocyte differentiation-related protein* (*ADRP* or more rarely *ADFP*), is expressed ubiquitously among different tissues (Heid et al. 1998). Some studies referred that when not bound to a LD ADRP is unstable and is degraded (Gross et al. 2006). However, recent research on cyclists has shown through confocal microscopy that ADRP is not always colocalized with skeletal muscle LDs, wherein at least ~36% is cytosolic (Shaw et al. 2009). The same findings were further extended to adipocytes through fluorescence recovery after bleaching (FRAP) studies (Wang et al. 2009).

In 2003, mutant research on molecular properties of ADRP revealed that interaction with LD can actually occur in two different, not overlapped amino acid (aa) locations. The same study identified ADRP specific aa for targeting mitochondria (Nakamura & Fujimoto 2003). Nonetheless, besides localizing in LD membrane, ADRP as well as perilipin and TIP47 are PAT proteins already reported to occur inside the core of adipocyte LDs as well (Robenek et al. 2005).

In adipocytes and fibroblasts, ADRP was shown to associate mostly with small LDs during cell differentiation phases (Brasaemle et al. 1997; Bickel et al. 2009). In fact, several studies generally suggest ADRP to be involved somehow in the formation and development of small new LDs by coating them throughout early stages. Therefore, situations like increased FFA uptake, TAG esterification and decreased TAG hydrolysis are often positively correlated with the rise of both ADRP protein and mRNA levels (Brasaemle et al. 1997; Gao & Serrero 1999; Imamura et al. 2002; Chang et al. 2006; Bickel et al. 2009). ADRP was also shown to bind to vimentin and dynein, thus suggesting that in muscle, transport of LD and PAT occurs in microtubular systems (Meex et al. 2009).

Similarly to perilipin - but in earlier LD development stages - rather than a lipogenic effect, ADRP has a more inhibitory effect on lipolysis, acting as a shielding barrier

against TAG hydrolysis by suggested repellence of lipases and co-lipases (ATGL, HSL and CGI-58) from the LD surface (Listenberger et al. 2007; Bickel et al. 2009).

In adipocytes however, ADRP seems to have a rather weaker protective effect against lipolysis, given that it has been shown to permit elevated hydrolyzation rates both in basal and stimulated lipolysis. Furthermore, inversely to perilipin, close interaction of ADRP with HSL was observed and under basal conditions only (Wang et al. 2009). While, interestingly, in skeletal muscle ADRP colocalization with HSL increased significantly after both muscle contraction and adrenalin stimulation (Prats et al. 2006).

ADRP-deficient mice display impairment in LD formation and are resistant to diet-induced fatty liver (Chang et al. 2006), while weight loss programs seem to increase ADRP expression along with insulin sensitivity in diabetic skeletal muscle (Phillips et al. 2005). Given such findings, Phillips and others hypothesize ADRP to serve as a capturer of potentially toxic cytosolic lipids.

However like other PAT proteins, ADRP behaves in a complex manner, providing many contrasting findings. Note, for instance, Minnard and colleagues' work, where ADRP protein levels were shown to correlate positively with insulin resistance and parallel lipid contents in skeletal muscle of both T2D and BMI matched controls (Minnaard et al. 2008; Minnaard et al. 2009).

4.3 TIP47

This protein was identified first by Pfeffer laboratory and was then described as an endosomal protein involved in intracellular transport between endosomes and the Golgi complex (Diaz & Pfeffer 1998). However, such functions do not seem to be supported by recent research which increasingly strengthens TIP47 having a role as a LD coating protein (Bulankina et al. 2009). Yet, Wolins and colleagues already pointed out that TIP47's function probably is much more complex than simply shuffling between cytosol and LD (Wolins et al. 2005; Wolins et al. 2006). Moreover, by not being regulated by peroxisome proliferator-activated receptors (PPARs), TIP47 is likely the closest PAT

family member to the original common gene between all PATs (Wolins et al. 2006; Wolins et al. 2006).

TIP47 is expressed ubiquitously like ADRP and is stable both in cytosol and in LDs surface (Ohsaki et al. 2006; Bickel et al. 2009). Also, it appears that in hepatocytes and fibroblasts, within 10 minutes after oleic acid administration, cytosolic TIP47 translocates towards small non-neutral lipid containing structures, which eventually originate small neutral lipid containing LDs. Such observations led the researchers to conclude that TIP47 may have a function in LD biogenesis (Bulankina et al. 2009).

In liver, TIP47 was not detected within LDs after feeding in mice. On the other hand, after FA esterification caused by fasting, TIP47 was increasingly present in the same LDs (Wolins et al. 2001; Wolins et al. 2005; Ohsaki et al. 2006; Bickel et al. 2009). Interestingly, in skeletal muscle cells, differently from ADRP, TIP47 was observed both in LDs surface and cytosolic pools as well (Prats et al. 2006).

In ADRP deficient mice and cell culture studies, TIP47 replaces ADRP as the main PAT coating the LD, thus denoting some compensatory activity (Ohsaki et al. 2006; Sztalryd et al. 2006; Bickel et al. 2009). Reciprocally, Bulankina and colleagues also showed that in TIP47 knock-out (KO) cells, ADRP is overexpressed, suggesting compensation for the lack of TIP47. In the same study the authors observed that despite normal FA intake and TAG hydrolysis, LD maturation and growth are inhibited in TIP47 KO cells (Bulankina et al. 2009).

4.4 S3-12

S3-12 is perhaps the less studied PAT protein and it is most differentiated by having the lowest sequence of homology to the other PATs and by not having a PAT domain (Meex et al. 2009). Like OXPAT, S3-12 is stable in cytosol and coats LDs after FFA loading and being seen in the surface of newly formed LDs (Wolins et al. 2003).

This protein is expressed mainly in tissue specialized in fat storage, like the white adipose tissue (WAT) and not so much in skeletal muscle or heart (Wolins et al. 2003; Wolins et al. 2006; Dalen et al. 2007). Due to these facts, relative little attention is given to S3-12 in this skeletal muscle focused thesis.

4.5 OXPAT

Firstly referred as *PAT-1* (Miura et al. 2002), *OXPAT* is synthesized in cytosol by PPAR induction and is likely the last protein of the PAT family (Wolins et al. 2006). Several different groups claimed the first characterization of OXPAT as a PAT protein, thus giving it different designations, as it is also referred as *MLDP* (myocardial lipid droplet protein) (Yamaguchi et al. 2006); *Mldp* (muscle lipid droplet protein) (Granneman et al. 2009) and *LSDP5* (lipid storage droplet protein 5) (Dalen et al. 2007). This last reference is stated by the authors as being a comparable but different protein from OXPAT. Yet, recent research groups have treated it as being the same protein (Granneman et al. 2009). In this review, however, all these designations will be referred as *OXPAT*, since it belongs to the PAT family and it is present and expressed mostly in highly oxidative tissues (Wolins et al. 2006).

OXPAT is extensively expressed in tissues with high oxidative profile like the heart and brown adipose tissue (BAT), but is also seen in skeletal muscle, especially skeletal muscle with high oxidative capacity (Wolins et al. 2006; Yamaguchi et al. 2006; Dalen et al. 2007) like the IMTG-enriched and vastly type I fiber-composed *soleus* muscle containing mostly type I fibers (Vermathen et al. 2004).

Interestingly, in mice OXPAT and S3-12 are inversely expressed depending on the tissue, i.e., where one of these proteins is heavily expressed, the other one is timidly doing so and vice versa. For instance, in opposition to OXPAT, S3-12 is greatly expressed in WAT and considerably in quadriceps muscle but poorly expressed in the liver (Wolins et al. 2006). OXPAT is expressed in all tissues much like PPARα, i.e., mostly in red muscle, liver and heart (Dalen et al. 2007). This suggests again, that different members of the PAT proteins have different roles in different tissues. In fed

mice, like TIP47, OXPAT was not detected in hepatocyte LDs and its levels were increased after fasting-induced esterification occurred (Wolins et al. 2006). The same observations had been extended to cardiac muscle by Yamaguchi and his colleagues' weeks before in 2006 (Yamaguchi et al. 2006).

Not only fasting conditions, but also lipid loading enhances LD formation and OXPAT coating (Dalen et al. 2007). In fact, after oleate loading, OXPAT starts coating LDs, wherein it increases the period of time when rapid TAG storing occurs, thus resulting in bigger LDs (Wolins et al. 2006; Granneman et al. 2009). However, such enhanced TAG storing in LDs is not performed by OXPAT in lean cultured adipocytes (Wolins et al. 2006). In adipocytes, OXPAT seems to be recruited towards LDs proportionally as ADRP does. Still, OXPAT does not colocalize with bigger LDs where perilipin is strongly present (Yamaguchi et al. 2006). At the same time, OXPAT expression associates to increased lipolytic activity through enhanced FA uptake rates and raised levels of oxidative catabolic enzymes such as cytochrome c oxidase 4 (COX4) and several FA dehydrogenases (Wolins et al. 2006).

OXPAT also increases coating of LDs in PPARα overexpressed mouse muscle and the protein levels decrease in PPARα KO mice. So, PPARα appears to be required for the full expression of OXPAT (Wolins et al. 2006). The same researchers found this protein more expressed in fasting and insulin resistance, which are inducible metabolic circumstances for activation of PPARα and FA oxidation, but neither of these metabolic circumstances lead to OXPAT expression in liver of PPARα KO mice (Wolins et al. 2006). Contrary findings were reporter by Dalen and colleagues, who found that fasting induces OXPAT mRNA in liver even in the absence of PPARα (Dalen et al. 2007). Nevertheless, due to its PPAR induction, OXPAT may be an important molecule for selecting the fuel for ATP production, probably by intervening and permitting hydrolysis to occur in the LDs surface (Sugden et al. ; Wolins et al. 2006).

In mouse cardiomyocyte, OXPAT colocalizes with ADRP in some LDs, both proteins targeting towards small LDs. However, these proteins were also found individually on some LDs and interestingly, OXPAT was found present in averagely bigger LDs than

those where only ADRP was found (Granneman et al. 2009). Significantly and in total opposition to ADRP, OXPAT was demonstrated by fluorescence resonance energy transfer (FRET) to extensively colocalize with CGI-58, an activator protein for ATGL, suggesting functional activity between CGI-58 and OXPAT, thus directly highlighting the latter as a regulator for TAG hydrolysis (Lass et al. 2006; Granneman et al. 2009).

In absence of OXPAT, CGI-58 does not specifically target LDs in adipocytes but perinuclear membranes instead. Nevertheless, in the presence of OXPAT, CGI-58 is highly targeted towards LDs where OXPAT already is (Granneman et al. 2009). Besides occasional cytosolic colocalization, CGI-58 binds and interacts with OXPAT only in LD surface. Moreover, unlike ADRP, the interaction between OXPAT and CGI-58 is augmented almost 3 times with oleic acid treatment (Granneman et al. 2009). Furthermore, pharmacological inhibition of TAG synthesis led to suppressed interaction between OXPAT and CGI-58 (Granneman et al. 2009). Together, this data paradoxically suggests that OXPAT is closely involved in lipolytic activity, being however dependent of lipogenic phenomena to efficiently carry on lipolytic actions.

Furthermore, mutations of CGI-58 which are linked to neutral lipid storage disease - or CDS - in humans are also preventing this protein to interact with OXPAT, leading to lower effect upon ATGL activity (Granneman et al. 2009). Additionally, OXPAT binds to ATGL in the absence of CGI-58, but ATGL does not bind to CGI-58 in the absence of OXPAT (Granneman et al. 2009). Moreover, cells with ATGL expression but without OXPAT moderately accumulate LDs, but ATGL co-expressed with CGI-58 in absence of OXPAT occludes nearly all LD accumulation, and in cells containing ATGL and OXPAT well defined clusters of LDs were observed (Granneman et al. 2009).

All these observations suggest that the interaction of OXPAT with LD surface increases its affinity for CGI-58. The experiments made by Granneman and colleagues in 2009 demonstrate that OXPAT manages the physical and functional interface of CGI-58 and ATGL. Outlining, OXPAT seems to closely lead CGI-58 towards the LD surface, wherein ATGL activity is regulated (Granneman et al. 2009).

Apparently, at least in adipocytes, OXPAT has a stronger protective effect against lipolysis when comparing with perilipin since even PKA activation failed to increase basal lipolysis when OXPAT involves LDs (Wang et al. 2009). The same research observed that OXPAT lively interacts with HSL in both basal and stimulated lipolysis (Wang et al. 2009).

In normal circumstances, OXPAT is especially expressed in the heart and up-regulated by PPARα or fasting. Therefore, it is probable that OXPAT preferentially targets LDs of cells with elevated rates of lipolysis, assisting then, in the oxidation of intracellular TAG (Yamaguchi et al. 2006).

Perhaps at this stage, it is safe to state that the fate of TAG within the LD is under close judgement of OXPAT, a protein that is quite temperamental as it is differently expressed between physiological and pathophysiological conditions. A dilemma is settled, is OXPAT a lipolytic or lipogenic protein? Noticeably, this is a question that cannot be answered lightly. While it seems to be involved in key lipolytic mechanisms as it gears up LDs for TAG hydrolysis and as it indulges oxidative enzymes to perform, OXPAT also seems pretty much to enjoy TAG esterification by being present in the formation and nourishment of LDs. Most likely, the best way to interpret OXPAT is by facing it as a booster, a catalyser of the cell's entire lipid metabolism, accelerating TAG synthesis as it accelerates its hydrolysis. Still largely unsolved, OXPAT and the PAT family in general, are puzzling parts of the complex machinery that maintains cellular lipid metabolism.

4.6 Relevant models and facts

All PAT proteins seem to move around the LD phospholipid monolayer surface and are not rigidly attached to it (Wang et al. 2009). Due to their protein recruiting capacity, the PAT family seem to regulate the access of lipases and their activators into LD (Wolins et al. 2006). However, lipase binding to PAT proteins, does not seem to be enough to

dictate the rate of lipolysis, as Wang and colleagues demonstrated for HSL in adipocytes (Wang et al. 2009).

According to Wolins and coworkers, OXPAT may play a role in packaging lipids for short-termed hydrolysis while S3-12 mediates lipid storage for long-termed hydrolysis. Additionally, OXPAT could work by displacing other PATs from LDs. The same group suggests that by boosting FA oxidation, OXPAT may serve as a "feedfoward" mechanism to fight metabolic states like fasting, IR or the excessive cytosolic FFA (Wolins et al. 2006).

Finally, an attractive model of the ER as a lipid "superhighway" has been discussed, where lipids could efficiently travel between several organelles and where LDs could serve as network storages, being able to deliver, fuse and share its contents accordingly to the system needs (Murphy et al. 2009).

5 SKELETAL MUSCLE LIPID METABOLISM IN INSULIN RESISTANCE

5.1 Metabolic overview

The average man body weight is comprised 40% of skeletal muscle and since this organ is responsible for production of movement it is highly prepared for processing chemical energy within its metabolism. Nonetheless, the same organ is a major processor of energy metabolism even during rest. It has been discussed if and how the misuse or dysfunction of skeletal muscle fuelling can lead to development of OB or T2D states or instead, if these diseases are merely a cause for muscle metabolic dysfunction rather than a consequence of it. The association between OB and T2D populations and IR has long been known, especially when concerning high blood glucose levels. Lately however, much focus has been placed on lipid metabolism besides glucose avaiability, not only in the competition and selection between both fuel natures, but also in the cellular and molecular implications that unregulated lipid metabolism have in IR (Ehrman 2003; Blaak 2005).

Initially, the relation between intramyocellular lipids (IMCL) and IR was considered to be linear, wherein elevated IMCL contents paired the increase in IR, thus explaining alone the development of IR in OB and T2D. However, researchers soon dismantled this dogma when they repeatedly demonstrated that endurance athletes – which are highly IS individuals – had even higher IMCL contents than highly IR individuals like T2D (Goodpaster et al. 2001; van Loon et al. 2004; van Loon & Goodpaster 2006; Moro et al. 2008). Such evidence switched research attention from quantitative, towards qualitative aspects of IMCL regulation (Figure 12).

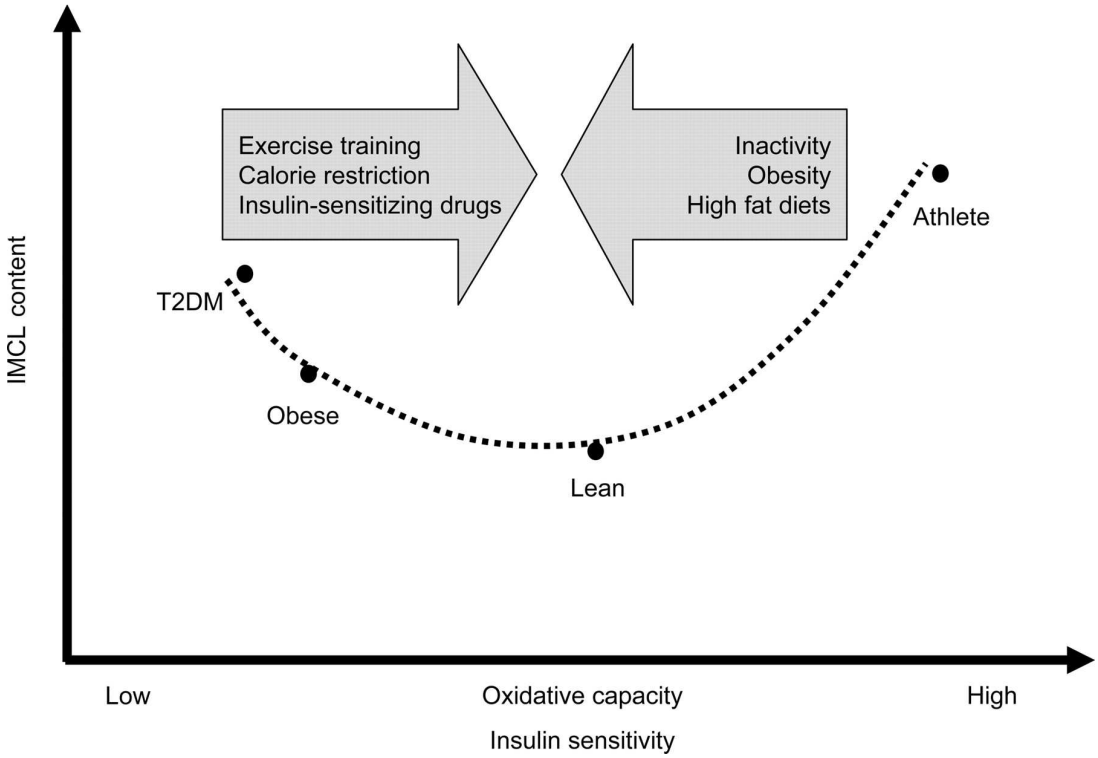

FIGURE 12. Model for the relationship between IMTG content, oxidative capacity and IS in humans. Gray arrows represent directional influence of environmental factors (Moro et al. 2008).

It is still questionable how exactly IMTG might be causing IR in OB and T2D. However, the most believed model and proved to some extent, begins by justifying this connection due to elevated cytosolic lipid by-products, such as DAGs and ceramides. These by-products can be originated by inefficient and uncoordinated TAG hydrolysis in LDs along with impaired mitochondrial oxidative work (Moro et al. 2008). The accumulation of DAGs and ceramides in cytosol seems to initiate IR signaling cascades, resulting in insulin receptor substrates (IRS) inhibition and protein kinase B (PKB) deactivation (Machann et al. 2004; Bruce et al. 2007; Watt 2009). Ultimately, these events lead to a decrease in GLUT-4 translocation towards the sarcolemma. Consequently, glucose transport is impaired and results in hyperglycemia (Figure 13).

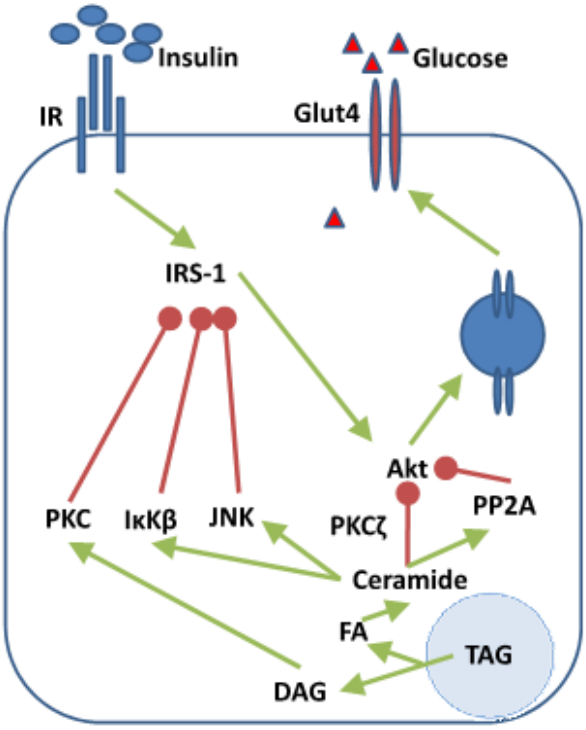

FIGURE 13. Fatty acids mediators on insulin resistance. DAG results in activation of several PKC isoforms that may induce serine phosphorylation of IRS-1. FA hydrolyzed from TAG are used for de novo ceramide synthesis. Ceramide activates protein phosphatase 2A (PP2A), which dephosphorylates and deactivates Akt. By activating PKCζ, ceramide also prevents Atk translocation. Ceramide also activates JNK and IκKβ, inhibiting insulin signal transduction by serine phosphorylation of IRS-1 (Watt 2009).

It is known that both OB and T2D individuals have impaired capacity for utilizing lipids as energy, as precise molecular events involved in such impairments have been extensively researched lately and will be here briefly mentioned. Among these are for example, FA transport capacity, potential for beta-oxidation and oxidation capacity (Blaak 2005).

5.2 Intracellular lipid transport

Many times, IS was tried to be correlated with FFA transport related variables, although, many results remain unclear. Human T2D subjects were shown to have lesser amounts of FABP3 in *vastus lateralis* muscle. In addition, T2D and OB also revealed impaired

plasma FFA uptake and oxidation during forearm balance technique (Kelley & Simoneau 1994; Turpeinen et al. 1999; Blaak et al. 2000; Mensink et al. 2001).

However, a different study in abdominal muscle, when compared to lean controls, T2D and OB showed higher rates of FFA influx, higher rates of FA esterification and increased levels of sarcolemmal CD36, all being associated with increased levels of IMTG but unaltered FFA oxidation rates (Bonen et al. 2004). Moreover, endurance trained men skeletal muscle revealed higher concentrations of FABPpm than in non-trained subjects' (Kiens et al. 2004).

In general, IR populations seem to be somewhat metabolically impaired when comparing to healthy IS populations, but the inconsistency of many results suggests that FFA transportation might not be the key point for developing IR. Conversely, it may be an upstream phenomenon rather than a causable issue.

Nevertheless, genetic predisposition of FA transporters has been linked to the development of metabolic diseases. For instance, FABP3 polymorphism was shown to associate with the risk of developing T2D (Shin et al. 2003). While CD36 gene seems to associate with deficient lipid metabolism and hypertriglyceridemia (Aitman et al. 1999).

5.3 Efficiency of TAG hydrolysis and β-Oxidation

Both T2D and OB have been extensively associated with impaired oxidation rates. Many believe that such impairment may be the crucial axis connecting by-product accumulation and the development of IR (Kelley & Simoneau 1994; Machann et al. 2004; Blaak 2005). However, some still discuss that the reduced oxidative enzyme capacity in T2D muscle is probably due to lower percentage of type I fibres (Oberbach et al. 2006).

In OB skeletal muscle of mice, high IMTG levels are logically followed by low ATGL protein levels while ATGL mRNA however, is higher than in lean controls. This

suggests ATGL is considerably downregulated somewhere after being transcribed into RNA but before protein translation (Meex et al. 2009). Furthermore, ATGL knockout mice show elevated and excess intracellular TAG content in the form of LD. ATGL over-expression in skeletal muscle led to increased intramyocellular content of DAG and ceramide. Unbalanced coordination between ATGL and HSL activities might be one of IR's geneses by excessive cytosolic lipolysis, generating by-products as DAGs and ceramides. However, such has not been demonstrated in T2D subjects yet. Here, PAT proteins may be of crucial importance since they were shown to differently interact and regulate these lipases (Meex et al. 2009).

FA oxidation rates are higher in SS mitochondria when compared to IMF mitochondria in gastrocnemius (Koves et al. 2005). Expectedly, SS mitochondria electron transport activity was shown to be lower in T2D, followed by OB when compared to healthy controls. However, IMF mitochondria electron transport activity was similar between T2D and OB but decreased when compared to controls (Ritov et al. 2005). Besides impaired mitochondrial function, T2D have smaller sized mitochondria in vastus lateralis than OB and lean controls (Kelley et al. 2002). Nevertheless, it is still unknown if mitochondria inefficiency is a cause for IR, or if it is an adaptational consequence of the same IR and/or physical inactivity (van Loon & Goodpaster 2006; Moro et al. 2008).

Reduced oxidation in OB and T2D may also be caused by impaired FA transport into mitochondria via carnitine (Simoneau et al. 1995). However, in skeletal muscle of IR and OB rodents, elevated rates of infused intramuscular FFA did not seem to impair mitochondrial function, in fact, it increased the oxidation capacity (Turner et al. 2007). Such leads some authors to consider that reduced FA oxidation in skeletal muscle of T2D is likely genetic (Gaster et al. 2004). However, taken all together, this only suggests that smaller and impaired mitochondria in OB and T2D are not just simply due to increased intramuscular FA.

Perhaps, other poorly studied intervenients in skeletal muscle lipid metabolism play a more central role in IR signaling, as the PAT proteins for instance.

5.4 Lipid droplets and PAT proteins

Just like physical activity, OB and T2D seem to increase total IMTG, which positively correlates with percentage of body fat, mitochondrial decreased size and function (Hulver et al. 2003; Goodpaster & Wolf 2004; Schrauwen-Hinderling et al. 2006; Schrauwen-Hinderling et al. 2007). On the other hand, endurance training equally increases total IMTG but also the number of LD, size of mitochondria, LD colocalization with mitochondria and therefore, also FA oxidation (Tarnopolsky et al. 2007). Interestingly, T2D have shown bigger LDs than controls, while endurance exercise programs cause smaller LDs (He et al. 2004). Moreover, Phillips and colleagues found a direct correlation between decreased size of LDs and IS (Phillips et al. 2005).

Therefore, it has been suggested that populations with enhanced aerobic function such as endurance athletes, may have a higher turnover of IMTG, in other words, increased usage/restoration cycle of IMTG (Moro et al. 2008). Due to physical inactivity, sedentary individuals are more unprotected from lipotoxicity, as they have a decreased IMTG turnover which tends to lead towards lipid peroxidation and possibly trigger IR (Russell 2004). Such disclosure led to the problem that maybe IR is not so much about the amount, but rather the quality and regulation of the TAG depots in the form of LDs. Moreover, such observations were extend into groups of sedentary individuals subjected to exercise intervention, suggesting that increased IMTG might very well be an beneficial adaptation as well (van Loon & Goodpaster 2006). However, these results were not always found by other groups when using biochemical methods rather that microscopy or spectroscopic methods (Bruce et al. 2003).

Nevertheless, as known, type I fibers are more oxidative and have greater IMTG contents when compared to type II fibers. Knowing that athletes have higher percentage of type I fibers, it might offer an explanation for total IMTG differences between these populations. According to van Loon and coworkers however, such does not seem to occur, as higher IMTG in athletes is not totally dependent on fiber type distribution (van Loon et al. 2004).

The PPARs – principal PAT inducers – have been previously associated with reduced myocardial infarct size, ischemia prevention and even with reduced risk of developing T2D (Stumvoll & Haring 2002; Wayman et al. 2002). Hence, PAT proteins became a focus of IR etiological research.

OXPAT expression in non-diabetic human WAT correlates negatively with BMI and positively with IS, wherein it was suggested to be decreased in OB due to IR (Wolins et al. 2006). However, later on, OXPAT and ADRP protein levels in *vastus lateralis* were shown invariant between T2D and BMI-matched controls and were also shown to increase along with IR and IMCL content. (Minnaard et al. 2008; Minnaard et al. 2009). Additionally, no significant differences were find in *vastus lateralis* ADRP expression between non-diabetic OB and diabetic OB (Phillips et al. 2005).

However, despite the ambiguous analysis on protein content, there are indeed reports wherein PAT proteins KO led to unregulated LD metabolism, including uncontrolled LD fusion, increased lipase access to LDs, increased lipolysis and alteration of pathways concordant with IR signaling. Consequently, ATGL KO was able to correct the IR signaling caused by PAT KO. Moreover, after microscopy studies showed protein terminal association with mitochondria, ADRP has been pointed as facilitator of FA delivery to this organelle (Nakamura & Fujimoto 2003; Phillips et al. 2005). Therefore, one can infer that PAT proteins have a direct role upon LD regulation and a consequent role in insulin signaling (Phillips et al. 2005; Bickel et al. 2009). Perhaps, the limitation factor of PAT proteins in IR populations is in post translational events, as impaired targeting for example.

Further physiological function studies of PAT family members, should not only contribute to the growing knowledge concerning LDs, but also to better understand lipid metabolism as a whole, helping to fight abnormal lipid accumulation originated disorders.

6 PURPOSE AND HYPOTHESES OF THE STUDY

From among the issues identified in literature, the present work is centered on two raised problems. The first one, not fully explained yet, relies on the repeatedly reported paradox of similar IMTG quantities between IS and IR individuals (Goodpaster et al. 2001). Secondly, as discussed, the ratio between IMTG synthesis/storage and IMTG lipolysis coped with cellular necessity is a complex but crucial machinery for establishing lipid status and likely IR. Proteins from the PAT family are intimate managers of this machinery, wherein the question arises, how are the PAT proteins coordinating IMTG as a selected fuel in different population skeletal muscle? OXPAT spots out from the rest of the PAT family by its high expression in highly oxidative tissues and by being proposed to pack TAG for immediate hydrolysis (Wolins et al. 2006).

Thus, given both the importance and subcellular location of IMTG hydrolysis and FA oxidation and given the interesting referred paradox, the purpose of this study is to assess LD and OXPAT intracellular distribution between different insulin sensitivity key groups and therefore, better understand the LDs and OXPAT role and behaviour in skeletal muscle lipid metabolism.

We hypothesise that, despite the paradoxal similarity in increased amount of IMTG, the differences in lipid metabolism efficiency between IS and IR populations, can be seen through different intramyocellular geography of LDs and OXPAT. We further hypothesise that similarly to what occurs with mitochondria, increased SS OXPAT might be related to improved IMTG turnover and consequently improved IS (Figure 14).

We believe that different patterns will arise from different groups:

1- Insulin sensitivity associates with OXPAT and LD peripheral distribution.
2- Insulin sensitivity associates with degree of peripheral OXPAT colocalization with LDs.

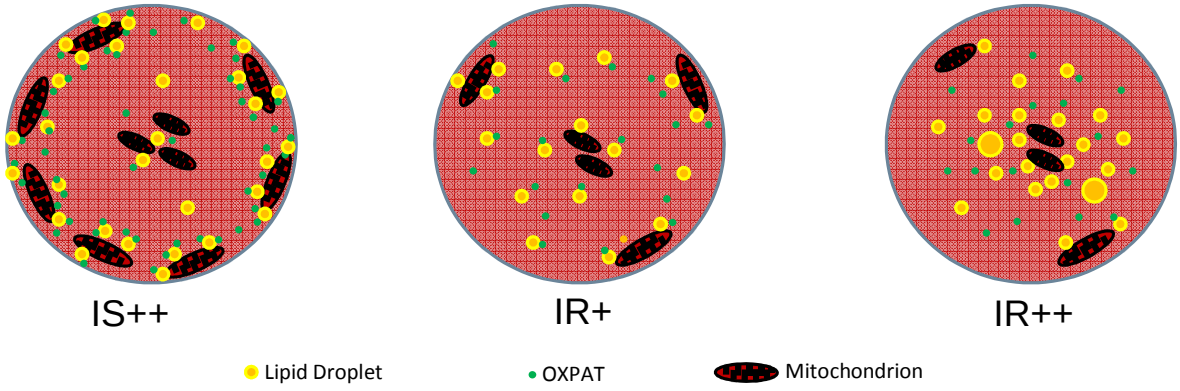

FIGURE 14. Illustration of proposed hypotheses. Insulin sensitive populations (IS) would have more peripheral LDs, OXPAT and their colocalization. More insulin resistant populations (IR) would have more internalized and uncolocalized LDs and OXPAT.

Besides the proposed numerical comparisons between groups, it is a complementary purpose of this study to further analyze, descriptively, the general human intramyocellular relative localization of LDs, OXPAT, mitochondria and myosin heavy-chain.

7 METHODS

7.1 Subjects

Subjects (males, 39-67 years) were divided into three different study groups according to their health status and weight. Group T2D consisted of subjects with type 2 diabetes mellitus (n= 10). In addition, diabetic subjects had other diseases related to diabetes mellitus, such as high blood cholesterol, and elevated or high blood pressure. Most of the diabetic subjects were also obese.

In the group OB were non-diabetic obese subjects (n= 8). Some of the obese subjects had metabolic syndrome, because they had elevated blood glucose level and other symptoms related to the disease. For the groups T2D and OB, the criterion set for obesity was a body mass index (BMI) over 30kg.m^{-2}.

Lean, non-diabetic subjects were in group of lean controls (LC) (n= 7). Subjects were considered lean if their BMI did not exceed 26 kg.m^{-2} or if their fat percent was in normal range (10-20%).

Subjects were recruited by public advertisements. Before attending to measurements, the subjects underwent a physical examination performed by a physician. If the subject had difficult injuries in spine or joints that could inhibit exercise, or high risk of heart attack, he was excluded from the study. Subjects were volunteers and they were informed about the study and risks involved with the measurements. Written informed consent and health questionnaire were obtained from all volunteers before starting any measurements. Study plan was approved in the ethical committee at the University of Jyväskylä.

Muscle biopsies utilized for the present study were previously obtained from subjects from different earlier projects. During 2008, the referred subjects were studied for different purposes, being then measured for diverse anthropometric variables such as body weight and BMI. More measurements were performed for bioimpedance variables as body fat percentage (FAT%), body fat mass (FM) and body free fat mass (FFM). Blood variables were also assessed, like total cholesterol (TCHOL), high-density lipoproteins (HDL), low-density lipoproteins (LDL), triacylglycerol (TAGemia) and glucose (Glycemia). Furthermore, maximal oxygen consumption (VO_2max) was directly measured in 20 of the studied subjects (10 T2D + 8 OB + 2 LC), being this variable only indirectly estimated in the remaining 5 CO subjects. The assessed values can be briefly consulted in Appendix II or more thoroughly in the cited work (Kivistö 2008).

7.2 Muscle biopsy

Prior to collecting the muscle biopsy, subjects retained from physical exercise for 48 hours. The skin area, where the biopsy would be taken, was shaved and cooled with ice for about ten minutes before local anaesthetic (Lidocain 20 $mg.ml^{-1}$ c. adrenalin) was injected. The muscle biopsy was taken with the Bergström biopsy needle from the vastus lateralis muscle approximately 15 cm above the patella tendon and 2 cm away from the fascia. The samples were covered with Tissue-Tek and frozen immediately in isopentane cooled with liquid nitrogen. The samples were stored at -80ºC until further analyses.

7.3 Immunocytochemistry

Sectioning and Fixing. From the muscle biopsies, 5µm cross and longitudinal sections were taken in a cryostat at -25ºC (Leica CM 3000, Germany). Sections were collected in 13mm round coverslips and immediately fixed in 4% paraformaldehyde for 15 minutes at RT.

Negative Controls. Negative controls were performed by staining without primary antibody, without secondary antibody and without primary and secondary antibodies.

Blocking and Primary Antibody incubation. After 3x5 minutes PBS washing, the sections were blocked with 3% BSA for at least 30 minutes and then washed briefly with PBS. All primary antibody dilutions were made in 1% BSA as seen in Table 1, and incubated for 1 hour in dark/moisture at RT. Mitochondria labelling experiments were subjected to 0.05% saponin permeabilization in all steps mentioned in this paragraph.

TABLE 1. Primary antibodies used and respective dilutions in 1%BSA.

Puropose	α-gene	Species	Code	Manufacturer	Dillution
Fast Myosin	Fast Myosin Heavy-chain	Mouse	MY32	SIGMA	1:50
Mitochondria	COX subunit IV	Mouse	A21347	Invitrogen	1:50
OXPAT	OXPAT	Guinea Pig	GP31	Progen	1:200
Fast Myosin	IgM	Mouse	4.519	DSHB	1:10

Secondary Antibody and LipidTox incubation. Next, the samples were washed 3x15 minutes with PBS before incubated with secondary antibodies in 1% BSA for 1 hour in dark/moisture RT accordingly to Table 2. A 3x10 minutes PBS washing followed, till this point all steps were still performed with 0.05% saponin. Lipid Droplets were then stained with LipidTOX™ Green (FITS, Molecular Probes) after neutral lipids, using a 1-100 dilution in PBS for 30 minutes in dark RT. Excess dye was removed with 2x 1 brief drop of PBS right before mounting.

TABLE 2. Secondary antibodies used and respective dilutions in 1%BSA.

Puropose	α-species	Species	Code/nm	Manufacturer	Dillution
Fast Myosin	Mouse IgG	Donkey	AMCA 346	Jackson ImmunoResearch	1:50
OXPAT	Guinea Pig IgG	Donkey	594	Jackson ImmunoResearch	1:50
Mitochondria	Mouse IgG	Donkey	546	Jackson ImmunoResearch	1:50
Fast Myosin	Mouse IgM	Donkey	488	DSHB	1:50

Mounting. The mounting medium utilized was Mowiol with 2.5% DABCO for anti-fading effects. The medium was left to dry for at least 1 hour in the dark at 4C°. All

samples for quantitative purposes were observed under microscopy within 12 hours after mounting in a glass slide.

7.4 Epifluorescence microscopy

Raw data collection was performed with widefield technology by an *Olympus BX50 BX-FLA*. Images were collected using a 40x objective. Fluorphores were excited with a mercury lamp, through U-MWU, U-MWB and MWG excitation cubes.

Preformed with the software *AnalySIS 5.0* (Soft Imaging Systems), fluorescent signal coming from the samples was gray-scale recorded by a *ColorViewIII* (Soft Imaging Systems) camera. As much as possible, similar exposure times were used when collecting images.

7.5 Image processing and raw data extraction

General image processing. After collection, all images were further processed with *ImageJ* software. For purposes of descriptive analysis and figure display in this document, images were treated and prepared accordingly to each observation intention. Image adjustments for properties like contrast, brightness or color balance for instance, were differently manipulated in order better reflect the observations to the reader. It should be kept in mind that many images presented are in fact the result of merging two or more original images. In few cases, the reader can also come upon with thresholded and binarized images for purposes explained further on.

Image preparation for numerical data extraction. However, for numerical analysis, the image processing followed a thorough, controlled and invariable methodology. Subsequently, all three channels – FastMyo (Figure 15A), LD (Figure 15B) and OXPAT (Figure 15C) – were merged (Figure 15D) wherein all cells in good physical condition were selected and hand cropped using a drawing tablet *Cadboy NGS*® with care in order

to avoid capillaries (Figure 15E). Every cropped cell was pasted into one new different image per subject (Figure 15F) still with all three channels merged. At this point, all images were equally background subtracted at 2 pixel value, where the channels were splitted and remerged in order to obtain a two-channel image of LD plus FastMyo and a second two-channel image of OXPAT plus FastMyo. Each one of these later sets was then merged into third background channel (respectively Figure 15G and Figure 15H) serving as cell membranes, required by the software application.

Intensity Correlation Analysis. Colocalization analysis was preformed over the previously prepared images, and done accordingly to Sylvain Costes and colleagues' method (Costes et al. 2004), available through one of *Image J*'s plug-in called *Intensity Correlation Analysis* (ICA). While traditional colocalization analysis is usually preformed by merging two different channels and assess qualitatively or quantitatively the area of the superimposed pixels, the ICA method however, assesses different channels' relationships not only in the geographic frame of reference but also accordingly to pixel intensity, more precisely, the pixel spread functions (PSF) of both channels are analyzed against each other. Putted in simple words, through spatial statistics, ICA calculates the degree of true colocalization (read Study limitations part), by ruling out random pixel colocalization. By applying this method, potential artifacts are greatly reduced and reliability of true colocalization of real structures is enhanced. For detailed information, the reading of Costes and colleagues work (Costes et al. 2004) is strongly recommended.

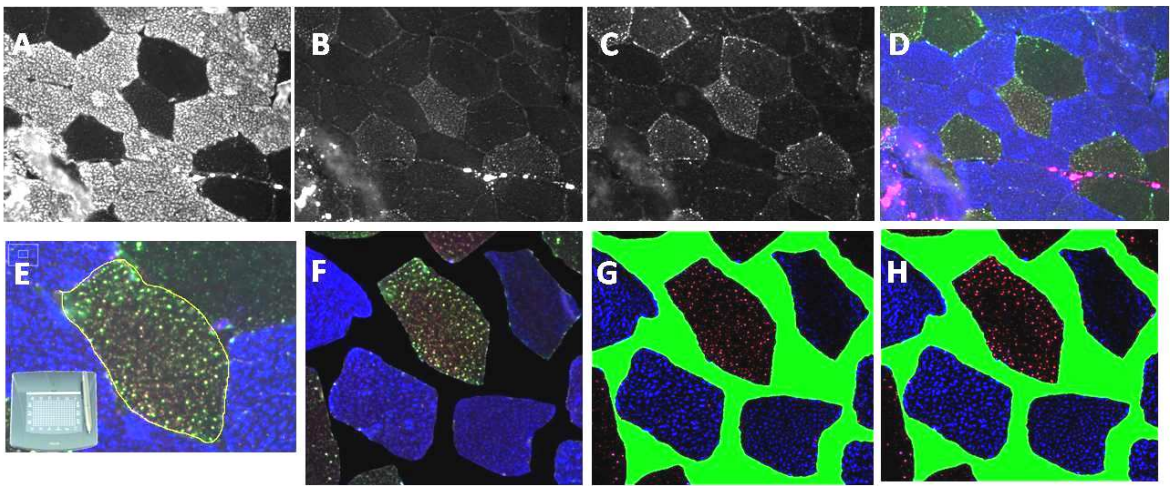

FIGURE 15. Simplified steps in preparation for image quantitative analyses. (A) Fast myosin. (B) LDs. (C) OXPAT. (D) Merge of A, B and C. (E) Individual cell crop. (F) Pasting in one image all analyzable cells per subject. (G) Ready image for LD analysis. (H) Ready image for OXPAT analyses. Note that software, regards green as the sarcolemma, i.e., the peripheral limit of each fiber.

Numerical data extraction from images. Intracellular topography of LD and OXPAT was assessed both qualitatively (descriptive observations) and quantitatively (coordinates, intensity and distance to membrane). The latter was obtained through *ImageJ*'s plug-in "*analyze cells*" developed by Tuomas Turpeinen, the same application was also able to differentiate from fiber type by recognizing FastMyo labelling. After running the images, the software application generated matrix files where both cell and related particle values were included. See Table 3 for number of analyzed cases. At this point, all matrixes arithmetics and further calculations were performed with Matlab©. Quantification of intracellular contents (IMTG, OXPAT and their colocalization) was calculated in each cell and is here expressed as total intensity value of positive pixels (from 1 to 255 intensity values) per total pixels within a fiber. Particle distances to membrane were calculated in each particle within each group and are referred as *Particle Closeness to Membrane*, which scale ranges from 0 to 100, wherein 0 represents the fiber (section) geometric center and 100 represents the sarcolemma.

TABLE 3. Number of analyzed cases. Depending on the measurement, different sampling was used for group calculations.

Group	Subjects	Cells (N)		Particles (N)					
				Type I			Type II		
		Type I	*Type II*	*LDs*	*OXPAT*	*COLOC*	*LDs*	*OXPAT*	*COLOC*
LC	7	343	273	110951	104943	84732	44130	22478	8238
OB	8	189	132	86404	102556	69066	41348	26524	10606
T2D	10	167	150	59428	75719	55173	31222	17829	7232

7.6 Statistics

All statistical analyses were performed using Matlab© with exception for *Spearman* correlations carried out by SPSS©. Correlation significance levels were set at $P<0.05$ (represented as *) and $P<0.01$ (represented as **).

Data distribution failed to fit normality using *Lilliefors*, *Shapiro-Wilk*, *Chi-Square* and *Jarque-Bera* tests. For group median comparisons on particle variables, a *Mann-Whitney U* test was used with significance level set at $P<0.001$ (represented as ***). For group median comparisons on cell variables, a *Mann-Whitney U* test was used with significance levels set at $P<0.05$ (represented as *) and $P<0.01$ (represented as **). Even though data did not fit normality, given the high number of analysed cases, a *two-sample Student's t-test* for unequal variances (*Satterthwaite's approximation*) was used to compare mean values between groups, with significance levels set at $P<0.05$ (represented as †), $P<0.01$ (represented as ††). All comparisons were performed between either the OB or the T2D groups against the assumed healthy LC group. Data variability is reported with standard deviations.

8 RESULTS

Although OXPAT and LDs are completely distinct biomolecules, for practical reasons, the reader will come upon the term “particles”, referring to LDs, OXPAT and the intentional artifacts generated from their colocalization analysis (COLOC). It should also be noticed that for the purpose of presenting image results and where not stated otherwise, OXPAT signal will be shown to the reader as *green*, neutral lipids (LDs included) as *red*, fast myosin as *blue* and the colocalization between LDs and OXPAT as *yellow*. One more commentary should be regarded concerning the term “colocalization”, as it simply represents the overlaying of two signals sharing equal image pixels and by all means, does not imply – merely suggests – functional interaction between particles (See Study Limitations in Discussion chapter).

8.1 Descriptive observations

8.1.1 Lipid droplets and OXPAT appearance

It is easily seen that OXPAT signal is mainly colocalizing with LDs signal, sometimes being even possible to observe OXPAT coating LD in a ring-like form (Figure 16B). However, when examining carefully, a reduced but considerable amount of OXPAT particles appeared completely cytosolic. The inverse situation however, was much more clearly observable, i.e., greater number of LDs appeared to be “free” from OXPAT (Figure 16A).

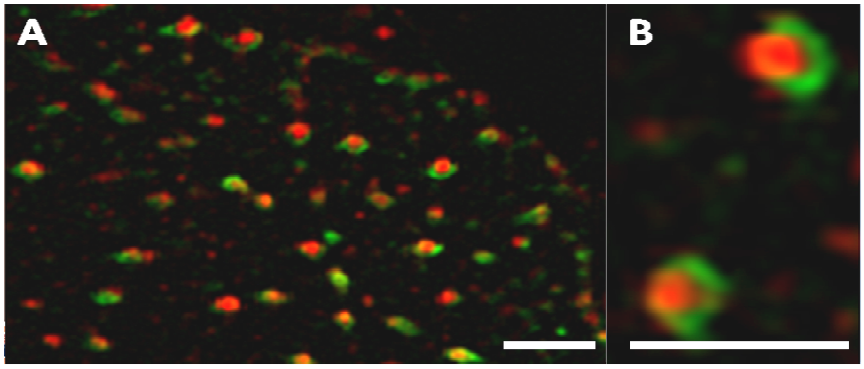

FIGURE 16. Intramyocellular LDs and OXPAT. (A) Despite frequent alliance between both biomolecules, some of these seem unassociated and completely cytosolic, especially LDs. (B) Careful examination further reveals OXPAT "rings" (green) coating LDs (red). Bars 4 µm.

Type I fibers presented a very plastic neutral lipid profile, from completely saturated of LDs and OXPAT to nearly devoid of these, containing from thousands of minute droplets to scarce bigger LDs. Likewise, type II fibers also presented a variable LD and OXPAT pattern profile, despite the general weaker and lesser signal from both labelings, never reaching the same saturation as some type I fibers. Therefore, although type I and type II fibers present several overlapping profiles, it is easily observed that generally, type I fibers have indeed more LDs and OXPAT than type II fibers (Figure 17).

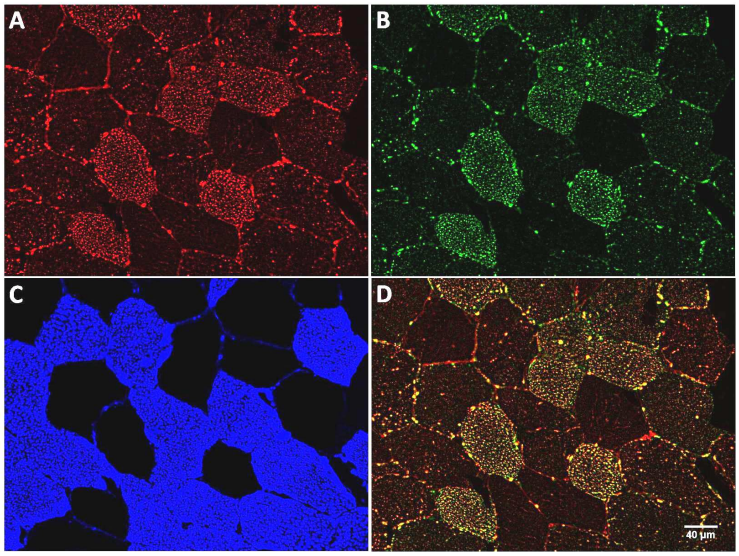

FIGURE 17. LDs and OXPAT in different skeletal muscle fibers. (A) Lipid Droplets. (B) OXPAT. (C) Fast Myosin. (D) Merge of A and B. Bar 40 µm.

However, OXPAT signal seemed many times stronger in type I fibers than type II even in the circumstances where LD signal looked similar between fiber types, giving type II cells a more reddish appearance while type I fibers tended to present a more yellowish look in the merged channel (Figure 18D), in other words, for the same amount neutral lipid signal, type II fibers seem to have less OXPAT signal. In many fibers, especially in type I, the majority of bigger droplets were observed closer to the periphery while smaller and minute LD were generally numerously extended throughout all cytoplasm (Figure 18A).

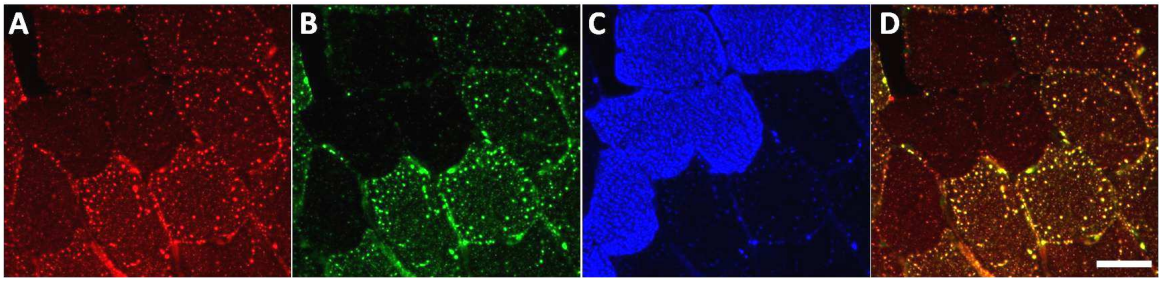

FIGURE 18. Big peripheral particles. (A) Lipid Droplets. (B) OXPAT. (C) Fast Myosin. (D) Merge of A and B. Note the reddish appearance of type II fibers in D, originated by poor OXPAT labelling in these fibers. Bar 40 µm.

What is more, besides bigger and more LDs being repeatedly observed in periphery, interestingly, OXPAT not only followed this behavior, but it seems to do so in a more obvious way, i.e., the intensity contrast of OXPAT signal between peripheral and inner regions is greater than LDs' (Figure 19).

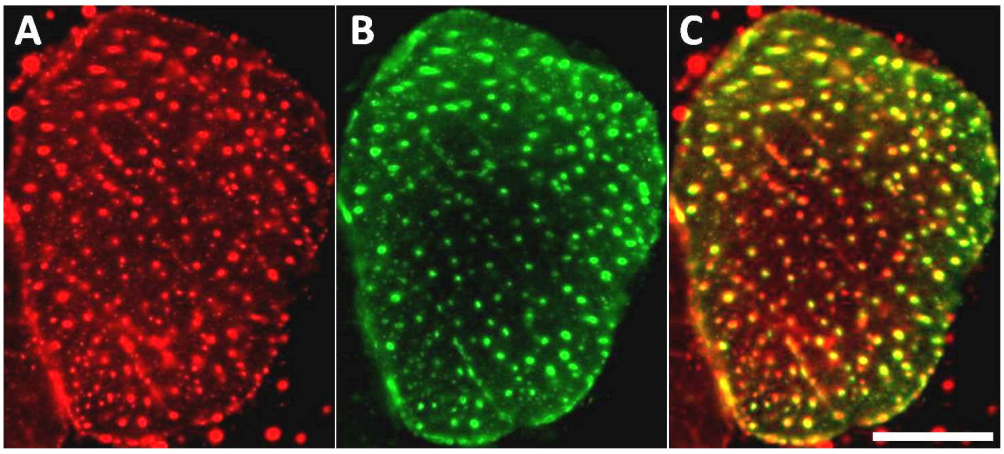

FIGURE 19. Different region label intensity. (A) Lipid Droplets. (B) OXPAT. (C) Merge of A and B. Note the reddish appearance in inner regions of C, originated by poor intermyofibrillar OXPAT labelling. Bar 20 µm.

More or less consistently, bigger LDs and the following OXPAT revealed huge (up to 50 micrometers) structural-like outlines throughout many cells. Sporadically these phenomena were quite obvious and represented sizeable dimensions considering the cell area. Repeatedly, these structures seemed connected to the sarcolemma (Figure 20).

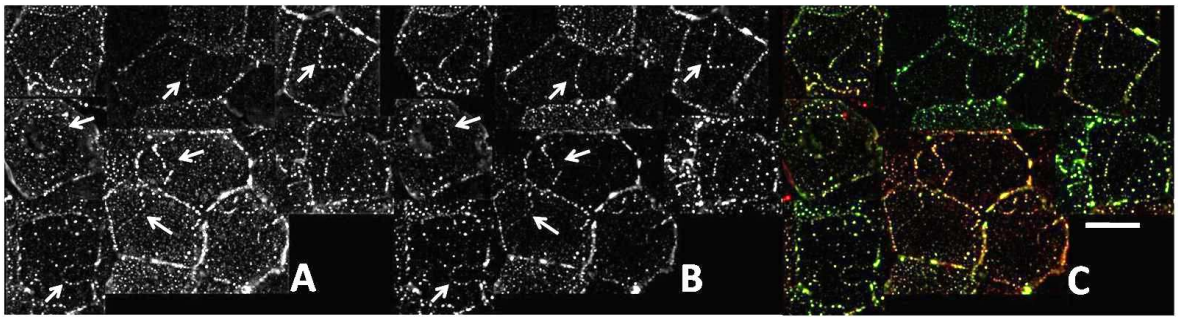

FIGURE 20. LDs and OXPAT big structures. (A) Lipid Droplets. (B) OXPAT. (C) Merge of A and B. Note non random aspect of structures, even shaping circles. Bar 40 µm.

Few longitudinal sections were equally stained for neutral lipids and OXPAT, wherein LD showed a similar pattern to Shaw and coworkers (Shaw et al. 2008) who studied LD in skeletal muscle longitudinal sections. In our images, we can also observe partial but strong colocalization between LD and OXPAT (Figure 21).

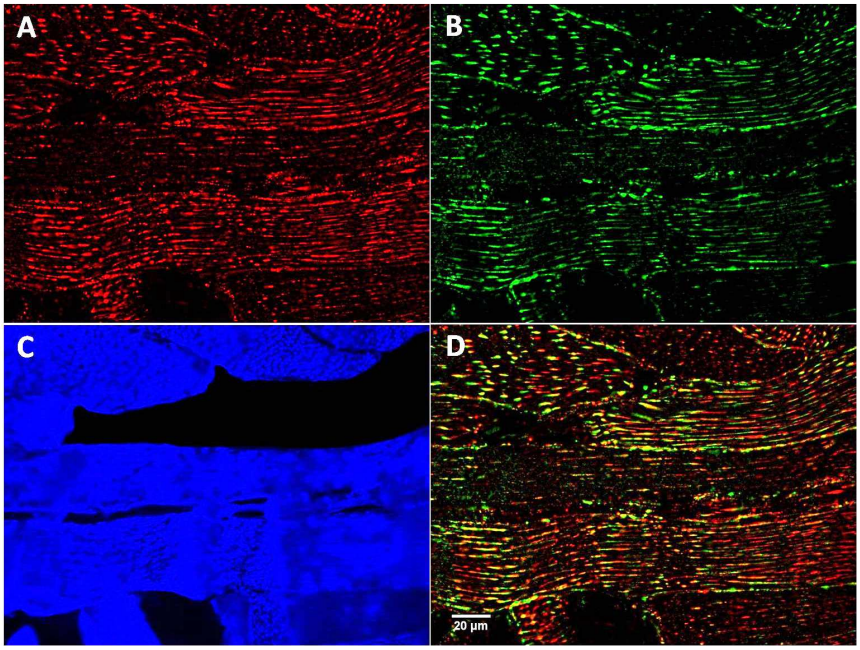

FIGURE 21. LDs and OXPAT in longitudinal sections. (A) Lipid Droplets. (B) OXPAT. (C) Fast Myosin. (D) Merge of A and B. Bar 20 µm.

Furthermore, we strengthened our group's previous observations which pointed out to a very fine network structure produced by neutral lipid staining with LipidTOX®. This structure had the appearance of a delicate reticulum occupying all cell area with even intensity, composed by minute semi-elongated polygons in the range of ~1-3 micrometers wide (Figure 22).

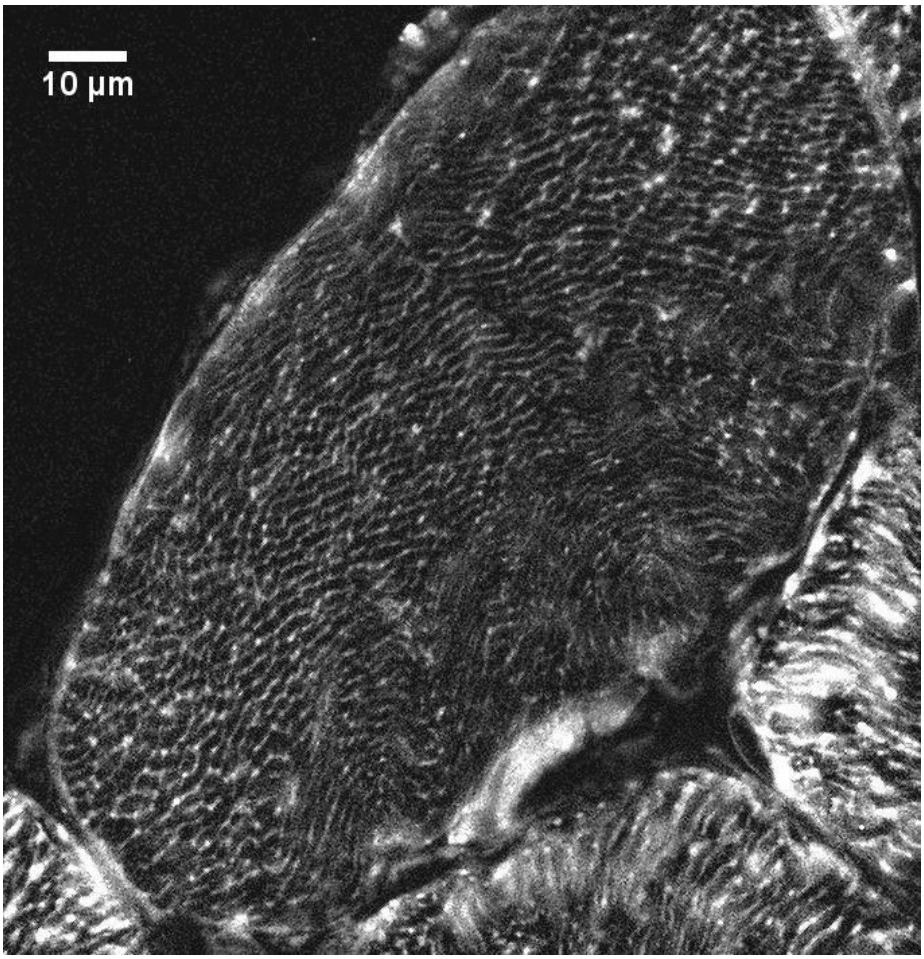

FIGURE 22. Neutral lipid network enhanced by contrast manipulation. Bar 10 µm.

Additionally, it appears that LDs (more intense and roundish neutral lipid staining) were part of such network as points were neutral lipids were more intensely accumulated (Figure 23). Interestingly, this repeatedly observed structure was perpendicularly inserted from the sarcolemma towards inner regions of the cell (Figure 23C).

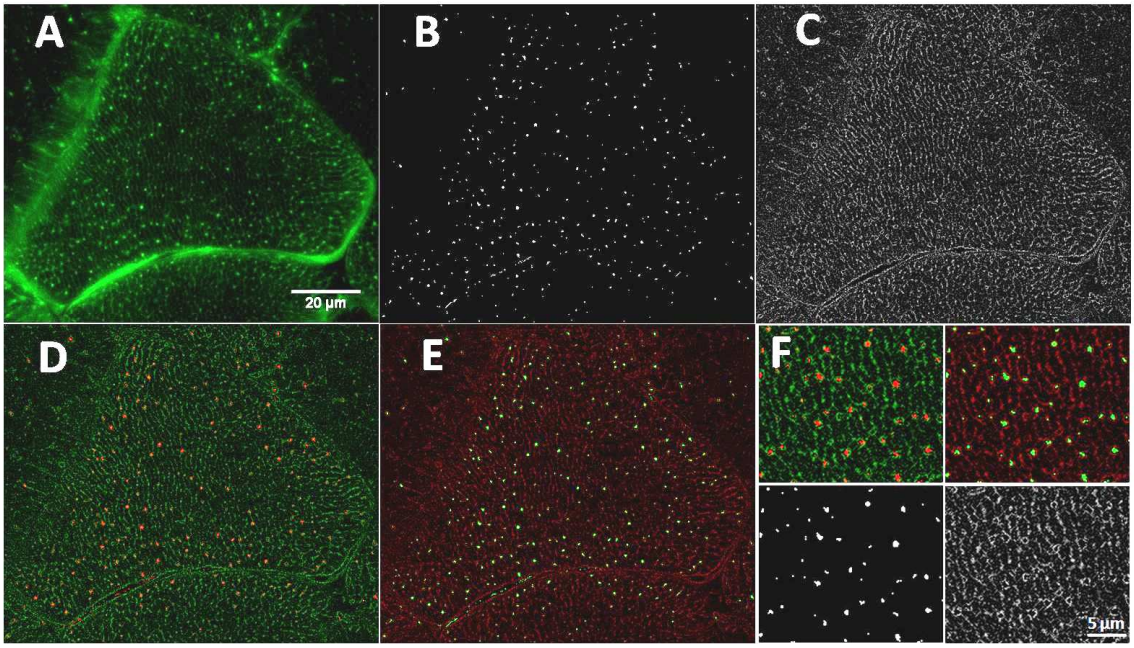

FIGURE 23. Separated neutral lipids, network versus LDs. (A) Raw neutral lipid staining. (B) LD isolation. (C) Network isolation and enhancing. (D and E) Merge of B and C as different channels. (F) Region zoom of B, C, D and E. Bars 20 µm (A) and 5 µm (F).

8.1.2 Relative localization of LD, mitochondria and myosin

When observing COX labeling it is also visible mitochondria more densely distributed in peripheral regions and more scarcely present in central regions. Some fibers however, were quite evenly supplied of mitochondria, throughout peripheral and central regions (Figures 24A). Just like LDs and OXPAT, some barely stained fibers greatly contrasted with neighbor cells with intensely stained neutral lipids and COX (Figure 24).

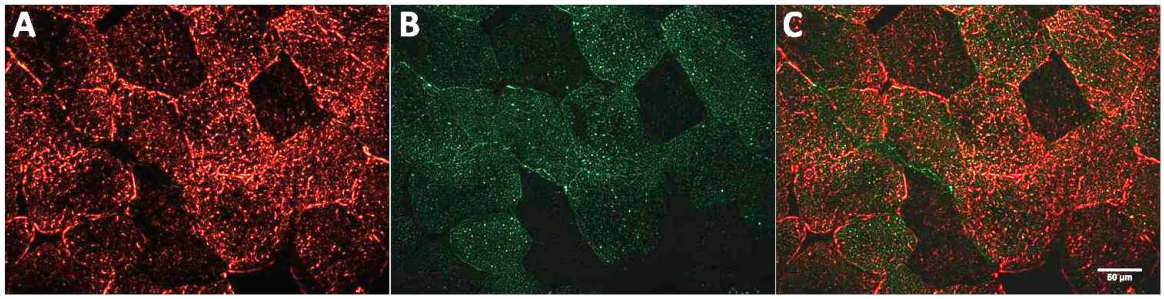

FIGURE 24. Mitochondria and LDs. (A) COX. (B) Neutral Lipids. (C) Merge. Bar 50 µm.

Labeling of COX allowed many times the observation of a semi polygonal structure-like pattern throughout the cell (Figure 25), being also observable LD colocalizing in many regions where mitochondrial signal is strong, even though neutral lipid staining did not fully exhibit the same complete pattern drawn by mitochondria. Such incomplete mitochondrial drawn polygons had a rather equiangular (not so elongated) shape with diameters in the range of the ~4-10 micrometer (Figure 25B).

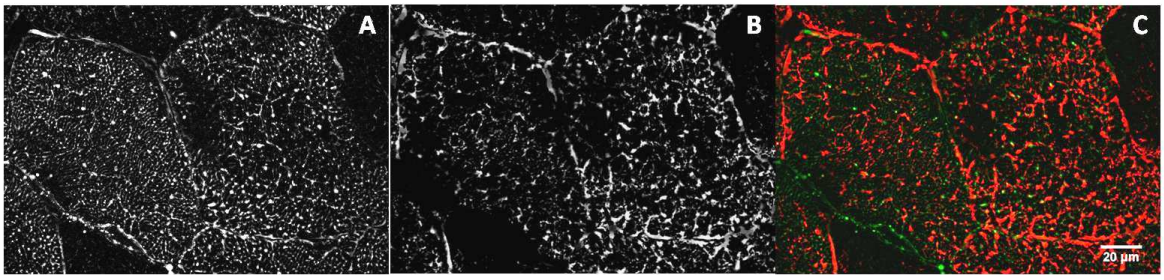

FIGURE 25. Mitochondria and LDs. (A) Neutral Lipids. (B) COX. (C) Merge. Bar 20 µm.

As expected, experiments involving LD and Fast Myosin heavy-chain stainings show a strong tendency for non-colocalization between both structures, however, sporadic colocalization was indeed observed. Nevertheless, different sized LDs tend to carefully surround Myosin staining (Figure 26).

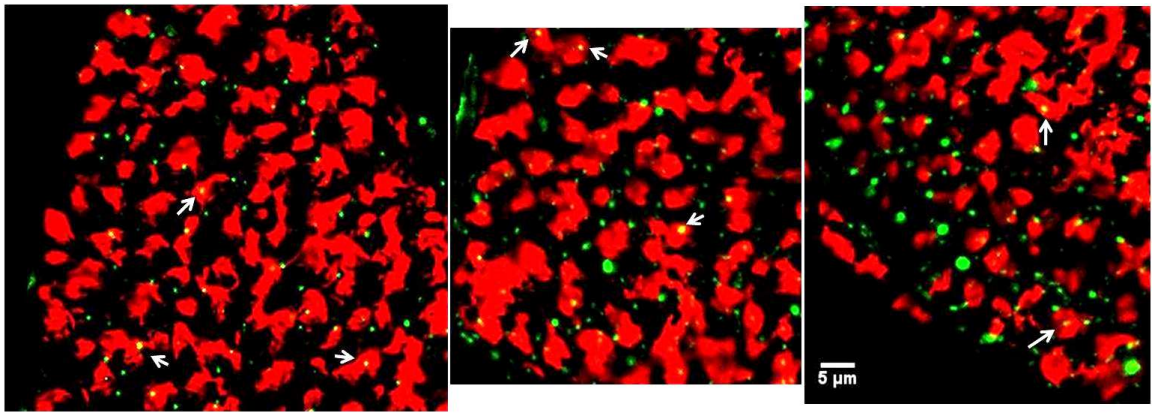

FIGURE 26. LDs surrounding Myosin. White arrows point to scarce unexpected colocalization (yellow) between neutral lipids (green) and fast myosin (red). Otherwise, LDs are seen carefully organized around myosin filaments. Bar 5 µm.

8.2 Numerical results

8.2.1 Lipid droplet and OXPAT intracellular distribution

Lipid Droplet Closeness to Membrane. Assumed as normal population values, the LC group revealed a median LD closeness to plasma membrane of 91.55 ± 14.57 in type I fibers. In this fiber type, both the OB and T2D groups showed significantly higher values (94.15 ± 13.39 and 93.09 ± 13.93 respectively) than LC group. For type II fibers, LC group presented a LD closeness to membrane of 92.95 ± 12.23, which was a significantly lower value than OB and T2D groups, respectively 93.21 ± 14.23 and 94.83 ± 13.66. See Figure 27A.

OXPAT Closeness to Membrane. Similarly, LC values for type I and type II fibers were significantly farther away from the membrane (respectively 93.36 ± 13.76 and 96.29 ± 13.18) when comparing to closer values of OB (respectively 95.10 ± 12.47 and 97.17 ± 12.41) and T2D (respectively 94.88 ± 12.84 and 99.19 ± 11.09). See Figure 27B.

LD and OXPAT Colocalization Closeness to Membrane. Once again, type I fibers present significantly closer to membrane values in OB and T2D groups (95.12 ± 12.47 and 95.12 ± 12.24 respectively) when comparing to LCs (93.35 ± 13.52). Despite very close values among all groups in type II fibers, OB and T2D higher values (respectively 99.03 ± 12.72 and 99.72 ± 10.25) still reached statistical significance when comparing to LC group (98.92 ± 11.72). See Figure 27C.

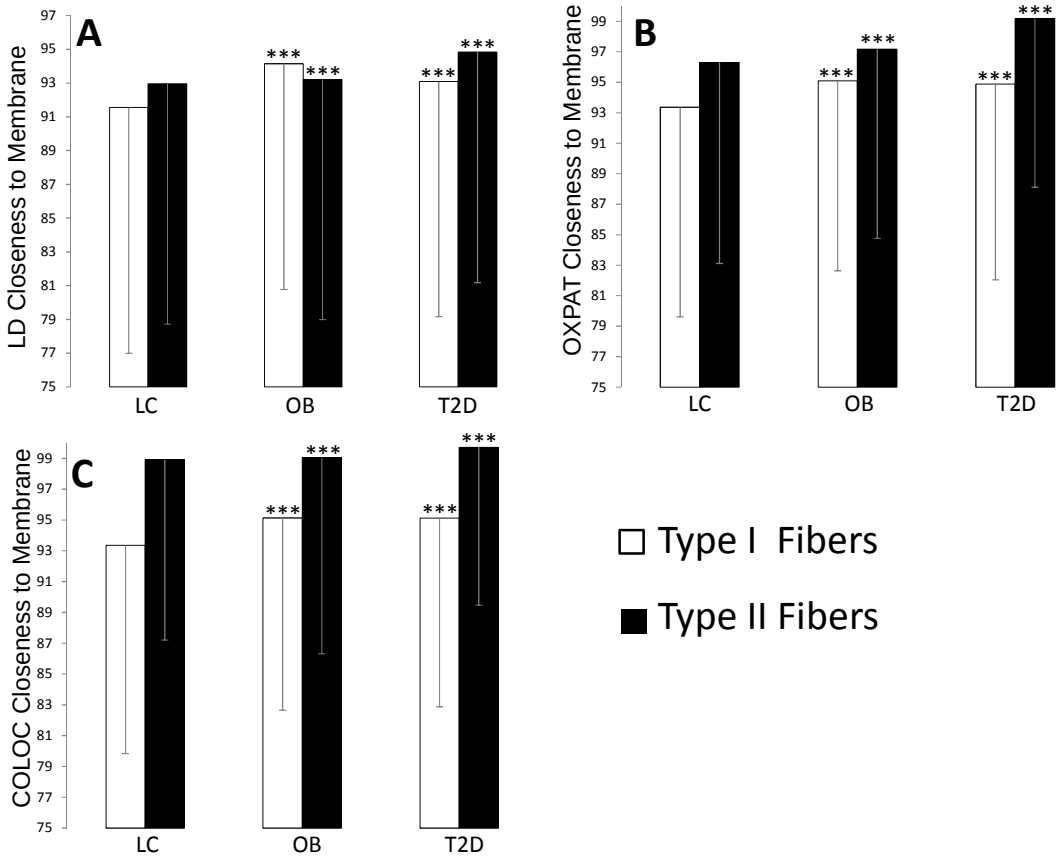

FIGURE 27. Particle Closeness to Membrane. Median values are reported. The scale top is the 100 value representing the sarcolemma, wherein the zero value is the geometric center of cells. (A) Median position of all analyzed LDs. (B) Median position of all analyzed OXPAT. (C) Median position of all analyzed LD and OXPAT colocalizing particles. ***P< 0.001.

Intracellular Particle Topography. After assessing all particles median position relative to the sarcolemma, we further examined intramyocellular distribution of different intensity particles. Regardless from fiber type and group analyzed, it is visible in Figures 28, 29 and 30 that different intensity LDs, OXPAT and their colocalization are spread throughout all cell regions. However, this positioning clearly follows a peri-sarcolemmal tendency, wherein most particles, low and high intensity, localize more abundantly closer to the plasma membrane. Moreover, low intensity particles seem to be more abundant than high intensity ones, even in cell periphery where high intensity particles localize extensively. Also, it is clear that type II fibers have considerably lesser quantity of particles than type I fibers, especially when examining OXPAT (Figure 29) and colocalization of LDs and OXPAT (Figure 30).

Next, in order to better detect and understand possible group differences in distribution behavior, we obtained a second degree polynomial function from the plotted particles. The LC group shows a concave line behavior in both cell types (Figure 28A and 28D), denoting relative higher number of low intensity LDs than high intensity LDs in central regions of cells when comparing to periphery. However, the OB group has a convex line behavior, especially in type I fibers, denoting a relative higher number of high intensity LDs than low intensity ones in central regions when comparing to periphery (Figure 28B and 28E). In turn, the T2D group shows a slightly convex line behavior in type I fibers in opposition to a rather concave line in type II fibers (Figure 28C and 28F).

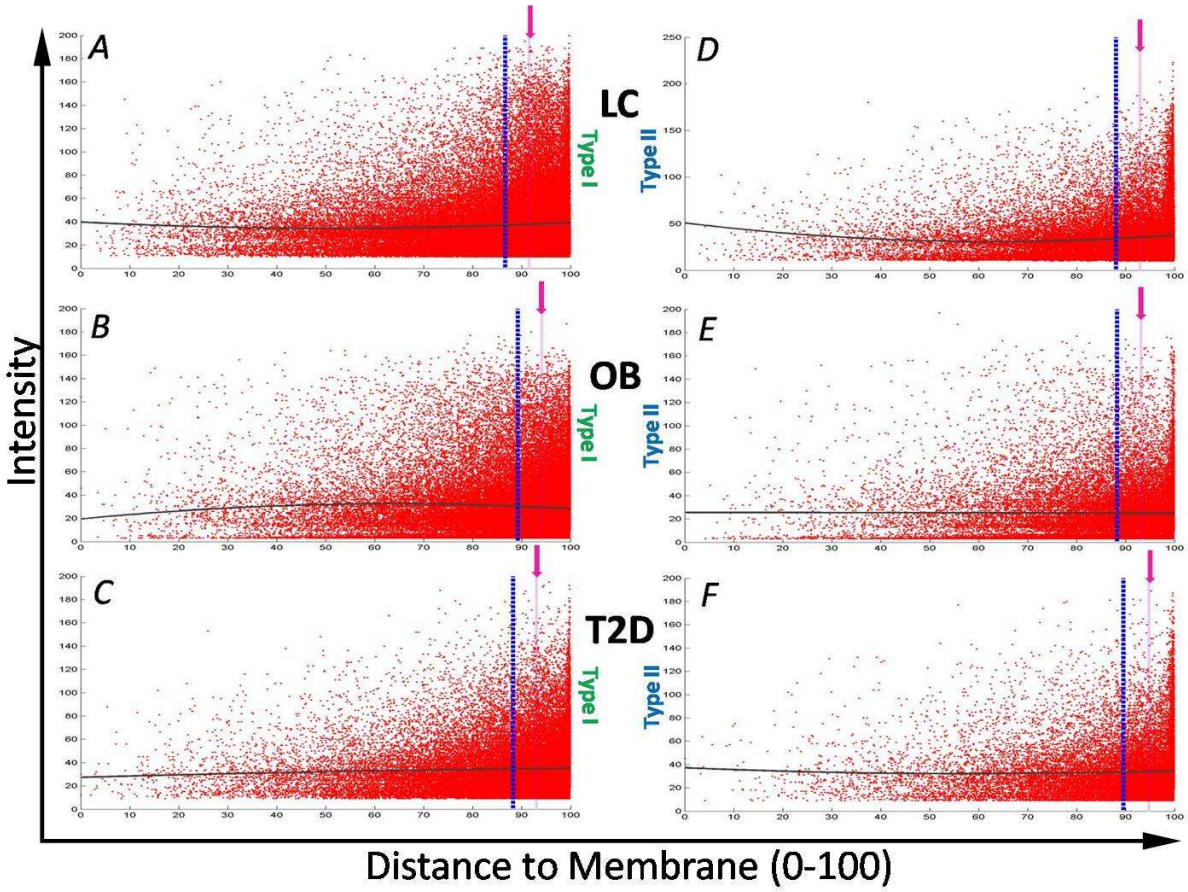

FIGURE 28. Lipid Droplet Distribution plots. (A) LDs in type I fibers of LC group. (B) LDs in type I fibers of OB group. (C) LDs in type I fibers of T2D group. (D) LDs in type II fibers of LC group. (E) LDs in type II fibers of OB group. (F) LDs in type II fibers of T2D group. Thick vertical blue lines show mean closeness to membrane. Thin vertical lines (with pink arrow) show median closeness to membrane. Black horizontal line is a 2nd degree polynomial of plotted data. Each dot represents a droplet.

With a somewhat decreased number of detected particles, OXPAT distribution patterns resemble LD distribution patterns, especially in the LC and T2D groups. Thus, only type I fibers of T2D group is showing a slightly convex line behavior (Figure 29C), being the type II fibers of T2D and both fiber types of LC showing concave curves (Figure 29F, 29A and 29D respectively). However, OB shows fairly different OXPAT patterns in comparison to LDs, especially in type I fibers wherein the OXPAT straight polynomial line (Figure 29B) contrasts to LDs' quite convex line (Figure 28B), denoting OXPAT uncorrespondance to high intensity LDs in central regions when comparing to periphery.

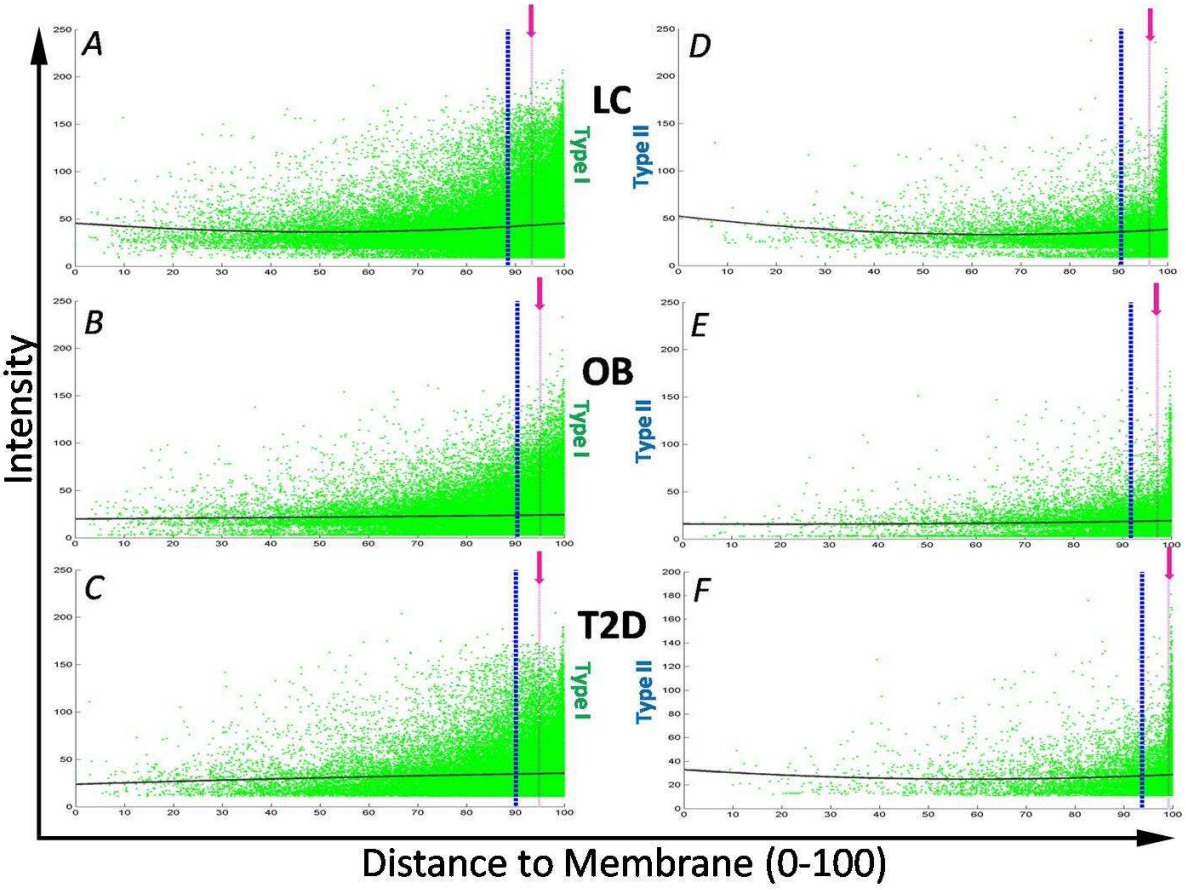

FIGURE 29. OXPAT Distribution plots. (A) OXPAT in type I fibers of LC group. (B) OXPAT in type I fibers of OB group. (C) OXPAT in type I fibers of T2D group. (D) OXPAT in type II fibers of LC group. (E) OXPAT in type II fibers of OB group. (F) OXPAT in type II fibers of T2D group. Thick vertical blue lines show mean closeness to membrane. Thin vertical lines (with pink arrow) show median closeness to membrane. Black horizontal line is a 2nd degree polynomial of plotted data. Each dot represents a detected OXPAT particle.

Despite the colocalized particle amount being more similar to OXPAT amount and considerably less than LDs (See Appendix III), the polynomial curve behavior of the colocalized particles resembles more LD distribution patterns. That is, while both fiber types of LC and type II fibers of T2D show concave lines (Figure 30A, 30D and 30F respectively), the OB group shows convex lines in both fiber types (Figure 30B and 30E), denoting relative higher number of high intensity colocalization in central regions of cells when comparing to peripheral regions.

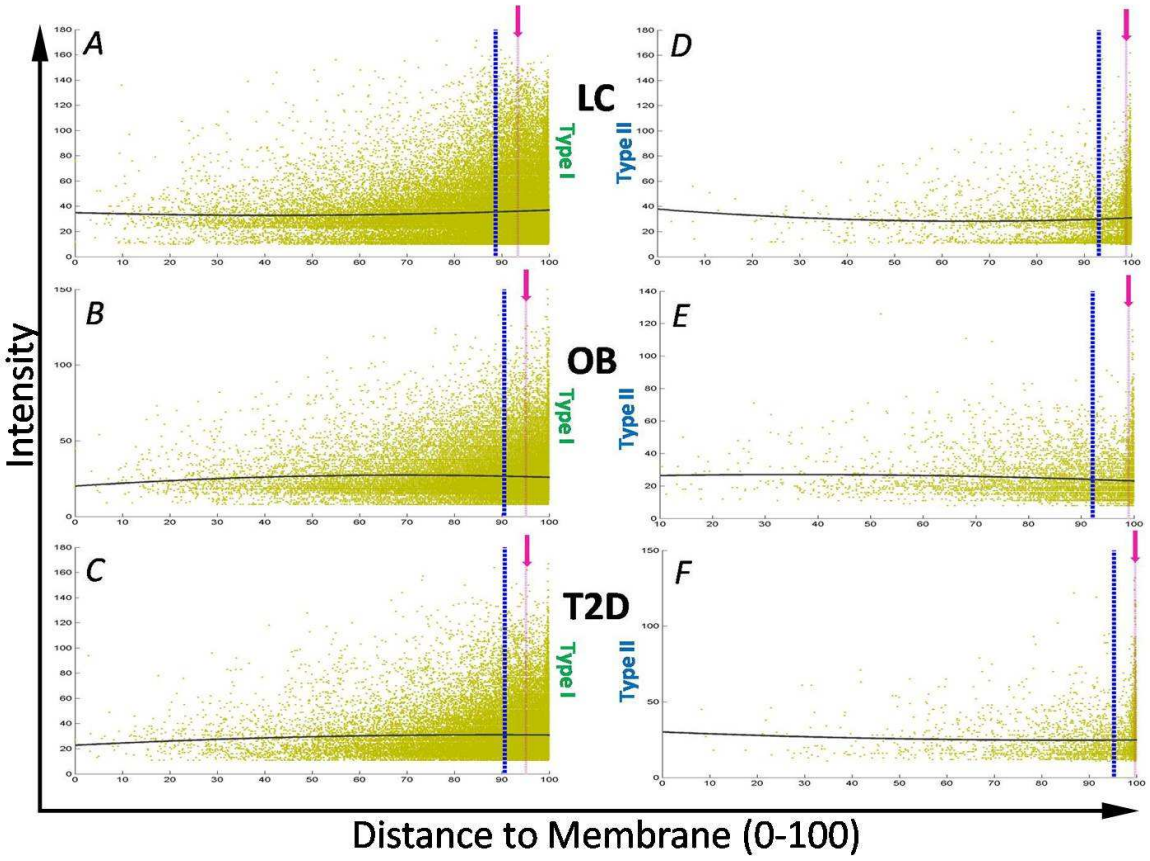

FIGURE 30. Colocalization Distribution plots. (A) COLOC in type I fibers of LC group. (B) COLOC in type I fibers of OB group. (C) COLOC in type I fibers of T2D group. (D) COLOC in type II fibers of LC group. (E) COLOC in type II fibers of OB group. (F) COLOC in type II fibers of T2D group. Thick vertical blue lines show mean closeness to membrane. Thin vertical lines (with pink arrow) show median closeness to membrane. Black horizontal line is a 2nd degree polynomial of plotted data. Each dot represents detected colocalized particles.

8.2.2 Correlations with anthropometrical and plasma data

Next we performed a *Spearman's* correlation analysis in order to find possible associations between previously assessed variables (See 7.1) and and our present measurements (See 7.5). However, only the most relevant correlations are reported in this chapter, the full tables can be found in Appendix IV.

Systemic lipids versus intramyocellular particle content. When analyzing all the groups toghether (n=25), a mild positive correlation (P<0.05) was found between TAGemia and type II fibers colocalized content (fast_COL_content) (P=0.030). The same mild correlation was also found when analyzing the LC group (n=7) (P=0.036). In the OB group (n=8), fast_COL_content also associated with TAGemia (P=0.017) in addition to FAT% (P=0.047) and FM (P=0.028). In T2D group (n=10), fast_COL_content correlated positevely with body weight (P=0.019) and negatively with HDL (P=0.018). Moreover, still in T2D, strong correlations (P<0.01) were found between type II fibers LD content (fast_LD_content) with BMI (P=0.004) and body weight (P=0.008).

Systemic lipids versus intramyocellular particle closeness to membrane. Several correlations were found between tissue/plasma lipids and intracellular particle closeness to membrane, interestingly all in T2D group. For instance, strong associations between colocalized particle closeness to membrane in type II fibers (fast_COL_closeness) and TCHOL (P=0.008) and LDL (P=0.005). Moreover, mild correlations were found between OXPAT closeness to membrane in type II fibers (fast_OXPAT_closeness) and TCHOL (P=0.030) and FAT% (P=0.043). Furthermore, several positive associations were found between FAT% and membrane closeness variables, such as LD closeness to membrane in type II fibers (fast_LD_closeness) (P=0.016), OXPAT closeness to membrane in type I fibers (slow_OXPAT_closeness) (P=0.019) and colocalized particle closeness to membrane in type I fibers (slow_COL_closeness) (P=0.016). The latter particle closeness correlations were also observed with FM (P=0.016; P=0.029 and P=0.033 respectively). I addition, LD closeness to membrane on type I fibers (slow_LD

closeness), associated positevely with FM (P=0.038), BMI (P=0.043) and body weight (P=0.029).

Intramyocellular particle closeness to membrane versus VO_2max. The LC group showed strong associations between VO_2max and both slow_LD_closeness (P=0.007) and slow_OXPAT_closeness (P=0.000), plus a mild correlation with fast_LD_closeness (P=0.014). Interenstingly, the OB group also revealed some strong associations between VO_2max and particle closeness to membrane (slow_OXPAT_closeness (P=0.007; fast_LD_closeness (P=0.000) and fast_COL_closeness (P=0.004)). On the other hand, T2D revealed a negative association beteween VO_2max and some particle closeness to membrane variables (slow_OXPAT_closeness (P=0.022); slow_COL_closeness (P=0.025) and fast_LD_closeness (P=0.038)).

8.2.3 Other performed measurements

Additionally, more measurements were performed collaterally to this dissertation's main purpose. Among these, there are the IMTG and OXPAT content analysis based on particle area and intensity (Appendix V) and also ICA, a draft of LD/OXPAT colocalization analysis between different groups (Appendix VI).

9 DISCUSSION

9.1 Study limitations

Despite many times utilizing more than quite reliable and appropriate technology for its purposes, this study has also some considerably harsh limitations, which in hand, might have caused possible misinterpretations of the final numerical results, or at least did not permit total assurance of these. Therefore, in this part I will mention all these aspects which I consider that at least might have added noise to some results.

Colocalization analysis, despite being done accordingly to Costes method, it still only analyzed “copixelization”, i.e., only spatial interrelationship was measured. Still, spatial interrelationship would not be so limitative if confocal technology was used rather than the widefield epifluorescence microscope used in this study. Such setup can provide only to the researcher, the possibility to observe the total sectioned volume (5µm in Z-axis depth in this case) and assuming that the majority of intramuscular LDs is under 1µm, it leaves the researcher with little certainties that “copixelization” means in fact, real interaction.

Biopsy samples had different collection circumstances, but more significantly, had different and excessive manipulation, which resulted in some poorly shaped biopsies and many worthless fibers, limiting the number of analyzable fibers. Also, there is always the possibility then, that lipid displacement or protein denaturation might have occurred.

Unfortunately, most of T2D group subjects were medicated against IR. Some of the used medication was specifically up regulating AMPK pathways, resulting in improved

lipolysis through increased rates of β-oxidation. Many times, as observed, this led to conflicting results for the T2D group, showing more than once, similarities more towards the LC group rather than the OB one. We consider the use of this kind of medication, the main probable cause for the OB group being the more contrasting one towards LC group, rather than the T2D group in some results.

The number of subjects in each group could be indeed bigger, especially in the LC where only 7 subjects were analyzed. Possibly even more limiting, was the fact that different individuals and different groups had different number of cropped and analyzed cells, where some individuals were only analyzed through one or two dozens of cells, others could be more reliably analyzed through hundreds of cells. Better assessment of these limitations can be further checked in Appendix III.

In our study we used a methodology based on fluorescence microscopy, which has limited resolution when comparing to electron microscopy for instance. This limitation is significant when considering the difficulty in distinguishing between subsarcolemmal (SS) and intermyofibrillar (IMF) regions for instance. On the other hand, fluorescence microscopy allows us to better differentiate between fiber types and to more extensively quantify intramyocellular particles.

9.2 Particle distribution in different groups

9.2.1 Observed results versus proposed hypotheses

The proposed hypotheses of distinct particle distribution between groups were based on the fact that IR seems to be partially caused by the accumulation of by-products originated from poor or inefficient TAG hydrolysis, rather than increased IMTG content. We believed this impaired IMTG turnover in IR populations could be linked to more central or internalized LDs in skeletal muscle fibers and therefore, harder accessed by oxygen and other oxidative agents coming from sarcolemma direction.

The main hypothesis of this study was that different LD and OXPAT distribution patterns would arise from the three different studied groups, therefore, since this situation indeed occurred, the main hypothesis succeeded. However, our predictions about how exactly this groups would differ in terms of intramyocellular distribution of LDs and OXPAT, clearly failed. In fact, our results show an opposite tendency to our expectations, i.e., T2D was the group having more peripheral LDs, OXPAT and their colocalization, immediately followed by the OB group while LC presented more internalized particles, contrarily to our sub hypotheses.

In our opinion, these membrane proximity results can be partly explained by our correlation analysis. That is, there were repeated positive correlations between particle content/closeness to sarcolemma and tissue/plasma lipid concentrations, especially in T2D group (See 8.2.2). This only suggests that there is a direct implication of tissue and plasma fat with intramyocellular lipid internalization. However, since blood glucose levels showed no correlation whatsoever, the idea of LD closeness to membrane being directly related to IR, loses some power. Nevertheless, we did not measure glucose tolerance in this study and the fact that we found no Glycemia correlations with particle closeness to membrane does not mean the latter is unrelated to developing or having IR.

While this thesis was being written, Nielsen and his colleagues released a study wherein by means of electron microscopy they assessed IMTG content in IMF and SS regions of T2D, BMI-matched obese and endurance athletes. In accordance with our results, Nielsen and colleagues found that indeed T2D had significantly higher absolute and relative values of SS IMTG while athletes presented more internalized lipids. In addition, they were able to find a strong negative correlation between IS and SS lipids (Nielsen et al. 2010). The same researchers suggested that besides increased plasma lipid availability, the impairment of SS mitochondria oxidative capacity previously reported (Ritov et al. 2005), might be one of the causes for accumulation of SS LDs. When trying to link increased SS lipids with IR, Nielsen et al. further speculated that SS lipids could contribute more for insulin signaling cascade than IMF lipids, due to the absence of SR network in SS regions, which in turn, could serve as a protective barrier for IMF LDs

against signalling proteins. Therefore, this could lead to more significant formation of IR precursors in SS regions, as DAG for instance (Nielsen et al. 2010). In fact, when compared to more internalized DAG, a decrease in membrane-bound DAG was previously shown to associate with PKCθ inhibition and consequent IS improvement (Bruce et al. 2007).

9.2.2 OXPAT more peripheral than LDs

One interesting fact when analysing Figure 27 is that in both fiber types of all three groups, OXPAT median position is always closer to sarcolemma than LD median position, especially in type II fibers where this closeness increment is more obvious. This analysis allows us to conclude two things: *1)* it corroborates our descriptive observations wherein we saw that OXPAT only appears to mimic LD presence (See 8.1.1) when a closer look reveals that there are some unassociated cytosolic pools of both biomolecules (Figure 16); *2)* OXPAT exists more peripherally than LDs in skeletal muscle which leads us to anticipate that peripheral LDs in general are more prone to interact with OXPAT than internal LDs are (Figure 19), especially in type II fibers. In what concerns the first point, our results match the literature, wherein OXPAT was already shown to be stable in cytosol when unbound to LDs (Yamaguchi et al. 2006). On the other hand, as far as we know, the fact that in skeletal muscle OXPAT tends to be closer to the membrane than LDs is a novel observation. Equally unreported, our additional analyses of colocalized particles (Figure 27C and Appendix VI) also strengthen our descriptive observations (See 8.1.1), in which we state that there are more LDs devoid of OXPAT than the other way around and that these “OXPAT-free” LDs are indeed in inner regions of fibers (Figure 19), especially in type II fibers.

When trying to interpret these results meaning biologically, our set of data seems logical if we acknowledge the fact that cytosolic FA activate PPARα and consequently induce OXPAT expression, resulting in OXPAT protein coating new nourishing LDs (Yamaguchi et al. 2006). Therefore it makes sense that OXPAT is more peripheral than LDs due to its employment in organizing newly endocytosed lipids, while mature,

organized and more internal LDs would have less need for OXPAT's intervention in boosting IMTG turnover (Figure 31).

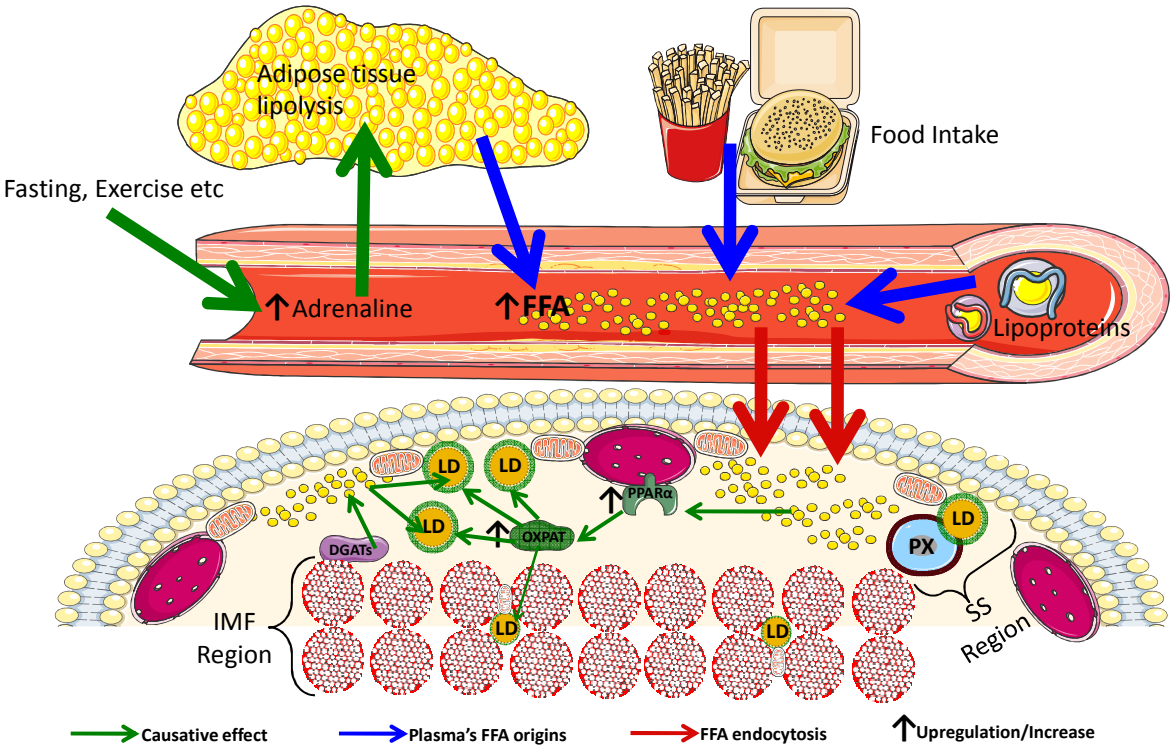

FIGURE 31. Model for LD and OXPAT more peripheral distribution. LDs are more abundant in SS region due to FFA internalization and increased mitochondrial activity. OXPAT is more peripheral than LDs due to OXPAT's function in managing freshly esterifying lipids for more immediate hydrolysis and oxidation in SS region. PX stands for peroxisome.

However, our results show both fiber types of OB and T2D groups having significantly closer OXPAT and COLOC to sarcolemma when comparing to LC group. An immediate explanation for this could be that T2D and OB have higher amount of FA in peripheral regions to be processed into LDs by OXPAT. Such FA could have two possible origins: *1)* internalized FFA from circulation; *2)* intracellular provenience by failed/impaired esterification or by peroxisomal/mitochondrial insufficiency to β-oxidize hydrolyzed FA (Figure 31). About the first hypothesis, despite our results showing several associations between tissue/plasma lipids (FAT%, FM, TCHOL, LDL, HDL and TAGemia) with particle closeness to membrane, we did not measure FFA uptake rates or even FFA concentrations in plasma. In fact, while some studies support that IR populations have higher rates of FFA uptake (Bonen et al. 2004), several other state

contrarily (Kelley & Simoneau 1994; Turpeinen et al. 1999; Blaak et al. 2000). Secondly, mitochondrial inefficiency uncoordinated with TAG hydrolysis (Kelley et al. 2002; Ritov et al. 2005) can result in leakage of FA into the SS region, possibly contributing for more peripheral OXPAT in OB and T2D groups. Moreover, it has been shown that during mechanical interaction with LDs, incapacitated peroxisomes which are unable to oxidize FA, promote the formation of the so called “gnarls”, which apparently are distorted LDs in the form of serial arranged layers of accumulated FFA (Binns et al. 2006). Therefore impaired peroxisomal function may also increase the need for OXPAT’s intervention in reorganizing LDs where they exist in higher number, in cell’s periphery.

9.2.3 Fiber type differences

A common pattern between groups was observed in particle closeness to membrane in different fiber types, especially in OXPAT and COLOC where type II fibers consistently show closer median position to membrane (Figure 27). Biologically, this could be mainly explained by the general lower capacity of type II fibers for internalizing and metabolizing lipids, being the fewer existing intracellular lipids in more peripheral regions as the SS region, thus in close proximity to where FFA internalize and where type II fiber lesser concentrations of myoglobulin could deliver oxygen to mitochondria and peroxisomes. In opposition, type I fibers have the capacity for processing higher quantity and more widespread distributed lipids, explaining thus the more internalized median position of LDs, OXPAT and COLOC.

However, our results interestingly show that LD closeness to membrane has an inverted tendency in the OB group, i.e., type I fibers have more peripheral LDs than type II fibers (Figure 27A). Such occurrence could be explained by one or both of the following: *1)* Type I fibers have higher rates of peripheral LD accretion given this fiber type higher capacity in internalizing and accumulating lipids coped with the increased tissue/plasma lipid concentrations in OB group; *2)* Type II fibers have excessive lipid internalization/esterification for its capacity to oxidize them, resulting in excessive

unprocessable IMTG in type II fiber inner regions. Concerning the first hypothesis, indeed OB and T2D have been already associated with higher FFA membrane and cytosolic transporters as CD36 and FABPpm, which in turn, have been shown be significantly more present in type I fibers (Bonen et al. 1998; Bonen et al. 2004). Moreover, Goodpaster's research group recently released a paper were they found a positive correlation between IR and higher IMTG in type I fibers but not in type II (Coen et al. 2010). Concerning the second possibility, one collection of type II fibers from OB subjects definitely show us high amount of LDs in inner regions, resembling even type I fibers (Figure 32). Indeed, our correlations (See 8.2.2) showed a positive association of fast_COL_content with both FAT% and FM. Furthermore, it has been suggested that IR is related with the presence of fat in tissues not well prepared for having fat itself, i.e., tissues with low oxidative capacity as type II fibers for instance. Consequently, given this scenario, it might not be too risky to conjecture that type I fibers having more peripheral LDs than type II fibers, might be a precursor or symptomatic condition for IR.

Nonetheless, when looking at LD closeness to membrane in T2D, we do not find the observed inverted fiber type tendency (Figure 27A). In our opinion this could be due to most subjects of this group being under T2D specific medication.

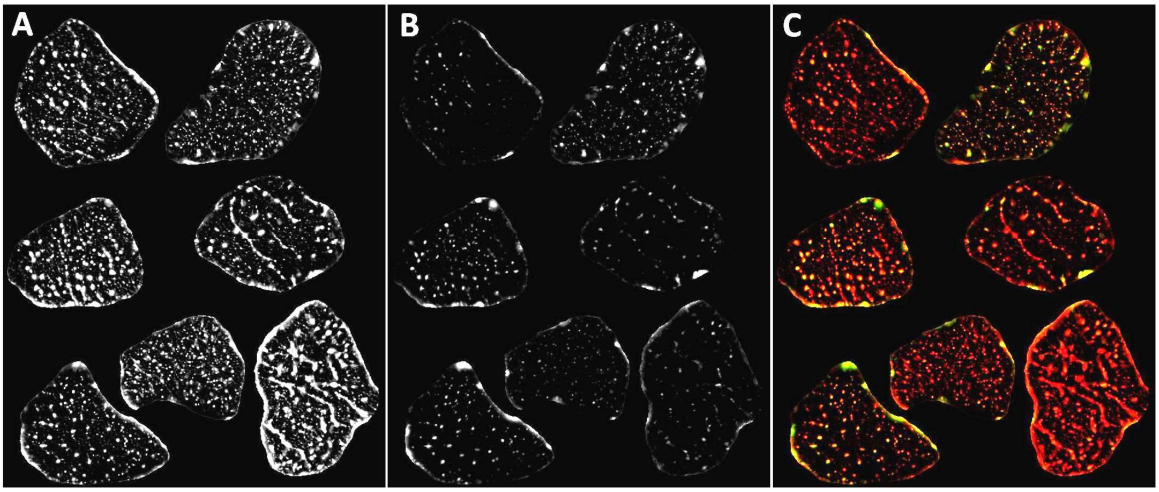

FIGURE 32. Type II fibers of OB group. Note abnormal content (intensity and number) of LDs in central regions (A), followed by weaker OXPAT labeling (B), resulting in strong reddish appearance of fibers (C). All images were equally manipulated in order to maintain true relative intensity.

9.2.4 Additional insights revealed by polynomial functions

The 2nd polynomial function line presented in figures 28, 29 and 30, is calculated upon the geography and intensity of each plotted particle. In our perspective, normal and healthy distribution patterns are shown by the LC group, where higher relative number of high intensity particles is in the periphery of cell and not in more central regions, thus resulting in a concave polynomial line. The OB group however, shows a convex polynomial line, revealing relative higher amount of high intensity LDs in central regions of cells. The fact that these high intensity inner LDs in OB are not equally followed by high intensity inner OXPAT, suggests that this group may have metabolic halted and ancient intramyocellular lipids, continuously esterified since long in the past with little oxidation occurring from then on.

Once again, T2D results are discordant with our perspective, since they show a balance between LC and OB groups. Likewise, we believe this might be a consequence of T2D medication most subjects were under (See 9.1).

9.3 Intramyocellular architecture and machinery

Mitochondria and Lipid Droplets. When detecting higher presence and intensity of LD and mitochondria in more peripheral regions of cells, an immediate and logic conjecture is brought by the need and closeness of oxygen provided from the sarcolemma. Hence, it is to be expected that oxygen dependent agents, like mitochondria, would be closer to where the former is provided, while LDs as important fuel providers and as FFA absorbers, are expected to be closer to oxidizers like mitochondria and closer to the plasma membrane where FFA are internalized.

Despite not colocalizing with the majority of mitochondrial signal, LDs are in fact mainly colocalized by the first, being the polygonal-like patterns observed in

mitochondria partly “imitated” by LD staining as if they coexist in the same physical architecture. In other words, it seems there is a strong behavioural pattern of LDs following oxidation active micro domains, but not so strong inverse relation (Figure 25). This could go into accordance with the stated relative ease and quickness LD travel through microtubules when comparing to other organelles (Murphy 2001; Bostrom et al. 2005; Welte et al. 2005).

Given the experiments setup by labelling COX one can speculate that, at the time of the biopsy collection, uncolocalized mitochondria could still be in oxidative work. If so, this would mean that mitochondrial β-oxidation is not dependent of LD closeness (few nanometers range) and that carnitines or others would be able to perform FFA transport efficiently throughout relatively long distances (several micrometers range). Of course, mitochondrial staining was performed against COX, which by only existing does not mean it is in oxidative work. Further studies involving specific stainings against mitochondria in oxidative work together with LD for instance, would be necessary to better describe the spatial dependency between these two oxidative organelles.

Neutral Lipid network and cytochrome c oxidase staining patterns. Mitochondrial labelling revealed a tendency to form polygonal structures which did not appear to be randomly organized. In fact, this labelings seemed to follow an organized logical structure (Figure 25). When comparing our semi shaped polygons drawn by COX against immunolabellings of SR performed by fellow colleagues in the University of Oulu (Rahkila et al. 1997; Kaakinen et al. 2008), one is rather tempted to make the assumption that mitochondrial staining patterns closely follow SR structure (Figure 33A and 33B). In fact, several studies show EM longitudinal sections where mitochondria and LD are repeatedly localized in close contact with myofibrils over the Z-line region (Hoppeler et al. 1973; van Loon & Goodpaster 2006; Tarnopolsky et al. 2007; Shaw et al. 2008).

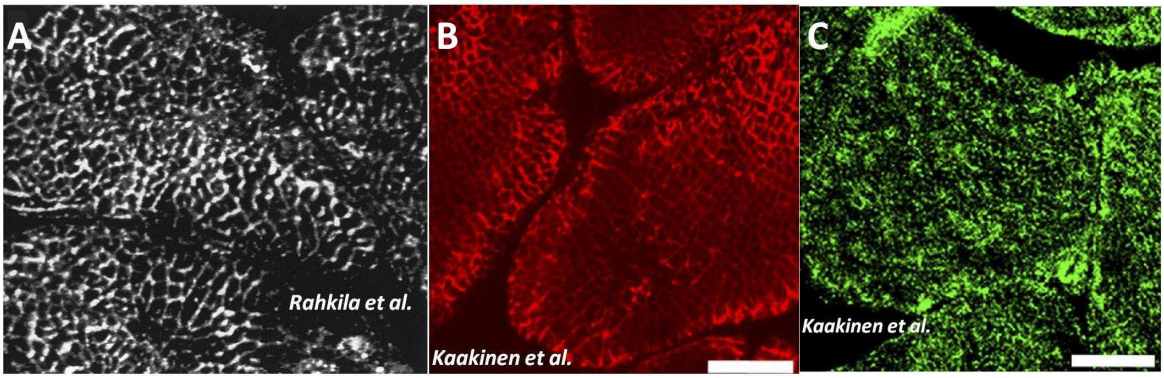

FIGURE 33. Sarcoplasmic and endoplasmic reticula immunolabelling. (A and B) SERCA label for SR (Rahkila et al. 1997; Kaakinen et al. 2008). (C) Sec61α label for ER (Kaakinen et al. 2008). Bars 10 µm.

On the other hand, despite LD partly colocalizing with the mentioned mitochondrial pattern, the fine network revealed by LipidTOX® stainings after neutral lipids seems a completely different structure. This impression is not only based on the dimensions of the smaller lipid polygons, but also on the more elongated shape of these throughout the cell (Figure 22). Different number and period of PBS washings were experimented and in all of these, the neutral lipid fine reticulum was still observed. In our opinion this network staining is hardly an artifact for it has been repeatedly seen in a dazzling well organized outline. In this phase of research where little is known about the phenomenon – even if it is real or not – many plausible explanations can arise, being the ER the most discussed possibility. By looking at Kaakinen and colleagues' sec61α labelings after ER in skeletal muscle cross sections (Figure 33C), it is possible to observe the complex abundance of ER network (Kaakinen et al. 2008), reinforcing, or at least not refuting, our suggestion that the neutral lipid network could be in fact the ER. If such network is real, more candidates besides ER can explain the phenomenon, as the SR in conjunction with the microtubular system for instance or perhaps a combination of the previous with ER itself. More real however, related or not, we repeatedly observed huge outlines formed by bigger LDs coated with OXPAT as if these were hanging in a common communicating structure (Figure 20).

No matter what organelle or organelles are shaping this neutral lipid reticulum, what could such an event mean biologically? Perhaps it could be a system in where neutral lipids transversely flow for normal cellular functions (See 3.3), being LDs only active

and ambulant storehouses where enzymes regulated by PAT proteins would more intensely manage the fate of neutral lipids. Despite never clearly demonstrate, this functional reticulum theory has been previously suggested by Murphy and colleagues (Murphy et al. 2009). Such a vision is supported by our observations (Figure 20) and by EM studies conducted on yeasts, where permanent contact and fusion between LDs were also documented (Binns et al. 2006).

Fast Myosin Heavy-Chain and Lipid Droplets. The first and main purpose for labeling Fast Myosin heavy-chain was to distinguish type II from type I fibers while looking at LDs and OXPAT in both. However, this also permitted an interesting observation, myosin heavy-chain labelling showed a strong tendency not to colocalize with LDs, being the latter many times surrounding the myosin bundles (Figure 26). If these bundles nicely shape the SR, one is tempted to suggest that, supporting what others have demonstrated with more appropriate setups (Meex et al. 2009), in skeletal muscle minute LDs exist in cytosolic extra SR space right between different myofibrils. However, in our fluorescent widefield images, a minority of these LDs appeared clearly colocalized with myosin bundles (arrows in Figures 26), leaving some room for discussion. The more reasonable explanation for this colocalization would be justifying it merely due to sectioning artifacts, being some droplets slightly deviated by the cryostat blade from the myofibril border towards the myofilaments cross sectioned surface, or maybe due to the biopsy taking with the Bergström needle. Or otherwise, can such considerably big organelles internalize the SR barrier towards myofibrils? Skeletal muscle LDs were already clearly shown by Meex and others to localize in between the myofibrils outside the SR (Meex et al. 2009) but could LDs be in the inner side of SR as well?

Lipid droplets are many times in regions where mitochondria are, that is, SS and IMF regions. However, it might not be too farfetched to hypothesize a pathological phenomenon where excess LDs would surpass SR and be placed in between myofilaments, causing mechanical and subsequent chemical impairments to the cell. The biggest constraint to this model is the reduced space between the densely packed and organized myofilaments, while it seems hard that considerably big structures like LDs could be able to pass through the SR (Figure 10). Such would probably require harsh

deformation or rupture of the SR itself. Nevertheless, it is known that the already mention CDS can cause myopathy accompanied with supra-sized LDs in skeletal muscle, thus it would not be too careless to consider intermediate conditions between healthy tissue and CDS tissue where the micro-biomechanics of skeletal muscle fibers would be negatively affected by over-sized LDs.

Although independent myosin bundles are easily distinguished, these are not the most suitable or reliable markers for SR visualization. Besides, fluorescent microscopy, has limited optimal resolution (>400nm) for such delicate magnitudes (<10nm). Therefore, these observations are under grave methodological constraints and further experiments are recommended.

10 CONCLUSIONS

Given the study purpose, our main finding was that from the three studied groups, LC had more internalized LDs, OXPAT and their colocalization and that T2D had more externalized LDs, OXPAT and their colocalization, while the OB group showed middle term values. We justify these results with the strong associations found between tissue plus plasma lipids and closeness of LDs and OXPAT to sarcolemma, suggesting that particle distance is directly dependent of systemic lipid abundance.

Our results are in accordance with very recent EM studies, which despite having higher resolution and better differentiate intracellular regions (Nielsen et al. 2010), lack the capacity for analysing the distribution of greater number of particles in different fiber types. Therefore, we developed an advantageous method where it is possible to measure intensity and relative geography of individual LDs and any other detected particle in huge numbers. We further found that type II fibers have more externalized particles than type I fibers and that this phenomenon is inverted in OB LDs, possibly reflecting symptomatic IR development.

As far as we are aware, this is the first study reporting OXPAT intramyocellular distribution and its association with LDs in different fiber types. Furthermore, we found that OXPAT is more peripheral than LDs and that the former very likely preferably associate with more peripheral LDs. Suggesting that increased OXPAT targets towards newly formed and/or energetically more active LDs.

Moreover, our polynomial functions revealed that OB group has more relative amount of high intensity centralized LDs than other groups, and that these LDs are not equally followed by high intensity OXPAT. Suggesting that these centralized lipids have different metabolic fates rather than being FA esterification sites for immediate

hydrolysis. Further research should be carried in order to conclude if these specific LDs are related with the development of IR.

Finally, in our descriptive observations, we also reported big LD/OXPAT intracellular structure-like outlines, in addition to a very fine network structure revealed by the neutral lipid dye. This network further needs to be proved real, but it already opens many doors for future research, as it can be the already hypothesized “neutral lipid highway” structure (Murphy 2001), where LDs would be no more than bulky deposits in a continuum of communicating lipids, active and coordinated in many cell functions.

11 REFERENCES

Aitman, T. J., A. M. Glazier, C. A. Wallace, L. D. Cooper, P. J. Norsworthy, F. N. Wahid, K. M. Al-Majali, P. M. Trembling, C. J. Mann, C. C. Shoulders, D. Graf, E. St Lezin, T. W. Kurtz, V. Kren, M. Pravenec, A. Ibrahimi, N. A. Abumrad, L. W. Stanton and J. Scott 1999. Identification of Cd36 (Fat) as an insulin-resistance gene causing defective fatty acid and glucose metabolism in hypertensive rats. Nat Genet 21(1): 76-83.

Bartz, R., W. H. Li, B. Venables, J. K. Zehmer, M. R. Roth, R. Welti, R. G. Anderson, P. Liu and K. D. Chapman 2007. Lipidomics reveals that adiposomes store ether lipids and mediate phospholipid traffic. J Lipid Res 48(4): 837-47.

Bickel, P. E., J. T. Tansey and M. A. Welte 2009. PAT proteins, an ancient family of lipid droplet proteins that regulate cellular lipid stores. Biochim Biophys Acta.

Binns, D., T. Januszewski, Y. Chen, J. Hill, V. S. Markin, Y. Zhao, C. Gilpin, K. D. Chapman, R. G. W. Anderson and J. M. Goodman 2006. An intimate collaboration between peroxisomes and lipid bodies. J. Cell Biol. 173(5): 719-731.

Blaak, E. E. 2005. Metabolic fluxes in skeletal muscle in relation to obesity and insulin resistance. Best Pract Res Clin Endocrinol Metab 19(3): 391-403.

Blaak, E. E., A. J. Wagenmakers, J. F. Glatz, B. H. Wolffenbuttel, G. J. Kemerink, C. J. Langenberg, G. A. Heidendal and W. H. Saris 2000. Plasma FFA utilization and fatty acid-binding protein content are diminished in type 2 diabetic muscle. Am J Physiol Endocrinol Metab 279(1): E146-54.

Bonen, A., J. J. Luiken, S. Liu, D. J. Dyck, B. Kiens, S. Kristiansen, L. P. Turcotte, G. J. Van Der Vusse and J. F. Glatz 1998. Palmitate transport and fatty acid transporters in red and white muscles. Am J Physiol 275(3 Pt 1): E471-8.

Bonen, A., M. L. Parolin, G. R. Steinberg, J. Calles-Escandon, N. N. Tandon, J. F. Glatz, J. J. Luiken, G. J. Heigenhauser and D. J. Dyck 2004. Triacylglycerol accumulation in human obesity and type 2 diabetes is associated with increased rates of skeletal muscle fatty acid transport and increased sarcolemmal FAT/CD36. FASEB J 18(10): 1144-6.

Bostrom, P., M. Rutberg, J. Ericsson, P. Holmdahl, L. Andersson, M. A. Frohman, J. Boren and S. O. Olofsson 2005. Cytosolic lipid droplets increase in size by microtubule-dependent complex formation. Arterioscler Thromb Vasc Biol 25(9): 1945-51.

Brasaemle, D., T. Barber, N. Wolins, G. Serrero, E. Blanchette-Mackie and C. Londos 1997. Adipose differentiation-related protein is an ubiquitously expressed lipid storage droplet-associated protein. J. Lipid Res. 38(11): 2249-2263.

Brasaemle, D. L., G. Dolios, L. Shapiro and R. Wang 2004. Proteomic analysis of proteins associated with lipid droplets of basal and lipolytically stimulated 3T3-L1 adipocytes. J Biol Chem 279(45): 46835-42.

Bruce, C. R., M. J. Anderson, A. L. Carey, D. G. Newman, A. Bonen, A. D. Kriketos, G. J. Cooney and J. A. Hawley 2003. Muscle oxidative capacity is a better predictor of insulin sensitivity than lipid status. J Clin Endocrinol Metab 88(11): 5444-51.

Bruce, C. R., C. Brolin, N. Turner, M. E. Cleasby, F. R. van der Leij, G. J. Cooney and E. W. Kraegen 2007. Overexpression of carnitine palmitoyltransferase I in skeletal muscle in vivo increases fatty acid oxidation and reduces triacylglycerol esterification. Am J Physiol Endocrinol Metab 292(4): E1231-1237.

Bulankina, A. V., A. Deggerich, D. Wenzel, K. Mutenda, J. G. Wittmann, M. G. Rudolph, K. N. Burger and S. Honing 2009. TIP47 functions in the biogenesis of lipid droplets. J Cell Biol 185(4): 641-55.

Chang, B. H., L. Li, A. Paul, S. Taniguchi, V. Nannegari, W. C. Heird and L. Chan 2006. Protection against fatty liver but normal adipogenesis in mice lacking adipose differentiation-related protein. Mol Cell Biol 26(3): 1063-76.

Coen, P. M., J. J. DubÃ©, F. Amati, M. Stefanovic-Racic, R. E. Ferrell, F. G. S. Toledo and B. H. Goodpaster 2010. Insulin Resistance Is Associated With Higher Intramyocellular Triglycerides in Type I but Not Type II Myocytes Concomitant With Higher Ceramide Content. Diabetes 59(1): 80-88.

Costes, S. V., D. Daelemans, E. H. Cho, Z. Dobbin, G. Pavlakis and S. Lockett 2004. Automatic and Quantitative Measurement of Protein-Protein Colocalization in Live Cells. Biophysical Journal 86(6): 3993-4003.

Dagenais, G. R., R. G. Tancredi and K. L. Zierler 1976. FREE FATTY-ACID OXIDATION BY FOREARM MUSCLE AT REST, AND EVIDENCE FOR AN INTRAMUSCULAR LIPID POOL IN HUMAN FOREARM. Journal of Clinical Investigation 58(2): 421-431.

Dalen, K. T., T. Dahl, E. Holter, B. Arntsen, C. Londos, C. Sztalryd and H. I. Nebb 2007. LSDP5 is a PAT protein specifically expressed in fatty acid oxidizing tissues. Biochim Biophys Acta 1771(2): 210-27.

Denton, R. M. and P. J. Randle 1967. Concentrations of glycerides and phospholipids in rat heart and gastrocnemius muscles. Effects of alloxan-diabetes and perfusion. Biochem J 104(2): 416-22.

Diaz, E. and S. R. Pfeffer 1998. TIP47: a cargo selection device for mannose 6-phosphate receptor trafficking. Cell 93(3): 433-43.

Ducharme, N. A. and P. E. Bickel 2008. Lipid droplets in lipogenesis and lipolysis. Endocrinology 149(3): 942-9.

Egan, J. J., A. S. Greenberg, M. K. Chang and C. Londos 1990. Control of endogenous phosphorylation of the major cAMP-dependent protein kinase substrate in adipocytes by insulin and beta-adrenergic stimulation. J Biol Chem 265(31): 18769-75.

Ehrman, J. K. (2003). Clinical exercise physiology. Champaign, IL ;, Human Kinetics.

Fujimoto, T., H. Kogo, K. Ishiguro, K. Tauchi and R. Nomura 2001. Caveolin-2 Is Targeted to Lipid Droplets, a New "Membrane Domain" in the Cell. J. Cell Biol. 152(5): 1079-1086.

Fujimoto, T., Y. Ohsaki, J. Cheng, M. Suzuki and Y. Shinohara 2008. Lipid droplets: a classic organelle with new outfits. Histochem Cell Biol 130(2): 263-79.

Ganong, W. F. (1987). Review of medical physiology. Norwalk, Conn., Appleton & Lange.

Gao, J. and G. Serrero 1999. Adipose Differentiation Related Protein (ADRP) Expressed in Transfected COS-7 Cells Selectively Stimulates Long Chain Fatty Acid Uptake. Journal of Biological Chemistry 274(24): 16825-16830.

Gaster, M., A. C. Rustan, V. Aas and H. Beck-Nielsen 2004. Reduced lipid oxidation in skeletal muscle from type 2 diabetic subjects may be of genetic origin: evidence from cultured myotubes. Diabetes 53(3): 542-8.

Glatz, J. F., F. G. Schaap, B. Binas, A. Bonen, G. J. van der Vusse and J. J. Luiken 2003. Cytoplasmic fatty acid-binding protein facilitates fatty acid utilization by skeletal muscle. Acta Physiol Scand 178(4): 367-71.

Goodman, J. M. 2008. The gregarious lipid droplet. J Biol Chem 283(42): 28005-9.

Goodpaster, B. H., J. He, S. Watkins and D. E. Kelley 2001. Skeletal muscle lipid content and insulin resistance: evidence for a paradox in endurance-trained athletes. J Clin Endocrinol Metab 86(12): 5755-61.

Goodpaster, B. H. and D. Wolf 2004. Skeletal muscle lipid accumulation in obesity, insulin resistance, and type 2 diabetes. Pediatr Diabetes 5(4): 219-26.

Granneman, J. G., H. P. Moore, E. P. Mottillo and Z. Zhu 2009. Functional interactions between Mldp (LSDP5) and Abhd5 in the control of intracellular lipid accumulation. J Biol Chem 284(5): 3049-57.

Gross, D. N., H. Miyoshi, T. Hosaka, H. H. Zhang, E. C. Pino, S. Souza, M. Obin, A. S. Greenberg and P. F. Pilch 2006. Dynamics of lipid droplet-associated proteins during hormonally stimulated lipolysis in engineered adipocytes: stabilization and lipid droplet binding of adipocyte differentiation-related protein/adipophilin. Mol Endocrinol 20(2): 459-66.

Guo, Y., K. R. Cordes, R. V. Farese, Jr. and T. C. Walther 2009. Lipid droplets at a glance. J Cell Sci 122(Pt 6): 749-52.

He, J., B. H. Goodpaster and D. E. Kelley 2004. Effects of weight loss and physical activity on muscle lipid content and droplet size. Obes Res 12(5): 761-9.

Heid, H. W., R. Moll, I. Schwetlick, H. R. Rackwitz and T. W. Keenan 1998. Adipophilin is a specific marker of lipid accumulation in diverse cell types and diseases. Cell Tissue Res 294(2): 309-21.

Hoppeler, H., P. Luthi, H. Claassen, E. R. Weibel and H. Howald 1973. The ultrastructure of the normal human skeletal muscle. A morphometric analysis on untrained men, women and well-trained orienteers. Pflugers Arch 344(3): 217-32.

Hulver, M. W., J. R. Berggren, R. N. Cortright, R. W. Dudek, R. P. Thompson, W. J. Pories, K. G. MacDonald, G. W. Cline, G. I. Shulman, G. L. Dohm and J. A. Houmard 2003. Skeletal muscle lipid metabolism with obesity. Am J Physiol Endocrinol Metab 284(4): E741-7.

Imamura, M., T. Inoguchi, S. Ikuyama, S. Taniguchi, K. Kobayashi, N. Nakashima and H. Nawata 2002. ADRP stimulates lipid accumulation and lipid droplet formation in murine fibroblasts. Am J Physiol Endocrinol Metab 283(4): E775-83.

Jiang, H. P. and G. Serrero 1992. Isolation and characterization of a full-length cDNA coding for an adipose differentiation-related protein. Proc Natl Acad Sci U S A 89(17): 7856-60.

Kaakinen, M., H. Papponen and K. Metsikkö 2008. Microdomains of endoplasmic reticulum within the sarcoplasmic reticulum of skeletal myofibers. Experimental Cell Research 314(2): 237-245.

Kanaley, J. A., S. Shadid, M. T. Sheehan, Z. Guo and M. D. Jensen 2009. Relationship between plasma free fatty acid, intramyocellular triglycerides and long-chain acylcarnitines in resting humans. J Physiol 587(Pt 24): 5939-50.

Kelley, D. E., J. He, E. V. Menshikova and V. B. Ritov 2002. Dysfunction of mitochondria in human skeletal muscle in type 2 diabetes. Diabetes 51(10): 2944-50.

Kelley, D. E. and J. A. Simoneau 1994. Impaired free fatty acid utilization by skeletal muscle in non-insulin-dependent diabetes mellitus. J Clin Invest 94(6): 2349-56.

Kiens, B. 2006. Skeletal muscle lipid metabolism in exercise and insulin resistance. Physiol Rev 86(1): 205-43.

Kiens, B., C. Roepstorff, J. F. Glatz, A. Bonen, P. Schjerling, J. Knudsen and J. N. Nielsen 2004. Lipid-binding proteins and lipoprotein lipase activity in human skeletal muscle: influence of physical activity and gender. J Appl Physiol 97(4): 1209-18.

Kivistö, R. (2008). Energy expenditure and substrate utilization during eccentric exercise in obese and diabetics. Department of Biology of Physical Activity. Jyväskylä, University of Jyväskylä. **Master:** 92.

Koves, T. R., R. C. Noland, A. L. Bates, S. T. Henes, D. M. Muoio and R. N. Cortright 2005. Subsarcolemmal and intermyofibrillar mitochondria play distinct roles in regulating skeletal muscle fatty acid metabolism. Am J Physiol Cell Physiol 288(5): C1074-82.

Krahmer, N., Y. Guo, R. V. Farese, Jr. and T. C. Walther 2009. SnapShot: Lipid Droplets. Cell 139(5): 1024-1024 e1.

Kuerschner, L., C. Moessinger and C. Thiele 2008. Imaging of lipid biosynthesis: how a neutral lipid enters lipid droplets. Traffic 9(3): 338-52.

Lass, A., R. Zimmermann, G. Haemmerle, M. Riederer, G. Schoiswohl, M. Schweiger, P. Kienesberger, J. G. Strauss, G. Gorkiewicz and R. Zechner 2006. Adipose triglyceride lipase-mediated lipolysis of cellular fat stores is activated by CGI-58 and defective in Chanarin-Dorfman Syndrome. Cell Metabolism 3(5): 309-319.

Lay, S. L. and I. Dugail 2009. Connecting lipid droplet biology and the metabolic syndrome. Prog Lipid Res.

Leber, R., E. Zinser, G. Zellnig, F. Paltauf and G. Daum 1994. Characterization of lipid particles of the yeast, Saccharomyces cerevisiae. Yeast 10(11): 1421-8.

Lieber, R. L., G. J. Loren and J. Friden 1994. In vivo measurement of human wrist extensor muscle sarcomere length changes. J Neurophysiol 71(3): 874-81.

Listenberger, L. L., X. Han, S. E. Lewis, S. Cases, R. V. Farese, Jr., D. S. Ory and J. E. Schaffer 2003. Triglyceride accumulation protects against fatty acid-induced lipotoxicity. Proc Natl Acad Sci U S A 100(6): 3077-82.

Listenberger, L. L., A. G. Ostermeyer-Fay, E. B. Goldberg, W. J. Brown and D. A. Brown 2007. Adipocyte differentiation-related protein reduces the lipid droplet association of adipose triglyceride lipase and slows triacylglycerol turnover. J. Lipid Res. 48(12): 2751-2761.

Liu, P., R. Bartz, J. K. Zehmer, Y. S. Ying, M. Zhu, G. Serrero and R. G. Anderson 2007. Rab-regulated interaction of early endosomes with lipid droplets. Biochim Biophys Acta 1773(6): 784-93.

Liu, P., Y. Ying, Y. Zhao, D. I. Mundy, M. Zhu and R. G. Anderson 2004. Chinese hamster ovary K2 cell lipid droplets appear to be metabolic organelles involved in membrane traffic. J Biol Chem 279(5): 3787-92.

Londos, C., D. L. Brasaemle, C. J. Schultz, J. P. Segrest and A. R. Kimmel 1999. Perilipins, ADRP, and other proteins that associate with intracellular neutral lipid droplets in animal cells. Semin Cell Dev Biol 10(1): 51-8.

Londos, C., C. Sztalryd, J. T. Tansey and A. R. Kimmel 2005. Role of PAT proteins in lipid metabolism. Biochimie 87(1): 45-9.

Machann, J., H. Haring, F. Schick and M. Stumvoll 2004. Intramyocellular lipids and insulin resistance. Diabetes Obes Metab 6(4): 239-48.

Malenfant, P., D. R. Joanisse, R. Theriault, B. H. Goodpaster, D. E. Kelley and J. A. Simoneau 2001. Fat content in individual muscle fibers of lean and obese subjects. Int J Obes Relat Metab Disord 25(9): 1316-21.

Martin, S. and R. G. Parton 2006. Lipid droplets: a unified view of a dynamic organelle. Nat Rev Mol Cell Biol 7(5): 373-8.

Maughan, R. J., M. Gleeson and P. L. Greenhaff (1997). Biochemistry of exercise and training. Oxford [England] ; New York, Oxford University Press.

Meex, R. C., P. Schrauwen and M. K. Hesselink 2009. Modulation of myocellular fat stores: lipid droplet dynamics in health and disease. Am J Physiol Regul Integr Comp Physiol 297(4): R913-24.

Mensink, M., E. E. Blaak, M. A. van Baak, A. J. Wagenmakers and W. H. Saris 2001. Plasma free Fatty Acid uptake and oxidation are already diminished in subjects at high risk for developing type 2 diabetes. Diabetes 50(11): 2548-54.

Minnaard, R., P. Schrauwen, G. Schaart, J. A. Jorgensen, E. Lenaers, M. Mensink and M. K. C. Hesselink 2009. Adipocyte Differentiation-Related Protein and OXPAT in Rat and Human Skeletal Muscle: Involvement in Lipid Accumulation and Type 2 Diabetes Mellitus. J Clin Endocrinol Metab 94(10): 4077-4085.

Minnaard, R., P. Schrauwen, G. Schaart, E. Lenaers, M. Mensink and M. Hesselink 2008. ADRP and OXPAT protein content in muscular lipid accumulation and insulin resistance. Chemistry and Physics of Lipids 154: S49-S49.

Miura, S., J. W. Gan, J. Brzostowski, M. J. Parisi, C. J. Schultz, C. Londos, B. Oliver and A. R. Kimmel 2002. Functional conservation for lipid storage droplet association among Perilipin, ADRP, and TIP47 (PAT)-related proteins in mammals, Drosophila, and Dictyostelium. J Biol Chem 277(35): 32253-7.

Mooren, F. and K. Völker (2005). Molecular and cellular exercise physiology. Champaign, IL, Human Kinetics.

Morgan, T. E., F. A. Short and L. A. Cobb 1969. Effect of long-term exercise on skeletal muscle lipid composition. Am J Physiol 216(1): 82-6.

Moro, C., S. Bajpeyi and S. R. Smith 2008. Determinants of intramyocellular triglyceride turnover: implications for insulin sensitivity. Am J Physiol Endocrinol Metab 294(2): E203-13.

Murphy, D. J. 2001. The biogenesis and functions of lipid bodies in animals, plants and microorganisms. Prog Lipid Res 40(5): 325-438.

Murphy, S., S. Martin and R. G. Parton 2009. Lipid droplet-organelle interactions; sharing the fats. Biochim Biophys Acta 1791(6): 441-7.

Nabi, I. R. and P. U. Le 2003. Caveolae/raft-dependent endocytosis. J Cell Biol 161(4): 673-7.

Nakamura, N. and T. Fujimoto 2003. Adipose differentiation-related protein has two independent domains for targeting to lipid droplets. Biochemical and Biophysical Research Communications 306(2): 333-338.

Nielsen, J., M. Mogensen, B. F. Vind, K. Sahlin, K. Hojlund, H. D. Schroder and N. Ortenblad 2010. Increased subsarcolemmal lipids in type 2 diabetes: effect of training on localization of lipids, mitochondria, and glycogen in sedentary human skeletal muscle. Am J Physiol Endocrinol Metab 298(3): E706-713.

Oberbach, A., Y. Bossenz, S. Lehmann, J. Niebauer, V. Adams, R. Paschke, M. R. Schon, M. Bluher and K. Punkt 2006. Altered fiber distribution and fiber-specific glycolytic and oxidative enzyme activity in skeletal muscle of patients with type 2 diabetes. Diabetes Care 29(4): 895-900.

Ohsaki, Y., J. Cheng, A. Fujita, T. Tokumoto and T. Fujimoto 2006. Cytoplasmic lipid droplets are sites of convergence of proteasomal and autophagic degradation of apolipoprotein B. Mol Biol Cell 17(6): 2674-83.

Ohsaki, Y., T. Maeda, M. Maeda, K. Tauchi-Sato and T. Fujimoto 2006. Recruitment of TIP47 to lipid droplets is controlled by the putative hydrophobic cleft. Biochem Biophys Res Commun 347(1): 279-87.

Olofsson, S. O., P. Bostrom, L. Andersson, M. Rutberg, J. Perman and J. Boren 2008. Lipid droplets as dynamic organelles connecting storage and efflux of lipids. Biochim Biophys Acta.

Phillips, S. A., C. C. Choe, T. P. Ciaraldi, A. S. Greenberg, A. P. Kong, S. C. Baxi, L. Christiansen, S. R. Mudaliar and R. R. Henry 2005. Adipocyte differentiation-related protein in human skeletal muscle: relationship to insulin sensitivity. Obes Res 13(8): 1321-9.

Pol, A., S. Martin, M. A. Fernandez, M. Ingelmo-Torres, C. Ferguson, C. Enrich and R. G. Parton 2005. Cholesterol and fatty acids regulate dynamic caveolin trafficking through the Golgi complex and between the cell surface and lipid bodies. Mol Biol Cell 16(4): 2091-105.

Prats, C., M. Donsmark, K. Qvortrup, C. Londos, C. Sztalryd, C. Holm, H. Galbo and T. Ploug 2006. Decrease in intramuscular lipid droplets and translocation of HSL in response to muscle contraction and epinephrine. J Lipid Res 47(11): 2392-9.

Prattes, S., G. Horl, A. Hammer, A. Blaschitz, W. F. Graier, W. Sattler, R. Zechner and E. Steyrer 2000. Intracellular distribution and mobilization of unesterified cholesterol in adipocytes: triglyceride droplets are surrounded by cholesterol-rich ER-like surface layer structures. J Cell Sci 113 (Pt 17): 2977-89.

Rahkila, P., K. Vaananen, J. Saraste and K. Metsikko 1997. Endoplasmic reticulum to Golgi trafficking in multinucleated skeletal muscle fibers. Exp Cell Res 234(2): 452-64.

Rajendran, L., S. Le Lay and H. Illges 2007. Raft association and lipid droplet targeting of flotillins are independent of caveolin. Biol Chem 388(3): 307-14.

Ritov, V. B., E. V. Menshikova, J. He, R. E. Ferrell, B. H. Goodpaster and D. E. Kelley 2005. Deficiency of subsarcolemmal mitochondria in obesity and type 2 diabetes. Diabetes 54(1): 8-14.

Robenek, H., I. Buers, O. Hofnagel, M. J. Robenek, D. Troyer and N. J. Severs 2008. Compartmentalization of proteins in lipid droplet biogenesis. Biochim Biophys Acta.

Robenek, H., M. J. Robenek, I. Buers, S. Lorkowski, O. Hofnagel, D. Troyer and N. J. Severs 2005. Lipid droplets gain PAT family proteins by interaction with specialized plasma membrane domains. J Biol Chem 280(28): 26330-8.

Robenek, H., M. J. Robenek and D. Troyer 2005. PAT family proteins pervade lipid droplet cores. J Lipid Res 46(6): 1331-8.

Russell, A. P. 2004. Lipotoxicity: the obese and endurance-trained paradox. Int J Obes Relat Metab Disord 28 Suppl 4: S66-71.

Schrauwen-Hinderling, V. B., M. K. C. Hesselink, P. Schrauwen and M. E. Kooi 2006. Intramyocellular Lipid Content in Human Skeletal Muscle[ast]. Obesity 14(3): 357-367.

Schrauwen-Hinderling, V. B., M. E. Kooi, M. K. Hesselink, J. A. Jeneson, W. H. Backes, C. J. van Echteld, J. M. van Engelshoven, M. Mensink and P. Schrauwen 2007. Impaired in vivo mitochondrial function but similar intramyocellular lipid content in patients with type 2 diabetes mellitus and BMI-matched control subjects. Diabetologia 50(1): 113-20.

Shaw, C. S., D. A. Jones and A. J. Wagenmakers 2008. Network distribution of mitochondria and lipid droplets in human muscle fibres. Histochem Cell Biol 129(1): 65-72.

Shaw, C. S., M. Sherlock, P. M. Stewart and A. J. Wagenmakers 2009. Adipophilin distribution and colocalisation with lipid droplets in skeletal muscle. Histochem Cell Biol.

Shin, H. D., L. H. Kim, B. L. Park, H. S. Jung, Y. M. Cho, M. K. Moon, H. K. Lee and K. S. Park 2003. Polymorphisms in fatty acid-binding protein-3 (FABP3) - putative association with type 2 diabetes mellitus. Hum Mutat 22(2): 180.

Silverthorn, D. U. (2007). Human physiology : an integrated approach. San Francisco, Pearson/Benjamin Cummings.

Simoneau, J. A., S. R. Colberg, F. L. Thaete and D. E. Kelley 1995. Skeletal muscle glycolytic and oxidative enzyme capacities are determinants of insulin sensitivity and muscle composition in obese women. FASEB J 9(2): 273-8.

Stumvoll, M. and H. Haring 2002. The peroxisome proliferator-activated receptor-gamma2 Pro12Ala polymorphism. Diabetes 51(8): 2341-7.

Sturmey, R. G., P. J. O'Toole and H. J. Leese 2006. Fluorescence resonance energy transfer analysis of mitochondrial:lipid association in the porcine oocyte. Reproduction 132(6): 829-37.

Su, X. and N. A. Abumrad 2009. Cellular fatty acid uptake: a pathway under construction. Trends Endocrinol Metab 20(2): 72-7.

Sugden, M. C., M. G. Zariwala and M. J. Holness PPARs and the orchestration of metabolic fuel selection. Pharmacological Research In Press, Corrected Proof.

Sztalryd, C., M. Bell, X. Lu, P. Mertz, S. Hickenbottom, B. H. Chang, L. Chan, A. R. Kimmel and C. Londos 2006. Functional compensation for adipose differentiation-related protein (ADFP) by Tip47 in an ADFP null embryonic cell line. J Biol Chem 281(45): 34341-8.

Tarnopolsky, M. A., C. D. Rennie, H. A. Robertshaw, S. N. Fedak-Tarnopolsky, M. C. Devries and M. J. Hamadeh 2007. Influence of endurance exercise training and sex on intramyocellular lipid and mitochondrial ultrastructure, substrate use, and mitochondrial enzyme activity. Am J Physiol Regul Integr Comp Physiol 292(3): R1271-8.

Tauchi-Sato, K., S. Ozeki, T. Houjou, R. Taguchi and T. Fujimoto 2002. The surface of lipid droplets is a phospholipid monolayer with a unique Fatty Acid composition. J Biol Chem 277(46): 44507-12.

Turner, N., C. R. Bruce, S. M. Beale, K. L. Hoehn, T. So, M. S. Rolph and G. J. Cooney 2007. Excess lipid availability increases mitochondrial fatty acid oxidative capacity in muscle: evidence against a role for reduced fatty acid oxidation in lipid-induced insulin resistance in rodents. Diabetes 56(8): 2085-92.

Turpeinen, A. K., T. O. Takala, P. Nuutila, T. Axelin, M. Luotolahti, M. Haaparanta, J. Bergman, H. Hamalainen, H. Iida, M. Maki, M. I. Uusitupa and J. Knuuti 1999. Impaired free fatty acid uptake in skeletal muscle but not in myocardium in patients with impaired glucose tolerance: studies with PET and 14(R,S)-[18F]fluoro-6-thia-heptadecanoic acid. Diabetes 48(6): 1245-50.

van Loon, L. J. and B. H. Goodpaster 2006. Increased intramuscular lipid storage in the insulin-resistant and endurance-trained state. Pflugers Arch 451(5): 606-16.

van Loon, L. J., R. Koopman, R. Manders, W. van der Weegen, G. P. van Kranenburg and H. A. Keizer 2004. Intramyocellular lipid content in type 2 diabetes patients compared with overweight sedentary men and highly trained endurance athletes. Am J Physiol Endocrinol Metab 287(3): E558-65.

van Manen, H. J., Y. M. Kraan, D. Roos and C. Otto 2005. Single-cell Raman and fluorescence microscopy reveal the association of lipid bodies with phagosomes in leukocytes. Proc Natl Acad Sci U S A 102(29): 10159-64.

Vance, J. E. and K. Moldave (2003). Molecular and Cell Biology of Phosphatidylserine and Phosphatidylethanolamine Metabolism. Progress in Nucleic Acid Research and Molecular Biology. In ed, Academic Press. **Volume 75:** 69-111.

Vermathen, P., R. Kreis and C. Boesch 2004. Distribution of intramyocellular lipids in human calf muscles as determined by MR spectroscopic imaging. Magn Reson Med 51(2): 253-62.

Vistisen, B., K. Roepstorff, C. Roepstorff, A. Bonen, B. van Deurs and B. Kiens 2004. Sarcolemmal FAT/CD36 in human skeletal muscle colocalizes with caveolin-3 and is more abundant in type 1 than in type 2 fibers. J Lipid Res 45(4): 603-9.

Vock, R., H. Hoppeler, H. Claassen, D. X. Wu, R. Billeter, J. M. Weber, C. R. Taylor and E. R. Weibel 1996. Design of the oxygen and substrate pathways. VI. structural basis of intracellular substrate supply to mitochondria in muscle cells. J Exp Biol 199(Pt 8): 1689-97.

Walther, T. C. and R. V. Farese, Jr. 2008. The life of lipid droplets. Biochim Biophys Acta.

Wang, H., L. Hu, K. Dalen, H. Dorward, A. Marcinkiewicz, D. Russell, D. Gong, C. Londos, T. Yamaguchi, C. Holm, M. A. Rizzo, D. Brasaemle and C. Sztalryd 2009. Activation of hormone-sensitive lipase requires two steps, protein phosphorylation and binding to the PAT-1 domain of lipid droplet coat proteins. J Biol Chem 284(46): 32116-25.

Watt, M. J. 2009. Storing up trouble: does accumulation of intramyocellular triglyceride protect skeletal muscle from insulin resistance? Clin Exp Pharmacol Physiol 36(1): 5-11.

Wayman, N. S., Y. Hattori, M. C. McDonald, H. Mota-Filipe, S. Cuzzocrea, B. Pisano, P. K. Chatterjee and C. Thiemermann 2002. Ligands of the peroxisome proliferator-activated receptors (PPAR-gamma and PPAR-alpha) reduce myocardial infarct size. FASEB J 16(9): 1027-40.

Welte, M. A. 2007. Proteins under new management: lipid droplets deliver. Trends Cell Biol 17(8): 363-9.

Welte, M. A., S. Cermelli, J. Griner, A. Viera, Y. Guo, D. H. Kim, J. G. Gindhart and S. P. Gross 2005. Regulation of lipid-droplet transport by the perilipin homolog LSD2. Curr Biol 15(14): 1266-75.

Wolins, N. E., D. L. Brasaemle and P. E. Bickel 2006. A proposed model of fat packaging by exchangeable lipid droplet proteins. FEBS Lett 580(23): 5484-91.

Wolins, N. E., B. K. Quaynor, J. R. Skinner, M. J. Schoenfish, A. Tzekov and P. E. Bickel 2005. S3-12, Adipophilin, and TIP47 package lipid in adipocytes. J Biol Chem 280(19): 19146-55.

Wolins, N. E., B. K. Quaynor, J. R. Skinner, A. Tzekov, M. A. Croce, M. C. Gropler, V. Varma, A. Yao-Borengasser, N. Rasouli, P. A. Kern, B. N. Finck and P. E. Bickel 2006. OXPAT/PAT-1 is a PPAR-induced lipid droplet protein that promotes fatty acid utilization. Diabetes 55(12): 3418-28.

Wolins, N. E., B. Rubin and D. L. Brasaemle 2001. TIP47 associates with lipid droplets. J Biol Chem 276(7): 5101-8.

Wolins, N. E., J. R. Skinner, M. J. Schoenfish, A. Tzekov, K. G. Bensch and P. E. Bickel 2003. Adipocyte protein S3-12 coats nascent lipid droplets. J Biol Chem 278(39): 37713-21.

Yamaguchi, T., S. Matsushita, K. Motojima, F. Hirose and T. Osumi 2006. MLDP, a novel PAT family protein localized to lipid droplets and enriched in the heart, is regulated by peroxisome proliferator-activated receptor alpha. J Biol Chem 281(20): 14232-40.

Zimmermann, R., A. Lass, G. Haemmerle and R. Zechner 2008. Fate of fat: The role of adipose triglyceride lipase in lipolysis. Biochim Biophys Acta.

12 APPENDICES

Appendix I. The “Egg-cup” phenomenon

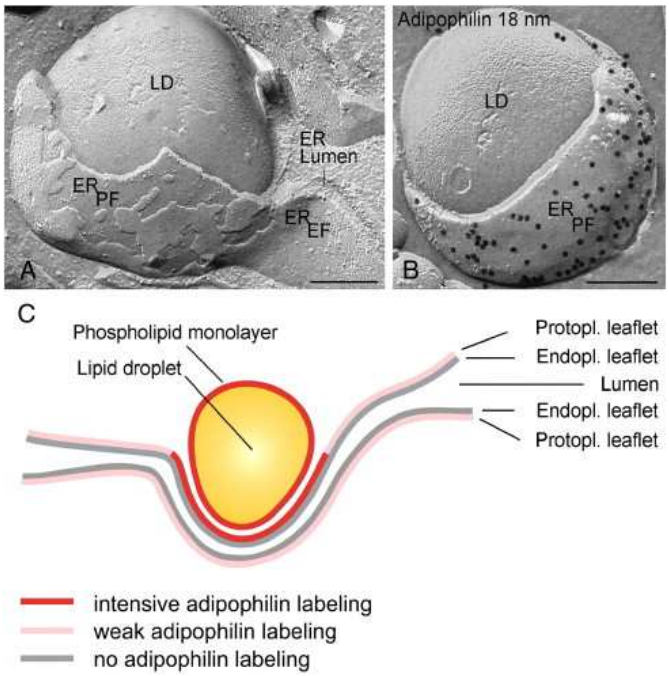

Up till date, LDs were never observed inside the ER lumen. Conversely, LDs seem to closely associate with ER protoplasmic membrane, under apparent ADRP regulation (Robenek et al. 2008).

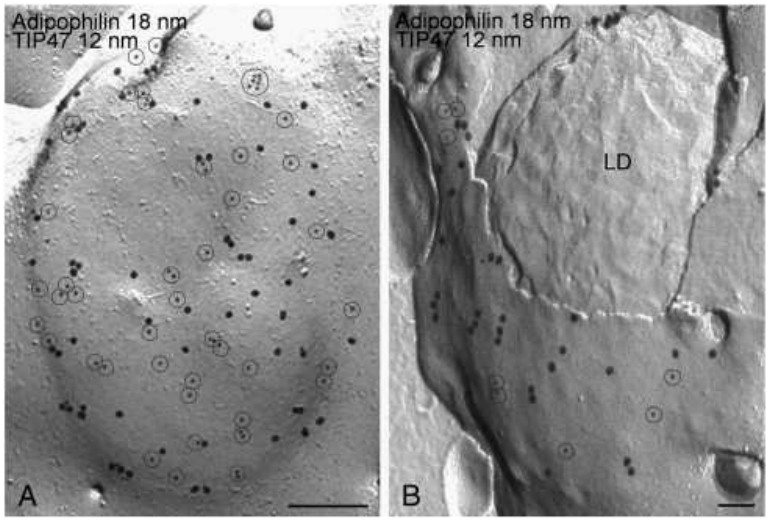

PAT proteins were shown to localize into membrane regions enriched by LDs, but with no necessary contact with LDs (Robenek et al. 2008).

Appendix II. Subject previously assessed data

	units	years	kg	kgm²	kg	kg	%	mmol/l	mmol/l	mmol/l	mmol/l	mmol/l	ml/min/kg
	subject	Age	Weight	BMI	FFM	FM	FAT%	TCHOL	HDL	LDL	TAGemia	Glycemia	VO_2max
Diabetic Type II	DM01	45	160.4	41.67	101.3	59.1	0.368	5.1	1.00	2.8	4.00	11.30	17.20
	DM03	53	91.3	30.16	67.0	24.3	0.266	6.3	1.10	3.9	3.00	6.00	34.20
	DM05	52	92.9	30.30	71.6	21.3	0.229	4.6	1.10	2.6	2.00	6.80	29.10
	DM06	60	115.0	37.13	84.3	30.7	0.267	3.6	1.30	2.2	1.00	5.40	21.90
	DM07	55	139.5	43.49	83.9	50.6	0.363	3.8	1.00	2.3	1.50	6.50	16.10
	DM08	60	102.9	31.76	74.5	28.4	0.276	3.6	0.90	1.6	2.80	6.60	23.70
	DM09	60	89.5	29.22	64.7	24.8	0.277	4.6	1.90	2.7	1.50	6.50	21.70
	DM10	52	112.1	31.32	78.0	34.1	0.304	8.7	0.70	.	8.60	19.00	17.70
	DM12	39	112.4	33.93	82.5	29.9	0.266	3.0	1.00	1.4	1.30	5.80	24.10
	DM14	51	104.2	31.32	72.9	31.3	0.300	4.5	1.30	2.2	1.90	6.30	24.20
Obese	OW01	54	89.3	31.08	61.9	27.4	0.307	6.6	1.50	4.6	1.20	5.50	31.60
	OW02	59	107.0	34.94	72.9	34.1	0.319	6.2	5.10	1.2	3.40	1.40	27.90
	OW05	42	91.9	32.56	59.9	32.0	0.348	5.2	1.20	3.4	1.50	4.90	23.30
	OW06	59	106.2	32.60	79.1	27.1	0.255	5.7	1.40	3.5	1.80	5.50	24.50
	OW07	40	132.2	37.60	81.6	50.6	0.383	3.5	0.90	2.1	1.30	4.60	27.60
	OW08	60	90.0	31.22	59.4	30.6	0.340	4.0	1.10	1.8	3.50	6.80	25.60
	OW09	59	85.4	29.00	61.7	23.7	0.278	4.7	1.50	2.7	1.20	6.20	26.60
	OW10	42	95.0	29.75	73.2	21.8	0.229	3.6	1.10	2.4	0.50	5.70	42.10
Controls	CO01	45	87.6	27.43	74.3	13.3	0.152	3.4	1.30	1.5	1.40	5.20	34.90
	CO03	57	76.8	25.99	60.8	16.0	0.208	6.8	1.60	4.6	1.10	5.00	31.30
	CO04	67	80.5	25.70	61.9	18.3	0.228	5.4	1.30	3.7	0.84	4.10	31.36*
	CO06	59	70.0	24.80	56.8	12.9	0.184	6.2	1.30	3.7	2.70	5.98	22.74*
	CO07	54	81.5	26.25	62.3	19.4	0.238	5.5	1.32	3.5	1.41	5.60	30.65*
	CO08	50	81.3	26.55	64.6	16.4	0.202	5.0	1.51	3.1	0.69	4.82	30.17*
	CO09	63	71.2	23.84	58.1	13.1	0.184	7.1	1.98	4.5	1.39	5.25	34.08*

*Estimated VO_2max

Appendix III. Number of analyzed cells per subject

subject	type I	type II
DM01	14	17
DM03	13	18
DM05	46	37
DM06	7	7
DM07	6	10
DM08	10	8
DM09	15	15
DM10	31	21
DM12	5	3
DM14	20	14
OW01	13	10
OW02	15	8
OW05	59	55
OW06	45	52
OW07	41	37
OW08	69	49
OW09	101	62
OW10	19	11
CO01	62	27
CO03	7	10
CO04	9	12
CO06	20	12
CO07	39	36
CO08	15	11
CO09	18	13

Number of different type cropped cells in each subjects.

Group	Particles per Cell					
	Type I			Type II		
	LDs	OXPAT	COLOC	LDs	OXPAT	COLOC
LC	323,5	306,0	247,0	161,6	82,3	30,2
OB	457,2	542,6	365,4	313,2	200,9	80,3
T2D	355,9	453,4	330,4	208,1	118,9	48,2

Average number of analyzed particles per cropped cell

Appendix IV. Correlations between previously and newly assessed variables

All Groups

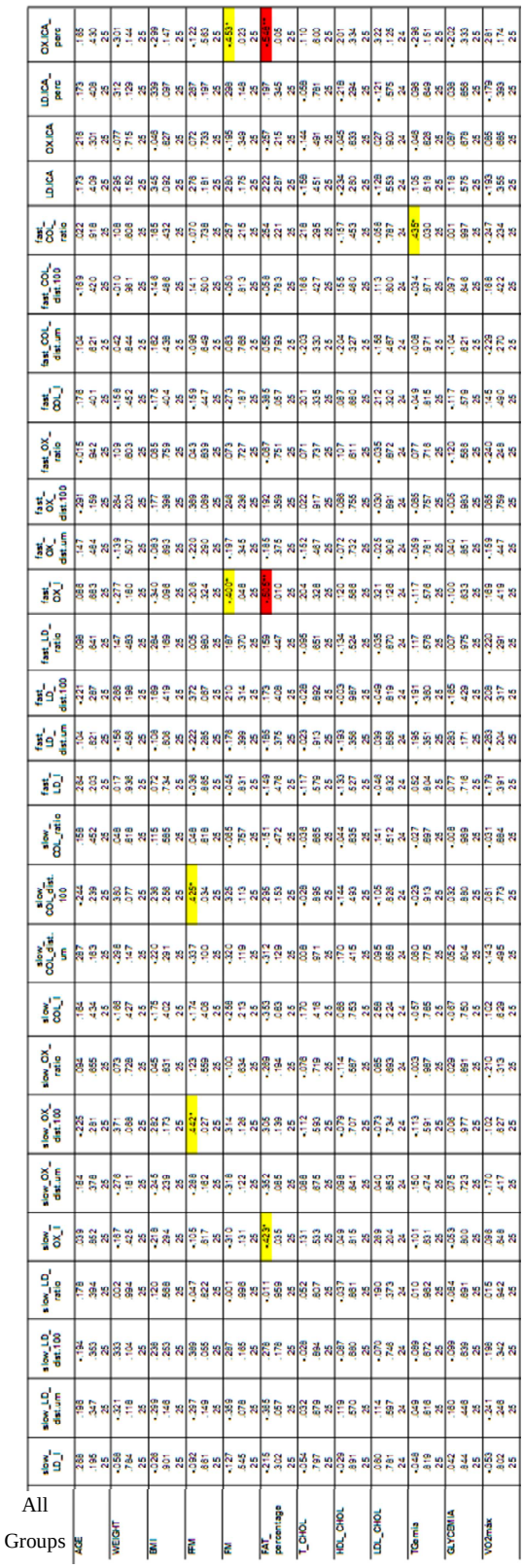

LC

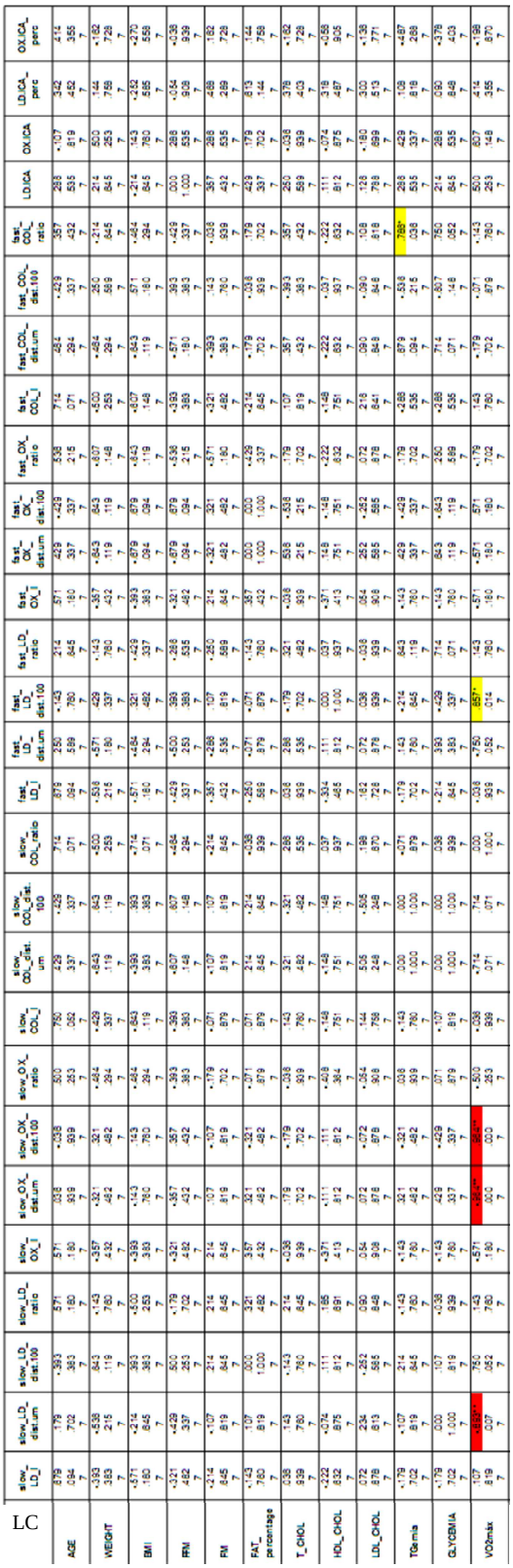

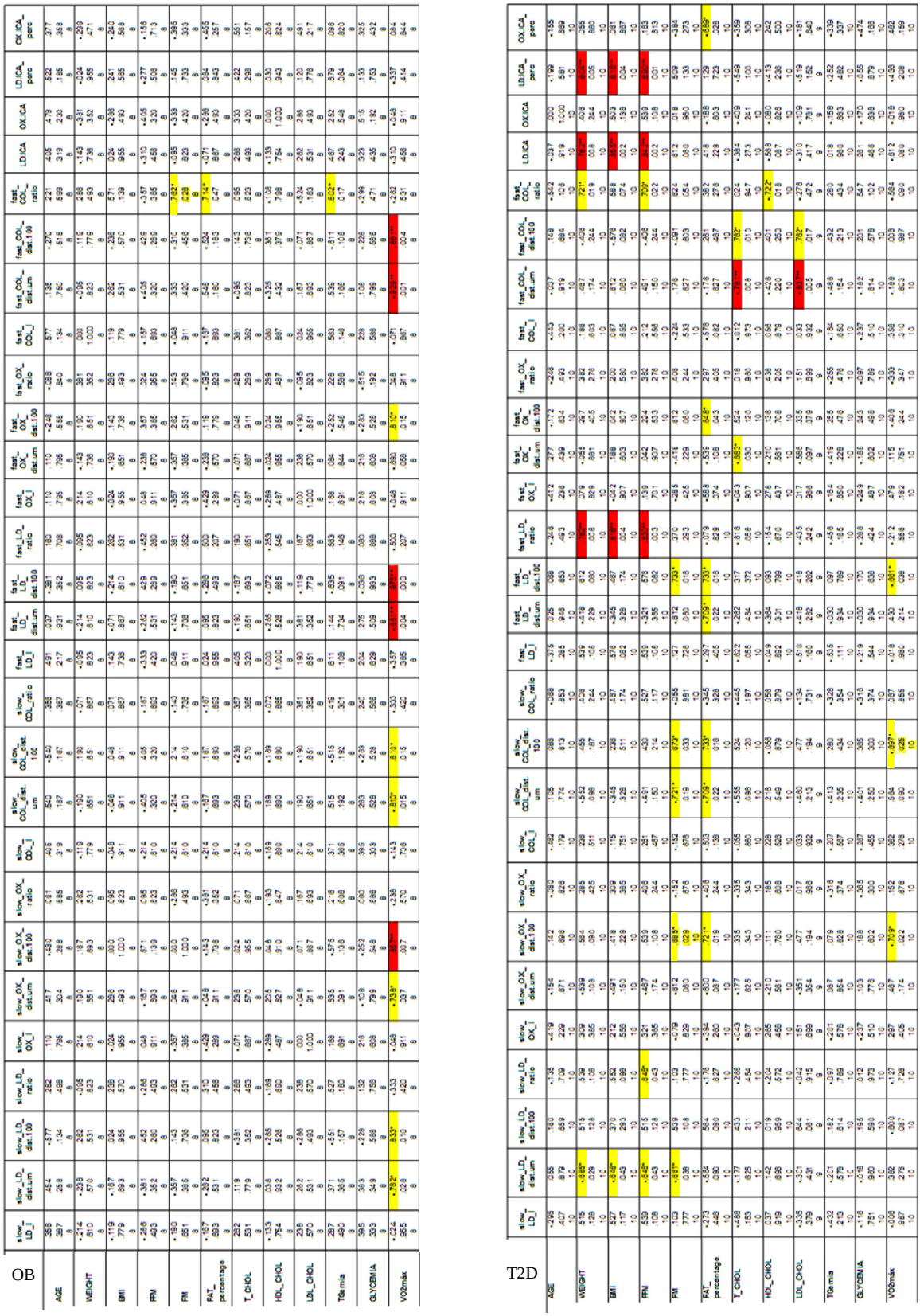

Spearman's correlations grid. Yellow represents mild correlations (P<0.05) and red stands for strong correlations (P<0.01).

Appendix V. Particle content Analysis

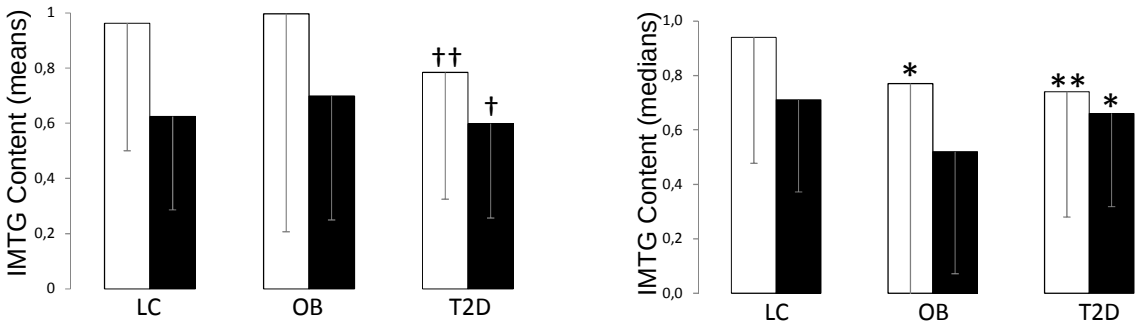

IMTG content between different fiber types of all groups. † and †† stand for P<0.05 and P<0.01 (*t-student*). * and ** stand for P<0.05 and P<0.01 (*Mann-Whitney*). White bars show type I fibers, black bars show type II fibers.

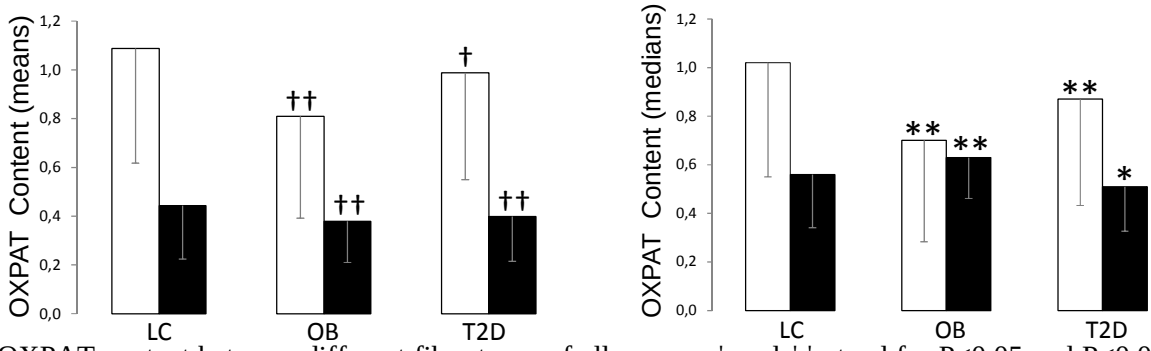

OXPAT content between different fiber types of all groups. † and †† stand for P<0.05 and P<0.01 (*t-student*). * and ** stand for P<0.05 and P<0.01 (*Mann-Whitney*). White bars show type I fibers, black bars show type II fibers.

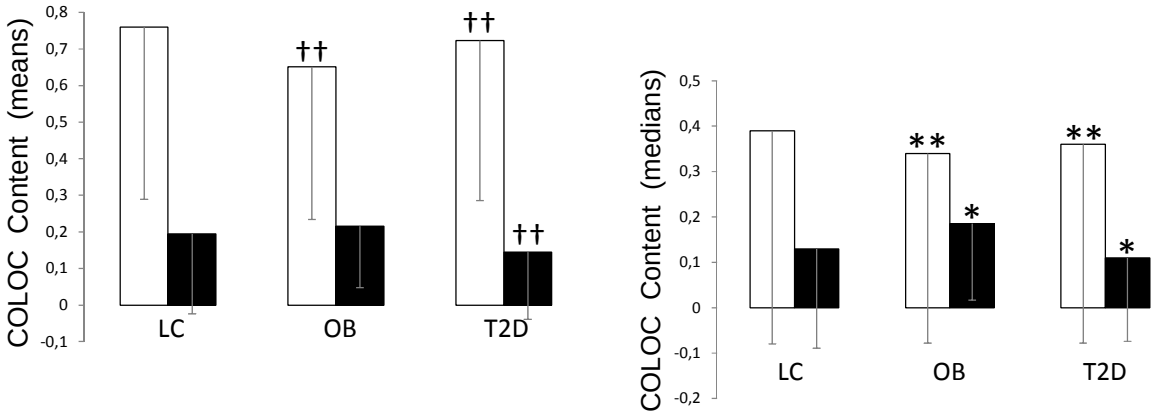

Colocalized content between different fiber types of all groups. † and †† stand for P<0.05 and P<0.01 (*t-student*). * and ** stand for P<0.05 and P<0.01 (*Mann-Whitney*). White bars show type I fibers, black bars show type II fibers.

Appendix VI. Intensity correlation analysis

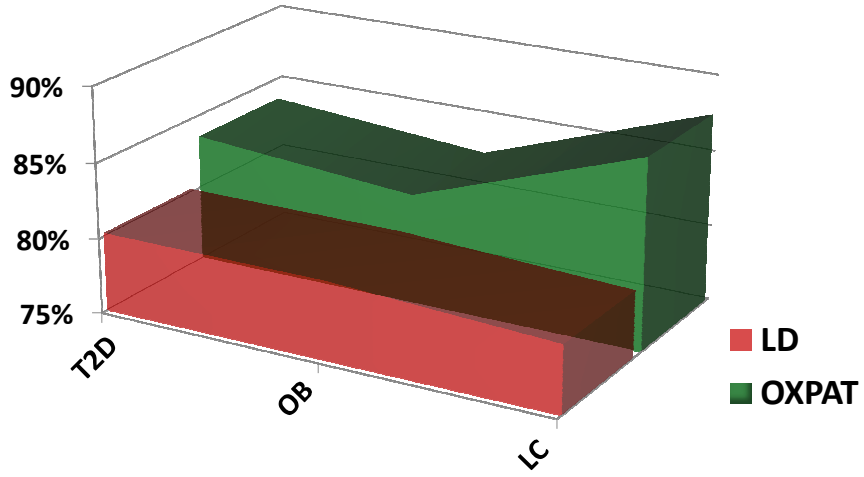

	Mander's OXPAT	Mander's LD	% colocalized OXPAT	% colocalized LDs
Diabetic	0,823	0,857	80,20%	83,52%
Obese	0,810	0,838	80,18%	82,29%
Controls	0,800	0,883	79,43%	87,54%

Intensity Correlation Analysis of LDs and OXPAT particles. Mander's correlations were performed for LDs and OXPAT separately in respect to each other after image data thresholding accordingly to Costes and colleagues (Costes et al. 2004).